CANADIAN THESES

THÈSES CANADIENNES

NOTICE

The quality of this microfiche is heavily dependent upon the quality of the original thesis submitted for microfilming. Every effort has been made to ensure the highest quality of reproduction possible.

If pages are missing, contact the university which granted the degree.

Some pages may have indistinct print especially if the original pages were typed with a poor typewriter ribbon or if the university sent us an inferior photocopy.

Previously copyrighted materials (journal articles, published tests, etc.) are not filmed.

Reproduction in full or in part of this film is governed by the Canadian Copyright Act, R.S.C. 1970, c. C-30.

AVIS

La qualité de cette microfiche dépend grandement de la qualité de la thèse soumise au microfilmage. Nous avons tout fait pour assurer une qualité supérieure de reproduction.

S'il manque des pages, veuillez communiquer avec l'université qui a conféré le grade.

La qualité d'impression de certaines pages peut laisser à désirer, surtout si les pages originales ont été dactylographiées à l'aide d'un ruban usé ou si l'université nous a fait parvenir une photocopie de qualité inférieure.

Les documents qui font déjà l'objet d'un droit d'auteur (articles de revue, examens publiés, etc.) ne sont pas microfilmés.

La reproduction, même partielle, de ce microfilm est soumise à la Loi canadienne sur le droit d'auteur, SRC 1970, c. C-30.

THIS DISSERTATION
HAS BEEN MICROFILMED
EXACTLY AS RECEIVED

LA THÈSE A ÉTÉ
MICROFILMÉE TELLE QUE
NOUS L'AVONS REÇUE

Canada

EVALUATION OF THE FLOCCULATION PROCESS IN GRANULAR MEDIA

by

Leszek W. Kuczynski

A thesis
submitted under the supervision of
Dr. Ronald L. Droste

in partial fulfillment of the
requirements for the degree of
Master of Applied Sciences
in
Civil Engineering

Department of Civil Engineering
University of Ottawa
Ottawa, Canada
K1N 9B4
November, 1985

ISBN 0-315-30979-2

DEDICATION

To my parents.

ACKNOWLEDGMENTS

The author would like to express his special appreciation to Dr. Ronald L. Droste, thesis supervisor, for his encouragement and continuous support during the course of this investigation.

Messrs. Francisco Aposaga, Robert Moore and Richard Moore are gratefully acknowledged for their technical support and assistance in performing the experimental work.

The author is indebted to Miss Deborah Wilson for her continuous support and invaluable assistance in typing and proofreading the thesis.

Financial assistance for this research was supplied by grant # NSERC A 0993 from the Natural Sciences and Engineering Research Council.

ABSTRACT

Coagulation and flocculation processes are commonly used by environmental engineers for the removal of turbidity causing particles from water and wastewater. Known mixing properties of granular media offer an excellent flocculation environment and promise better results, than those obtained from mechanical flocculators or contact filters.

This investigation evaluated the main variables governing flocculation of turbid waters during flow through porous media.

Work was performed in a declining flow rate regime, using as media spheres ranging in size from 14 to 32 mm, and hydraulic loads ranging from 0.17 to 1.08 cm/s.

It was determined that Reynold's number based on conductivity of the media is a useful parameter for monitoring and designing granular media flocculators.

It was found that above a certain value of Reynold's number a region exists where the effectiveness of flocculation increases and adverse effects of clogging are minimized.

In beds built of uniform spheres, particle size and medium porosity can be considered to be the main parameters of successful flocculation. This study also revealed that the effect of changing flow rate has only a small influence on

removal of turbidity but the effect of media size on removal is much more significant.

The experimental data were compared with those predicted from theory and gave a good correlation for flocculation in clean and in partially clogged beds.

I hereby declare that I am the sole author of this thesis. I further authorize the University of Ottawa to reproduce this thesis by photocopying or by other means, in total or in part, at the request of other institutions or individuals for the purpose of scholarly research.

Leszek W. Kuczynski

The University of Ottawa requires the signatures of all persons using or photocopying this thesis. Please sign below, and give address and date.

TABLE OF CONTENTS

LIST OF TABLES

LIST OF FIGURES

LIST OF SYMBOLS

A	area of bed, m^2
A'	projected area of the body on a plane normal to the flow, m^2
a , a'	coefficients
a_w	wetted surface, m^2
a_s	specific surface, m^2
B	breakup constant
b, b'	coefficients
C	mass concentration of substance, mg/L
C_D	drag coefficient
C_o	initial concentration of substance, area under dye mass concentration versus reduced time curve, mg/L
D	dispersion coefficient, m^2/s
D'	experimentally determined value of the size distribution function
D_d	convective dispersion, m^2/s
D_{IJ}	mutual diffusion of particles, m^2/s
D_M	molecular diffusion, m^2/s
d	particle diameter, mm
d_c	capillary tube diameter, mm
f	function of C/C_o
G	velocity gradient, 1/s
g	gravitational acceleration, m/s^2
H	headloss, m
h_o	initial headloss per unit depth [0]
I_{IJ}	number of contacts per unit time between particles, 1/s
J	hydraulic gradient [0]
K, K_1	constant
K_m, K_s	constant
k	constant, permeability, cm^2
L, L_o	length of vessel, depth of bed, m
M	coefficient
m	number of reactors
N	number of capillary tubes
N_m	mass of flocs in suspension after sedimentation
N_o	total mass of flocs, g
N_s	number of spheres
n, n_o	porosity, porosity of clean bed
n_I, n_J	number of concentrations
n_p	number of primary particles
Pe	peclet number
Q	volumetric flow rate, m^3/s, lps
q	specific discharge, m/s
R, r	radius, m
R_f	radius of floc, mm
Re	Reynold's number
R_K	Reynold's number based on permeability
R_I, R_J, R_{IJ}	radius of particle, mm

$R(c,t)$	chemical reaction
T,t	time, s
T_R	tortuosity
V	approach velocity, m/s
u	interstitial velocity, m/s
V_B	bulk volume of column, m^3
V_O	volume of vessel, m^3
V_S	volume of solids in V_B, m^3
V_V	volume of voids, m^3
W	work input, N-m
x,z	distance, m
α	coefficient
β	reciprocal of compaction factor
δ	function
ϕ_H	power dissipation per unit volume, N/m^2
λ	Ivasaki's filtration coefficient
μ	dynamic viscosity, $N\text{-}s/m^2$
ν	kinematic viscosity, m^2/s
ρ	fluid density, kg/m^3
σ_o	specific deposit [O]
σ_L^2	variance
σ^2	variance of time concentration formula

Abbreviations

CC	coefficient of correlation
CD	coefficient of determination
PF	plug flow
rms	root-mean-square
JTU	Jackson turbidity units
NTU	nephelometric turbidity units

Chapter I

INTRODUCTION

The slow settling rate of many particles found in water and wastewater requires extremely long detention times to achieve satisfactory removal in plain sedimentation basins. The expense of chemical addition is usually justified to promote agglomeration of particles of all sizes which results in improved removal in relatively short detention times. The chemical agents reduce forces that are responsible for the formation of colloidal suspensions.

Rapid mixing units in which chemical destabilization agents are added followed by flocculation units are common operations found in water treatment plants. The flocculation step, in which mildly stirred fluid induces dispersed particles to incorporate into flocs, produces effluent containing significantly less minute suspended solids particles. In flocculation, power is input into the fluid by means of mechanical or hydrodynamic devices which require energy; the amount depends on a number of factors.

The declining quality of water supplies and the increasing number of customers using existing treatment facilities as well as the increasing cost of energy magnify the importance of energy consumption in the design and operation

of all components of water treatment systems. Useful alternatives that promise energy savings for flocculation are static mixers and hydraulic flocculators.

The hydraulic flocculator utilizes hydrodynamic mixing of the stream of destabilized particles to promote their contact and to gradually form settleable or filterable agglomerates.

Mixing can be accomplished by using baffles, small-bore tubes, or granular media (Ives, *et al.*, 1978; Schulz and Okun, 1984). The most commonly used devices are baffles, which require a large area, steady flow rate and do not respond quickly to changing influent quality. Known mixing properties of granular media are commonly used in contact filters and pebble flocculators; the latter are gaining increased popularity in Brazil and India (Bhole and Mhaisalkar, 1977; Richter, 1977; Schulz and Okun, 1984).

The main difference between a contact filter and a pebble flocculator is the final product. The former produces clear water with maximum turbidity well below existing standards and is usually a final operation of the treatment process followed only by disinfection. The common problems encountered in contact filters treating high-turbidity waters are rapidly decreasing time between consecutive washing cycles and algae growth. The increased likelihood of breakthrough requires a greater amount of operational skill by plant personnel (Hutchinson and Foley, 1974).

The pebble flocculator produces water containing settleable or filterable agglomerates, called flocs, which have to be removed from the water by means of additional treatment. Coarse media, ranging in sizes from 2.0-20.0 mm, minimize filtration and settling phenomena and provide large void spaces which form numerous interconnected mixing chambers.

Only limited attention has been given to the development of process kinetics descriptions and design procedures for pebble flocculators, despite their obvious advantages. This has resulted in insufficient technical information regarding design criteria. The behaviour of pebble flocculators in changing environmental conditions related to the process is difficult to predict.

Schulz and Okun (1984) noted the high efficiency potential of pebble flocculators and their ability to store agglomerated flocs within the interstices or to form a floc blanket above the media. Their design procedure is closely related to that used for contact filters, since it underlines the importance of the floc-storing process in porous media. They assumed that flow through the gravel bed is laminar and presented equations to estimate headloss and velocity gradient.

Their design procedure was based on experience gained from numerous studies performed on sand filters and is hindered by lack of accuracy, especially for flow at higher Reynold's numbers. They confirmed the inaccuracy of this

procedure and suggested use of bench scale experiments to determine hydraulic gradient values. Other investigations presented in this study are similarly hindered by lack of accuracy.

Bhole and Mhaisalkan (1977) studied flocculation using sand ranging in size from 1.0 to 5.0 mm and a flow rate of up to 0.11 cm/s (2.0 Lpm). Their sample analysis performed after a 15 minute settling period indicated up to 80% reduction in turbidity, resulting from flocculation in a 40 cm bed. They observed the formation of a sludge blanket above the sand bed (approximately 1 m above the surface), which significantly improved effluent quality by entrapping flocs coming from the sand bed.

Richter (1977) used a 210 cm high column made of 6.7 mm gravel and hydraulic loadings ranging from 0.03 to 0.83 cm/s. He reported removal of turbidity, after settling, of up to 90% during test runs, and obtained similar results from a full-scale plant in Aracuaria, Brazil. The Aracuaria plant produces 1.04 MLd of water, providing for the needs of local industry and 12,000 inhabitants. The flocculator chamber had a volume of 3.8 m^3 filled with gravel. Graded gravel ranging from 10 to 20 mm was placed in layers from top to bottom. The direction of flow was upward and corresponding clean bed headloss in the granular medium was 7 cm. The construction cost was approximately $27,000 US for the plant.

Low hydraulic loading and the relatively small size of the grains indicated that results of these studies could be severely affected by filtration effects within the media. Kradille (1983) discussed a pebble flocculator constructed in 1977 for the Varangaon plant (India). The plant's water source is the Tapi river, which has a maximum turbidity of more than 3000 JTU compared to the average turbidity range of 30 to 50 JTU for raw water. The plant produces 4.2 MLd of water for a population of 35,000 in five villages. The pebble flocculator consisted of one 3.0 x 3.0 m chamber, with a 2.5 m deep gravel bed. Graded gravel ranging from 20 to 60 mm was placed in 60 cm layers from bottom to top. The direction of flow was downward and the surface loading rate was 9.7 m/h. The construction cost of the Varangaon plant was $50,000 - 30 to 50% of the construction cost of a conventional plant with the same capacity. It is postulated that use of coarser media and greater hydraulic loadings would provide a better mixing environment and prevent flocs from attaching to the grain; therefore, effluent floc becomes dense and will not clog the bed.

1.1 Objectives of the Study

This study was intended to contribute to the knowledge required to improve and formulate process design criteria for the granular media flocculation of turbid waters. The extent of the topic and available resources made it necessary to limit this study to investigation of the interrelationships among some performance and operating parame-

ters of the process. The optimum media size and flow rate are fundamental to the efficiency of the process of forming large suspended agglomerates. No study has been found which ties these variables together in a systematic manner. Therefore, these parameters were chosen to be the primary concern of the study. There are numerous parameters related to mixing which is the most important phenomenon in flocculation. Development of suitable mixing relations was also a primary aim of this research. Work was performed in a declining flow rate regime, taking full advantage of gravity flow, and reducing shear forces acting on flocs to minimize redispersion (Adin and Rebhun, 1974; Arboleda, 1974; Hutchinson and Foley, 1974).

The specific objectives were:

1. Evaluation of existing aggregation and transport theories in porous media models for analysis of relationships among process parameters;
2. Analysis of relationships between Reynold's number and dispersion abilities of the media.
3. Use of pilot plant scale flocculation experiments to study the effect of media size and flow rate on performance of the pebble flocculator.
4. Generation of preliminary design criteria and operational guidelines for granular media flocculation.

Chapter II

FLOCCULATION IN GRANULAR MEDIA - A LITERATURE SURVEY

Many areas of scientific inquiry are closely related to the specific interests of this study, and the available literature in these areas is extensive. This literature survey has therefore been limited to findings directly related to the investigation and to an interpretation of its results.

2.1.1 Flocculation Kinetics

Existing kinetic flocculation models enable one to distinguish among the phases involved in the flocculation process. The first phase, called perikinetic flocculation, arises from aggregation brought on by thermal agitation (Brownian movement) and is a random process. This phase is completed within seconds, since Brownian motion has little effect on flocs that are larger than 0.1 to 1.0 μm (Bratby, 1977). The second phase, called orthokinetic flocculation, is accomplished by inducing velocity gradients, whereby particles achieve mutual contact by movement of the surrounding liquid.

The extent of orthokinetic flocculation is therefore governed by applied velocity gradients and flocculation time. The increase of the velocity gradients induced in the

liquid results in more particle contact within a given time. However, as the velocity gradient increases, the size of the ultimate flocs produced decreases, because of a continuous breakdown of the larger flocs (Camp, 1968; Kao and Mason, 1975; Parker, 1970; Tambo and Watanabe, 1979a,b; Thomas, 1964). For this reason, for a given velocity gradient there will be a limiting flocculation time beyond which floc particles will no longer grow (Andreu-Villegas and Letterman, 1976).

2.1.1.1 Perikinetic Flocculation

Von Smoluchowski (1916) developed an expression for the rate of aggregation of bimodal floc during perikinetic flocculation in which the frequency of collisions was obtained from the diffusional flux of particles towards a single stationary particle. He assumed that particles are spherical and conjoin into a sphere of proportional volume upon contact.

$$I_{ij} = 4\pi D_{ij} R_{ij} n_i n_j \qquad (2.1)$$

where I_{ij} = number of contacts per unit time between particles of radius R_i and R_j
D_{ij} = mutual diffusion coefficient of particles I and J (approximately $D_i + D_j$)
R_{ij} = radius of interaction of the two particles, (*i.e.* $R_{ij} = R_i + R_j$)
n_i, n_j = number concentration of I and J particles respectively.

If velocity gradients, dv/dz, in the body of liquid are greater than approximately 5 s^{-1} (Bratby, 1980) and if particle sizes are larger than 1.0 μm, the effect of perikinetic flocculation is negligible. The simplified form

of von Smoluchowski's equation (Eq. 2.1) was adapted by Vold (1963) and Sutherland (1967) for computer simulation of perikinetic flocculation.

2.1.1.2 Orthokinetic Flocculation

A theoretical model of orthokinetic flocculation under laminar flow conditions was developed by von Smoluchowski (1917, Eq. 2.2) and popularized among civil engineers by Camp and Stein (1943).

$$I_{ij} = (4/3)\, n_i n_j R_{ij}^3 \,(dv/dz) \qquad (2.2)$$

where dv/dz = velocity gradient in laminar flow.

The application of the above equation is limited to laminar flow and a tubular reactor. This fact was recognized by Camp and Stein (1943); they tried to generalize von Smoluchowski's expression for laminar flow for the more commonly encountered turbulent condition. They replaced the velocity gradient term, dv/dz, by a measurable value called the root-mean-square (rms) velocity gradient, G. The value of G is obtained from the mean value of the work input per unit of time per unit volume (V_o). The total work per unit of time, W, was defined by the weight of the flowing fluid times headloss (Ives, 1978):

$$W = QgH\rho \qquad (2.3)$$

where Q = discharge
g = gravitational acceleration
ρ = density of the fluid
H = headloss.

The mean value of work input can be defined as:

$$\phi_m = W/V_o = AV\rho gH/AL = V\rho gH/L \qquad (2.4)$$

where V_o = volume of vessel
A = cross-sectional area of vessel
L = length of the vessel
V. = mean flow velocity

Therefore, G was defined by Camp (1943) as follows:

$$G = (\phi_m/\mu)^{1/2} \qquad (2.5)$$

where μ = dynamic viscosity

Camp and Stein (1943) state:

> If the flow pattern does not vary, the velocity gradient at any point in a mixing chamber over a period of time is directly proportional to the root-mean-square velocity gradient, and may be controlled by the work input to the chamber.

This statement allowed the formulation of a new version of von Smoluchowski's equation

$$I_{ij} = (4/3)\, n_i n_j R_{ij}^3 G \qquad (2.6)$$

or

$$I_{ij} = (4/3)\, n_i n_j R_{ij}^3 (\phi_m/\mu)^{1/2} \qquad (2.7)$$

From studying flocculation tanks, Camp (1955) found satisfactory results when the nondimensional number, GT, in which T is the total flocculation period, varied between $2*10^4$ and $2*10^5$, with the values of G varying between 20 and 74 s^{-1}. Several authors attempted to overcome the limitations of von Smoluchowski's theory and developed models which more closely describe the conditions encountered in water purification systems. The majority of them incorporated a floc breakup term and attempted to satisfy the physical realities of the continuous reactor, such as dispersion

and short-circuiting. Some of these studies briefly presented below demonstrate the complexity and extent of the problem.

Fair and Gemmell (1964), in an attempt to modify von Smoluchowski's equation (Eq. 2.1) based their theory on the oscillatory pattern of floc growth. In this model, particle growth is up to a maximum size, R_p, when larger particles break into smaller ones which return to the system. This model, like many others, is hindered by its necessary simplification of the complex nature of the floc growth/breakup mechanism.

$$\frac{dn_p}{dt} = (2/3)\left(\sum_{i=1}^{p-1} \sum_{j=p-i}^{} n_i n_j R_{ij}^3 - 2n_p \sum_{i=1}^{\infty} n_i R_{ip}^3 \right) \frac{dv}{dz} \qquad (2.8)$$

where $R_{ip} = R_i + R_p$

The first term in brackets represents the formation of particles of radius R_p from primary and complex particles. The second term describes the breakup of complex particles because of their collision with other particles.

Levich (1962), basing his theory on the characteristics of eddies and their velocity in the Komolgoroff "microscale", derived an equation similar to Camp's version of von Smoluchowski's formula:

$$I_{ij} = 12\pi\beta(\varepsilon_m/\nu)^{1/2} R_{ij}^3 n_i n_j \qquad (2.9)$$

where β = constant
ν = kinematic viscosity

A simplified version of Levich's equation was later verified in an experiment by Tambo and Watanabe (1979b).

Harris *et al.* (1966) generalized von Smoluchowski's equation for all collision possibilities between primary particles and other flocs up to a size p which was limited by breakup. They obtained the following:

$$\frac{dn_p}{dt} = -\frac{\alpha a^3}{\pi} \delta \phi n_1 \frac{dv}{dz} \qquad (2.10)$$

where α = fraction of collisions which result in aggregation
a = ratio of collision radius of a floc to its physical radius
ϕ = floc volume fraction
δ = size distribution function given by:

$$\delta = \frac{\sum_{I=0}^{p-1} n_I \left(I^{1/3} + 1 \right)^3}{\sum_{I=0}^{p} I n_I} \qquad (2.11)$$

Hudson (1965) assumed that in a continuous flow system, a simplified bimodal floc size distribution is valid and that removal of primary particles occurs because of their collisions with flocs. Consequently, he developed an equation similar in form to Harris's development (Harris *et al.*, 1966):

$$\frac{dn_p}{dt} = -(4/3)\alpha n_p n_p R_p^3 \frac{dv}{dz} \qquad (2.12)$$

where R_p = radius of flocs
n_p = floc number concentration
n_p = primary particles concentration
α = collision success factor

Noting that the floc volume fraction, ϕ, can be expressed by:

$$\phi = (4/3)\,\pi R_p^3 n_p \qquad (2.13)$$

Hudson re-expressed Eq. (2.12) as follows:

$$\frac{dn_p}{dt} = -\frac{\alpha\phi}{\pi} n_p \frac{dv}{dz} \qquad (2.14)$$

The surface erosion concept, used by Argaman and Kaufman (1970), recognized the continuous process of the aggregation of primary particles and small flocs to form larger flocs, and the breakup of the larger agglomerates into considerably smaller flocs.

$$\frac{dn}{dt} = -4\alpha\pi K_a R_p^3 n_p u^2 + B\frac{R_p^3}{R^2} n_p u^2 \qquad (2.15)$$

where K_a = proportionality coefficient
u^2 = mean square velocity fluctuation related to the rms velocity gradient G
B = breakup constant
α = fraction of particle collisions resulting in lasting aggregation

A simplified version of Eq. (2.15) for m reactors in series is given by:

$$\frac{N_o}{N_m} = \frac{(1+K_a GT/m)^m}{1 + K_a G^2 T/m \sum_{I=0}^{m-1} (1 + K_a GT/m)^I} \qquad (2.16)$$

where K_a and K_b are constants.
N_o = total mass of flocs
N_m = mass of flocs in suspension after sedimentation

For low values of G, Eq. (2.16) approaches the simplified version of Harris's equation listed earlier in this chapter.

Depending on assumptions, various parameters are incorporated into the aggregation and breakup constants. How-

ever, all of these models recognize the importance of G in the flocculation process and comply with each other in their range of validity.

2.1.2 Physicochemical Aspects of Flocculation

The rational investigation of the phenomena involved in the flocculation process requires an analysis of some of the physicochemical parameters affecting the growth of flocs.

This section will be chiefly concerned with the effects of temperature, coagulant concentration, and colloid concentration on flocculation with aluminum sulfate (alum). There are a large variety of coagulants, but alum is most commonly used. Finally, plug flow (PF) conditions and compartmentalization effects will be discussed.

2.1.2.1 Destabilization of Colloids with Aluminum Sulfate

Investigation of the mechanism of destabilization of colloids by means of numerous coagulant agents has been extensive (Bratby, 1980; Hudson, 1965; Ives, 1978; Stumm and Morgan, 1962; Stumm and O'Melia, 1968; Weber, 1972). For purposes of simplicity one can assume that reactions of aluminum sulfate ($Al_2(SO_4)_3*18H_2O$) in water proceed to the electroneutral precipitate, $Al(OH)_3$. Stumm and O'Melia (1968) have shown that the region for $Al(OH)_3$ stability lies in a pH range from 6 to 8. In water treatment practice, aluminum sulfate is usually used in the form of a solution

with a pH value ranging from 2.5 to 4.0, depending on the concentration of the solution.

The acidic properties of the alum solution produce a need to use alkaline reagents for pH control. The general reaction of alum with sodium bicarbonate is listed below.

$$Al_2(SO_4)_3 * 18H_2O + 6NaHCO_3 = 2Al(OH)_3 + 3Na_2SO_4 + 6CO_2 + 18H_2O$$

The quality of the final product of flocculation, the floc, depends mainly on:

1. coagulant concentration,
2. colloid concentration, and
3. temperature of the water.

Coagulant Concentration

Kawamura (1973, 1976) investigated the relationship between coagulant concentration and turbidity removal. He found that for the same coagulant dosage, its effectiveness decreases when the feed concentration of aluminum sulfate reaches a range between 1 and 3%. This effect decreases with increasing alum dosage and at 45 mg/L becomes negligible. The floc formation time is also affected by alum concentration in the feed and reaches a minimum at a concentration between 0.5 to 2.5%.

Colloid Concentration

Stumm and O'Melia (1968) investigated the effects of colloid concentration on the effectiveness of coagulation.

In the process of coagulating high turbidity water by changing the dosage of coagulant, they identified four zones:

1. Insufficient alum had been applied to destabilize the colloid suspension;
2. Effective destabilization was achieved;
3. Destabilization and then restabilization had taken place, due to overdosing;
4. Precipitation of large amounts of metal hydroxide species followed by the removal of turbidity.

For low concentrations of colloids, only zone number 4 is observed and often a large excess of alum must be added to obtain precipitation. Other authors (Bratby, 1980; Sanks, 1978; Weber, 1972) reported similar observations relating pH of treated water to coagulant dosage.

Water temperature

Morris and Knoche (1984) studied the effects of low temperatures on the rate of turbidity removal. Their investigation indicated that flocculation at low temperatures produces smaller floc with decreased settling abilities, compared to results obtained at 20°C. The authors attributed this discrepancy to a change in the kinetics of the reaction and to physical properties of water, such as viscosity and density. This phenomenon is more pronounced for flocculation with aluminum sulfate than it is for other coagulants (Sanks, 1978; Stumm and Morgan, 1962).

2.1.2.2 Flow Conditions

In flocculation systems, the degree of flocculation achieved within a unit also depends on the magnitude of the mean velocity gradient, G, the retention period in the unit, and the number of units. A simplified version of Harris's equation (Eq. 2.10) was utilized below to visualize these relationships. The simplified form of Eq. (2.10) is

$$\frac{N_o}{N_m} = \left(1 + K_1 G N_o \frac{T}{m}\right)^m \qquad (2.17)$$

where $K_1 = KD'$
D' = experimentally determined value of the size distribution function
K = experimentally determined rate constant

From the above equation, one can conclude that by progressively reducing the total retention time for a flocculation system while increasing the number of flocculation reactors one can achieve the same overall performance. The minimum possible retention time is achieved when the number of reactors in series is infinite, *i.e.*, during PF conditions. The second beneficial effect of compartmentalization is that it minimizes short circuiting.

Camp (1955) presented an equation describing the instantaneous dispersion curve for m compartments of equal size in series.

$$C/C_o = \frac{m^m}{(m-1)} \left(\frac{t}{T}\right)^{m-1} e^{-m(t/T)} \qquad (2.18)$$

where C = concentration of particles in the outlet from the last compartment after time t
C_o = initial concentration in inlet based on the total volume of m-tanks in series

The area under the dispersion curve at a given time t is equal to the fraction of a slug input of tracer which has left the system. Bratby (1980) solved Eq (2.18) and presented it as follows:

$$C/C_o = 1 - \frac{m^m e^{-(t/T)}}{m!}\left[(t/T)^{m-1} + (m-1)/m\ (t/T)^{m-2} + \frac{(m-1)(m-2)}{m^2}(t/T)^{m-3} + \ldots + \frac{(m-1)!}{m^{m-1}}\right] \qquad (2.19)$$

This development indicates that as the number of compartments increases, the time of maximum response approaches the nominal retention time, T.

Camp (1968) demonstrated that higher velocity gradients during flocculation produced lower floc volume concentrations and therefore more compact and less fragile flocs. Camp's investigation of floc volume concentration for G values between 80 and 1000 s^{-1} indicates that by providing a high velocity gradient in the first chamber and subsequently lower velocity gradients in the following compartments, denser floc should be produced (less sludge volume), compared to a system in which a single low G value was used in one or a series of tanks.

The superior performance of a multiple compartment flocculation unit working under a PF regime compared to a single unit with completely mixed conditions can be demon-

strated by means of solving Eq. (2.17) for total detention time, T:

$$T = \frac{m}{K_1 G N_o} [(N_o/N_m)^{(1/m)} - 1] \qquad (2.20)$$

As the number of chambers increases with the same overall performance, N_o/N_m, of the flocculator, the flocculation time tends towards the limit value:

$$T = \lim_{m \to \infty} \frac{m}{K_1 G N_o} [(N_o/N_m)^{(1/m)} - 1] \qquad (2.21)$$

substituting $m = 1/n_1$ into Eq. (2.21),

$$T = \lim_{n_1 \to o} \frac{1}{K_1 G N_o} \left[\frac{(N_o/N_m)^{n_1} - 1}{n_1}\right] \qquad (2.22)$$

results in

$$T = (\ln (N_o/N_m))/K_1 G N_o \qquad (2.23)$$

For a batch flocculator working under identical conditions (same N_o, N_m/N_o, K_1, G,) and m = 1, and for an equal time of flocculation t,

$$T = \frac{1}{K_1 N_o G} [(N_o/N_m) - 1] \qquad (2.24)$$

Comparing Eqs. (2.23) and (2.24) the minimum time for flocculation in an infinite number of compartments will always be a fraction of the flocculation time in a batch reactor for a given result, since $NO/N_m > 1$:

$$\ln (N_o/N_m) < (N_o/N_m) - 1 \qquad (2.25)$$

In summary, this investigation indicated the existence of several parameters directly involved in a successful flocculation process. Some factors, such as pH, temperature and concentration of the particles can be easily monitored and adjusted. Other factors, such as the number of compartments and flow conditions become a stumbling block on the way to improving flocculation efficiency. In this study Richter's (1977) approach to overcome these deficiencies by setting up flocculation in a granular medium, which could be considered as a flocculation basin with a great number of interconnected reactors, was investigated.

2.1.3 Structure of Fluid Motion in Porous Media

The flocculation models presented in Section 2.1 have been developed for reactors which are much larger in size than the largest floc. However, the velocity fluctuations of the particles moving in a granular medium appear to be analogous to velocity fluctuations during eddy motion in larger vessels (Scheidegger, 1960).

Scheidegger (1960), refers to this as "dispersivity". According to Scheidegger, "the hydrodynamics in a porous media may be thought of as analogous to the diffusivity of eddies... in turbulent motion."

Further investigation of flocculation in porous structures requires the analysis and selection of a suitable model, which can be easily applied to a variety of flows and

media.

2.1.3.1 Porous Media Models

Random distribution of pores, even for uniformly sized grains, results in the random nature of flow in granular materials. One can distinguish two different approaches: in one, the flow inside the conduits is analyzed; in the other, the flow around solid objects submerged in the fluid is considered (Bear, 1972). The first approach utilizes the Hagen-Poiseuille law governing the steady flow in a single, straight, circular tube. The second approach, based on an extension or generalization of Stokes law, has been successfully used in the design of suspended bed flocculators and clarifiers (Ives, 1978; Sanks, 1978).

The simplest conduit flow model consists of a bundle of straight cylindrical capillaries of uniform cross-section, oriented in one direction, with liquid flowing axially. These models have been developed based on the Hagen-Poiseuille law.

$$u = - \left(\frac{d_c^2 \rho g H}{32 \mu L} \right) \qquad (2.26)$$

where d_c = tube diameter
H = headloss in capillary
u = velocity, (interstitial velocity)
L = capillary length

If there are N such tubes per unit area of cross-section, then the overall specific discharge will be:

$$q = - NV (\pi d_c^2/4) \qquad (2.27)$$

Porosity, n, which consists of the ratio of the volume of voids within a sample to the bulk volume of the sample is given by:

$$n = V_v/V_m = N\,(\pi d_e^2/4) \qquad (2.28)$$

where V_v = volume of voids
V_m = bulk volume of sample

from which the intrinsic permeability, k, is found.

$$q = -\left(\frac{k\rho g}{\mu}\right)\frac{H}{L}\;;\quad k = \frac{nd_e^2}{32} \qquad (2.29)$$

Equation (2.29) is analogous to Darcy's law, with specific permeabilities related to porosity and pore diameters. The numerical coefficient 1/32 is meaningless as far as the actual porous medium is concerned, and is often replaced with a coefficient that represents tortuosity, T_R.

$$T_R = (L/L_e)^2 < 1 \qquad (2.30)$$

where L = straight line of length L connecting the two ends of tortuous tube of length L_e

The value of T_R estimated by different authors varies between 0.31 and 0.64 (Bear, 1972; Carman, 1937; Irmay, 1954).

The application of Eq. (2.29) to design has been hindered by the assumption that the diameters of the capillary tubes are uniform, and that the conduits have a circular shape. Consequently, the concept of hydraulic radius, R_H, defined as the ratio between porosity and wetted surface, a_w, per unit volume of bed, was introduced.

$$R_H = n/a_w \qquad (2.31)$$

where $a_w = a_s\,(1 - n)$
a_s = specific surface (total particles

surface divided by the volume of the particles).

Models based on the hydraulic radius visualize the porous medium as a network of interconnected channels and utilize some measurable property of porous media in the form of a shape factor.

One of the most widely accepted derivations of permeability is the Carman-Kozeny equation (Bear, 1972; Bird *et al.*, 1960):

$$k = (d_m^2/180)\ \frac{n^3}{(1-n)^2} \qquad (2.32)$$

which leads to:

$$V = \frac{\rho g}{\mu}\ (H/L)\ (d_m^2/180)\ \frac{n^3}{(1-n)^2} \qquad (2.33)$$

where d_m is defined as mean particle diameter = $6/a_m$
V = apparent velocity

Table 4 in Chapter 4 presents a brief review of permeability equations commonly encountered in existing literature.

The interstitial velocity is related to the volumetric flow rate and the cross-sectional area of a porous medium, A, by the Dupuit-Forchheimer relation:

$$u = Q/nA \qquad (2.34)$$

These two models have been successfully utilized in modelling filtration and flocculation processes in granular media (Bratby, 1980; Sanks, 1978; Schulz and Okun, 1984); other models, such as statistical, Ferrandon's and fissure models, have gained more popularity in geotechnical engi-

neering (Bear, 1972). The analogy among the presented models is obvious; any development based on the Hagen-Poiseuille law will lead to a linear relationship between the piezometric head gradient and the velocity. These models closely follow real conditions up to the value of Reynold's number, Re, equal to 1 (a discussion on Reynold's numbers and applicability range, is in Section 2.2), above which deviation increases; when the Re reaches a value of 10 (non-linear laminar flow regime), these models no longer apply. Fig. 1 shows the results of a typical one-dimensional experiment in which the flow rate is gradually increased. One can see clear deviations from Darcy's law and from the models which follow this law. This investigation will encompass higher flow rates that generate Reynold's numbers above 10. Thus, it is appropriate to investigate the relationships between the hydraulic gradient and the flux at large Re numbers.

2.1.3.2 Flow at Higher Re Numbers

The first attempt to find a nonlinear relationship between the hydraulic gradient and the flow rate was made by Forchheimer (1901). He attributed nonlinearity to the appearance of turbulence; this assumption was based on the similarity between flows in porous media and in rough pipes. His equation takes on the following form:

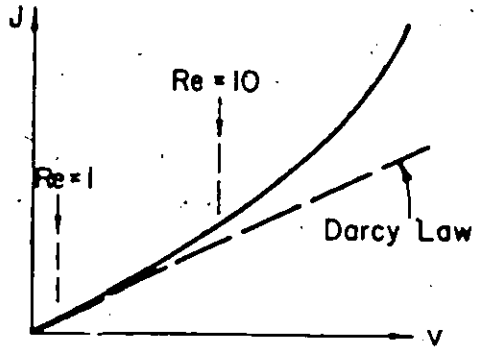

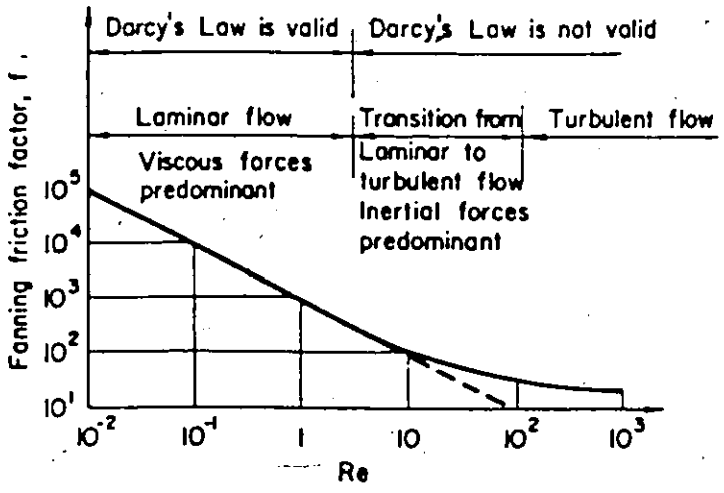

Figure 1 : SCHEMATIC CURVE REPRESENTING EXPERIMENTAL RELATIONSHIP BETWEEN FLUX AND HYDRAULIC GRADIENT (BEAR, 1972).

$$\Delta H/\Delta L = aV + bV^2 \qquad (2.35)$$

where a and b are constants.

Forchheimer's explanation has not been confirmed by experimental results which indicate that actual turbulence occurs at much higher Re values than Forchheimer suggested. Schneebeli (1955) conducted experiments to determine the Re at which turbulence begins. He observed the start of turbulence at Re 150; this indicates that nonlinearity (which occurs in a range of Re 1 to 10) cannot be caused by turbulence. He attributed nonlinearity to inertial forces, which at low Re are negligible in comparison to viscous forces (Bear, 1972; Schneebeli, 1955; Scheidegger, 1960). The inertial forces, which are proportional to the square of the velocity and are independent of viscosity, gradually become predominant as Re increases.

Another approach proposed by Ward (1964) uses drag forces to explain the deviation from Darcy's law. In a laminar region, Stoke's law which is analogous to Darcy's law, is used. At high Re, the drag resistance acting on a particle moving in a fluid is:

$$\text{Drag} = C_D A \rho \frac{V^2}{2} \qquad (2.36)$$

where A = projected area of the body on a plane normal to the flow
C_D = drag coefficient

Ward set a force balance and related C_D to a dimensionless friction factor, which depends on Re and pore geometry.

The final form of Ward's flow equation listed in Table 1 includes linear and quadratic terms.

These investigations resulted in a large number of non-linear motion equations which are identical in form except for their coefficients, and which incorporate the properties of media and fluid. A brief review of representative equations is presented in Table 1.

In this investigation, Forchheimer's type of equation has been utilized, because of its successful application in modelling fluid flow in porous media (Bear, 1972). It can also be applied to a wide range of flow rates (unlimited range of Re) and to a variety of porous materials. Of course all other formulas are also correct in their range of validity and they are not to be considered mutually exclusive.

2.2 Scaling Criteria For Flow and Dispersion in Granular Media

Scaling laws for flow in porous media have been investigated by numerous authors and therefore the available literature on this subject is extensive and detailed (Bear, 1972; Greenkorn, 1964; Gupta, 1972; Yalin, 1971). The scaling laws are usually derived from a dimensional analysis of the variables involved in investigated phenomena.

Table 1: Summary of Nonlinear Motion Equations for Fluid Motion in Porous Media (Bear, 1972)

No.	Author	Equation	Validity range and notation
1	2	3	4
1	Scheidegger (1960)	$J = C_1 \frac{\nu T^2}{gn} V + C_2 \frac{T^3}{gn^2} V^2$	where C_1, C_2 coefficients; T is tortuosity; and ν is kinematic viscosity
2	Ergun (1952)	$J = 150 \frac{(1-n)^2 \nu}{n^3 g d^2} V + 1.75 \frac{(1-n)}{n^3 g d} V^2$	
3	Schneebeli (1937)	$J = 1100 \frac{\nu}{gd^2} V + \frac{12}{gd} V^2$	for spheres; validity range for Re < 2
4	Carman (1937)	$J = 180 \frac{(1-n)^2 \nu}{n^3 g d^2} V + 2.87 \frac{\nu^{0.1}(1-n)^{1.1}}{n^3 g d^{1.1}} V^{1.9}$	empirical
5	Ward (1964)	$J = \frac{\nu}{gk} V + \frac{0.55}{g\sqrt{k}} V^2$	k, measured in a range of the transitional flow regime
6	Irmay (1954)	$J = 180 \frac{(1-n)^2 \nu}{gn^3 d^2} V + 0.6 \frac{1-n}{gn^3 d} V^2$	valid for Re > 1 ÷ 10

where $J = \frac{\Delta H}{\Delta L}$, hydraulic gradient

The second method utilized is a dimensional analysis of the equations that describe the system behaviour. A general description of these methods and their application in fluid flow in porous media has been presented by Greenkorn (1964) and Bear (1972). Fluid flow in a granular media involves numerous variables, some of which are listed below:

$$f (L,t,u,\mu,P,D,k,g,V,d,\rho) = 0 \qquad (2.36)$$

where P = pressure
D = dispersion
d = length perpendicular to flow direction

From these variables a set of dimensionless products representing the relationships among variables and coefficients can be obtained, thus allowing one to predict the behaviour of the prototype from experiments performed on a model that represents it. The complete derivation and a comparison of these products were given by Greenkorn (1964), and Gupta (1972).

In this study, the size of the media and the magnitude of the flow affect the viscous and inertial forces. The ratio between these two forces is the Reynold's number, defined by:

$$Re = VL/\nu \qquad (2.37)$$

Re has been primarily developed as a criterion for fluid flow in conduits to distinguish between laminar and turbulent flow. An analogy between the capillary bundle porous media model and flow in pipes leads to the application of Re as a criterion, describing flow in permeable materials.

Henceforth, in this study, Reynold's number is used as a primary criterion describing flow conditions in the model.

Although the form of Re seems very simple, its direct application for flow in granular media is not straight-forward and therefore requires a more detailed presentation.

2.2.1 Reynold's Number as a Flow Regime Criterion

Reynold's number in porous media is defined similarly to Eq. (2.37);

$$Re = Vd/\nu \qquad (2.38)$$

where d = length dimension of the porous media matrix

The application of Eq. (2.38) as a criterion of the flow regime has been hindered by the lack of a precise definition of a length dimension, d. Consequently, the value of Re for the same media and flow conditions can vary by a factor of 10 with respect to the representative length, d. The most popular definitions of the length dimension encountered in the literature are listed in Table 2.

Bear (1972) utilizes the mean grain diameter as the length dimension in his classification of the flow regimes. However, it seems more appropriate to use the value of $k^{1/2}$, where k is permeability, since it better represents the actual properties of the media.

Table 2: Definition of Length Dimension d, Representing Porous Matrix in Reynold's Number (Bear, 1972).

Notation	Definition
d_m	the mean grain diameter,
d_{10}	the grain size that exceeds the diameter of 10% of the material by weight,
d_{50}	the grain size that exceeds the diameter of 50% of the material by weight,
$(k/n)^{1/2}$	where k is permeability, and n is porosity,
$k^{1/2}$	

For beds consisting of uniform particles, porosity is independent of sphere size and can vary from 0.26 to 0.88. This variation greatly affects k and thus the corresponding value of Re. Using particle diameter as a length dimension would not change the value of Re, regardless of the packing porosity or tortuosity of the flow path. A review of the literature on this subject indicates the existence of several controversies with regard to parameter interpretations and in particular with regard to what parameter to use as a length dimension, d, of a porous matrix, and in assessment of the values of the critical Reynold's numbers.

Data reduction and analyses will consider the various definitions to arrive at the most consistent explanation of flocculation efficiency. The analyses presented later comfirmed that permeability was the best parameter and

therefore development in this chapter will be based on permeability.

Many authors distinguish three regions of flow through porous media (Bear, 1972; Morcom, 1946).

1. At low velocity, where the flow is laminar, viscous forces are predominant, and Darcy's law is valid. The upper limit of this range is characterized by a value of Re between 1 and 10.
2. As the velocity increases (for constant d and ν), inertial forces become more important, and at the upper end of the transition zone, flow passes into the turbulent regime. The upper part of the laminar flow regime is often called the nonlinear laminar flow regime. The Reynold's number for the upper limit of the nonlinear laminar flow regime is usually characterized by an Re value of 400 (Morcom, 1946). Bear (1972) suggests an Re of 100 for this limit.
3. Finally, it is agreed that flow becomes fully turbulent when Re exceeds 2000.

Scheidegger (1960) questions the existence of "universal" Reynold's numbers for porous media at which nonlinearity begins. The author pointed out that inertial effects depend on curvature of the tube; therefore, the critical Reynold's number would be different in some flow channels than in others. This would happen even if the cross-

sections of the channels were identical and even if they together formed a medium of identical porosity and tortuosity.

Although his approach seems to be correct, it is more suitable for phenomena in the microscale than for overall consideration. In this study, attention was directed to the flow in a nonlinear laminar flow region utilizing Re as a flow control parameter.

2.3 Theory Development

This section is chiefly concerned with the definition of the process performance as a function of operating variables. Existing theoretical developments applicable to flocculation in granular media will be discussed. In addition, a process performance model will be formulated to provide a basis for evaluation of experimental data.

The analysis of flocculation in granular media requires one to distinguish two simultaneous processes governing the behaviour of particles. The first process involves the transport of particles through the media and straining, usually described by deposition and differential mass balance equations. The second process involves flocculation, as described by the orthokinetic flocculation equation. For reasons of simplicity, they will be discussed separately. However, in real systems, these two processes complement each other.

2.3.1 Particle Transport in a Stream

The general mass balance equation in an infinitesimal increment of granular medium is as follows:

accumulation rate = (flow in) − (flow out) + generation

$$\frac{\partial C}{\partial t} + V\frac{\partial C}{\partial x} - D\frac{\partial^2 C}{\partial x^2} - R\,(C,t) = 0 \qquad (2.39)$$

where C = concentration of suspension
x = longitudinal distance
D = dispersion coefficient, including diffusion and hydrodynamic dispersion coefficients
R = chemical reaction in the liquid phase or reaction with the medium.

It is assumed that there is no chemical reaction between the medium and the liquid or suspended particles.

$$R\,(C,t) = 0 \qquad (2.40)$$

Therefore, for a semi-infinite medium having a plane source at x = 0, the governing differential equation is as follows:

$$\frac{\partial C}{\partial t} + V\frac{\partial C}{\partial x} - D\frac{\partial^2 C}{\partial x^2} = 0 \qquad (2.41)$$

The majority of researchers who hawe investigated flow and filtration phenomena agreed that the last term of Eq. (2.41) is negligible with respect to the other terms in the equation (Dullien, 1979; Herzig et al., 1970). However, it seems appropriate to discuss the dispersion term, since it represents the mixing properties of the media.

2.3.1.1 Dispersion in Porous Media

The process of longitudinal dispersion in flow through granular media has been studied by numerous authors (Bishoff and Levenspiel, 1962; Danckwerts, 1953; and Greenkorn, 1970; Levenspiel and Smith, 1957; Shamir and Harleman, 1967). Ogata and Banks (1961) presented a solution for Eq. (2.41) which allows one to find the concentration distribution and value of the dispersion coefficient.

In their model, at time t = 0, a quantity of the tracer was rapidly injected into the fluid. They assumed that the flow rate and degree of mixing are independent of radial position and that the plane of tracer would therefore move down the vessel with velocity V;

$$V = \frac{QL}{V_o} \qquad (2.42)$$

Its location at time t would be at x = Vt.

In porous media, the longitudinal velocity of any element of fluid relative to the plane at x = 0 will fluctuate randomly. At times, the element will be close to a solid surface and viscous forces will slow it down; otherwise, near the centre of a channel it will reach a velocity greater than the mean. If packing is randomly arranged, without any channeling, each element of fluid will travel at the same average velocity, and will experience fluctuations of the same average magnitude and frequency.

Assuming all of the above, Ogata's model can be accepted for overall consideration of dispersion phenomena in porous media.

The following boundary conditions allowed him to solve Eq. (2.41):

$$C(x, 0) = 0 \quad x > 0$$
$$C(0, t) = 0 \quad t \geq 0$$
$$C(\infty, t) = 0 \quad t > 0$$

and to obtain the following equation:

$$\frac{C}{C_o} = \frac{1}{2}\left\{ \operatorname{erfc}\left[\frac{x - Vt}{2(Dt)^{1/2}} \right] + e^{Vx/D} \operatorname{erfc}\left[\frac{x - Vt}{2(Dt)^{1/2}} \right]\right) \quad (2.43)$$

where erfc = complementary error function

Equation (2.43) can be presented in terms of dimensionless parameters:

$$\frac{C}{C_o} = \frac{1}{2}\left\{ \operatorname{erfc}\left[\frac{1 - \xi}{2(\xi\eta)^{1/2}} \right] + \exp\frac{1}{\eta} \operatorname{erfc}\left[\frac{1 + \xi}{2(\xi\eta)^{1/2}} \right]\right) \quad (2.44)$$

where $\xi = Vt/x$
$\eta = D/Vx$

Experimental data presented by Ogata and Banks (1961), indicated that the second part of Eq. (2.44) can be ignored without introducing errors in excess of experimental errors (Greenkorn, 1970; Ogata and Banks, 1961).

$$\frac{C}{C_o} = \frac{1}{2} \operatorname{erfc}\left[\frac{1 - \xi}{2(\xi\eta)^{1/2}} \right] \quad (2.45)$$

The solution to the above equation for the case under consideration is also known as Fick's second law of diffusion (Dullien, 1979; Levenspiel and Smith, 1957).

The initial conditions are (Bear, 1972):

$C\ (x,0) = C_\infty\ \delta(x)$

where $\delta(x)$ = a Dirac delta function

The Dirac distribution can be described by:

$\delta_m(x) = 1/m$ for $0<x<m$

$\delta_m(x) = 0$ elsewhere

where m is a small positive number

$$\frac{C}{C_\infty} = \frac{1}{2(\pi Dt)^{1/2}} \exp\left[- \frac{(x - Vt)^2}{4Dt} \right] \qquad (2.46)$$

In the case of a step change in inlet concentration from 0 to C_∞, the solution to Eq. (2.43) is as follows:

$$\frac{C}{C_\infty} = \frac{1}{2}\left\{ 1 \pm \operatorname{erf}\left[\frac{x - Vt}{2(Dt)^{1/2}} \right] \right\} \qquad (2.47)$$

where (+) is for $x - Vt < 0$
(−) is for $x - Vt > 0$
and point C/C_∞ moves with velocity V.

There are experimental difficulties in obtaining a true step function (Ebach and Withe, 1958), and the pulse function method is often used. The pulse function method is an extension of the step function approach and, as shown by Danckwerts (1953), the exit concentration profile for a unit pulse is the derivative of the distribution function for a step function.

The coefficient of dispersion has been found by calculating variance, σ^2, of Eq. (2.46), using a formula developed by Levenspiel and Smith, (1957).

$$\sigma^2 = \int_a^b x^2 f(x)dx - [\int_a^b xf(x)dx]^2 \qquad (2.48)$$

where $f(x)$ = Eq (2.45)
a, b = interval of variable x from 0 to infinity

The result of the integration of Eq. (2.48) is

$$\sigma^2 = 8(D/VL)^2 + 2(D/VL) \qquad (2.49)$$

or

$$D/VL = (1/8)[(8\sigma^2 + 1)^{1/2} - 1] \qquad (2.50)$$

where D/VL = a dispersion number equal to the reciprocal of Peclet number, Pe

2.3.1.2 Correlation of Dispersion and Velocity

Several studies have been conducted to examine the relationship between dispersion, D, in the media and flow parameters (Bear, 1972; Neung-Won Han *et al.*, 1985).

Bear (1972) summarized the results obtained by researchers working with a variety of media over a range of Pe in the form of a correlation between dispersion and Pe. The general form of this correlation is as follows:

$$D_m/D_d = \alpha\ (Pe)^m \qquad (2.51)$$

where D_m = molecular diffusion
D_d = convective dispersion
α, m = coefficients

The value of the coefficient m ranges from 0 to 1.2 for Pe between 10^{-2} to 10^4. In his development, the whole range was divided into several zones, with respect to predomination of molecular diffusion or mechanical dispersion. In the pure mechanical dispersion zone, where inertia effects

may no longer be neglected, the value of coefficient m tends to be less than one.

A weakness of Bear's theory lies in the difficulty of applying the equation to monitor and compare the mixing performance of the flocculation.

Scheidegger (1960) reported the results of his statistical analysis of the relationship between D and velocity, V, in the following form:

$$D = a\ (V)^b \qquad (2.52)$$

where b takes value from 1 to 2 according to the role played by molecular diffusion.
a = unspecified coefficient

Equation (2.52) has been tested and verified by numerous investigators and gained popularity because of its simplicity. Greenkorn (1970) investigated dispersion phenomena in granular beds with grains ranging in size from 0.06 to 0.894 mm and velocities ranging from 0.04 to 0.07 cm/sec. He found a good correlation between experimental data and Scheidegger's equation. However, some of the values of coefficient a were smaller than 1, which disagrees with Scheidegger's theoretical prediction.

Greenkorn extended Eq. (2.52) to investigate the correlation between dispersion and permeability or grain size:

$$D = a' \left(\frac{k^{1/2}}{n} V \right)^{b'} \qquad (2.53)$$

where a' = undefined coefficient related to nonuniformity

Furthermore, he expanded Eq. (2.53) to incorporate Reynold's number (R_k) based on conductivity (k):

$$D/\nu = a'(R_k)^{b'} \qquad (2.54)$$

A similar equation was earlier developed and tested with satisfactory results by Ebach and Withe (1958). Experimental results later confirmed Greenkorn's and Ebach's findings concerning Eqs. (2.52) and (2.54).

2.3.1.3 Floc Deposition in Granular Media

The solid-liquid separation process during the flow in porous media is a well-known phenomena, commonly utilized for filtration purposes. During the bed clogging process, there are several capture processes: inertia, sedimentation, hydrodynamic effects, direct interception and diffusion by Brownian motion. The clogging process commonly employed in filtration and contact flocculation is undesirable in pebble flocculation since it shortens the working cycle of the media. Adverse effects of clogging can be minimized by increasing media grain size, porosity of the bed or flow velocity.

Increase of flow velocity to the point where all deposition ceases (critical velocity) can be a useful alternative, limited mainly by floc strength and minimum contact time.

In a bed working under the constant flow rate regime, the process of clogging results in a decrease of porosity

and an increase of velocity, up to a critical velocity point (Maruodas and Eisenklam, 1965).

In contrast to the constant flow rate, in the declining flow rate regime a decrease in porosity results in a decrease of the flow rate, while the interstitial flow velocity remains approximately constant. Low interstitial flow velocity causes particles to attach to the media, therby producing large fragile flocs. This process continues until an equilibrium point is reached when shear forces overcome the strength of the floc. Therefore a sufficiently high initial flow rate is an extremely important factor in the design of flocculators working in the declining flow rate regime. The initial flow velocity allows critical velocity within the media to be achieved within a short time, resulting in a moderate decrease in flow rate and a longer run. Denser flocs produced at higher velocities requires shorter settling times and minimizes sludge production in the clarifiers.

Several studies have been conducted to enhance the understanding of the relationship between particle deposition and physical parameters in the process (Adin and Rebhun, 1974, 1977; Herzig *et al.*, 1970; Ives and Sholji, 1965; Maruodas and Eisenklam, 1965; Rebhun *et al.*, 1984; Tchobanoglous and Eliassen, 1970; Vigneswaran and Ben Aim, 1985). The majority of the studies directed at increasing removal efficiency were based on a simplified version of Eq. (2.41):

$$\frac{\partial C}{\partial t} = - V \frac{\partial C}{\partial x} \qquad (2.55)$$

and on Iwasaki's clarification equation:

$$\frac{\partial C}{\partial x} = - \lambda C \qquad (2.56)$$

where λ is a function of the amount of accumulated particles per unit volume of bed (σ_o) and therefore also of filtration time.

Equation (2.56) integrated for a given time t and depth L yields:

$$\frac{C}{C_o} = \exp (- \lambda / L) \qquad (2.57)$$

where C_o = influent concentration at t = 0 and for σ_o = 0 filtration coefficient $\lambda = \lambda_o$

Herzig (1970) presented an equation to estimate porosity of a clogged bed by the relation

$$n = n_o - \beta \sigma_o \qquad (2.58)$$

where n_o = porosity of the clean bed
β = reciprocal of compaction factor

He also substituted the following C in Eq (2.55) :

$$C = \sigma_o + nC \qquad (2.59)$$

Finally, by substituting Eq. (2.58) into (2.55) and using a few simplifying assumptions, he obtained:

$$\frac{\partial \sigma_o}{\partial t} + V \frac{\partial C}{\partial x} = 0 \qquad (2.60)$$

The term $\beta \sigma_o$ can be omitted with respect to n_o, when clogging is negligible. A further assumption, interpreted by other authors as well (Ives and Sholji, 1965; Maruodas

and Eisenklam, 1965) suggests that when the particle concentration change in the voids is marginally small, the term $n_o(\delta C/\delta t)$ is negligible. This assumption is valid when the value of nC is small compared with σ_o and can be applied to beds built of small particles when straining cannot be neglected.

Ives and Sholji (1965) presented equations representing the change of filter coefficient, λ, with respect to the specific deposit. These equations were primarily developed for filtration purposes; consequently they have only limited application to flocculation. The following equation was developed by Iwasaki, and represents change in λ during initial clogging and in a slightly clogged bed. Another equation, which includes terms representing coefficient change resulting from heavy accumulation of deposits, is more applicable in filtration processes.

$$\lambda = \lambda_o + k_1\sigma_o \qquad (2.61)$$

where λ = the filter coefficient for a clean bed
k_1 = constant

Equations (2.56), (2.60), (2.61) or other Ives filter coefficient equations, solved simultaneously, allow the quantity of deposits in any bed layer during a flocculation run to be found.

Direct application of this solution for any real system may be difficult, because of the lack of a precise definition of parameter λ, and a large number of simplifying assumptions. Ives and Sholji (1965) derived a formula for

change in a headloss in clogged bed based on their determination of specific deposit.

$$H = h_o L + K \int_0^L \sigma_o \, dL \qquad (2.62)$$

where h_o = initial headloss per unit depth
K = constant for given filtration rate, grain size, suspension and temperature.

2.3.2 The Working Equation

The development of a working equation was chiefly based on Richter's (1977) experience with granular media flocculation, from a study of the Araucaria treatment plant. Richter emphasized existence of a laminar flow regime in the flocculator, and consequently utilized Eq (2.18) to describe flocculation kinetics. The Ergun formula (Table 1) was used to describe flow conditions in a granular bed. The decision to use Ergun's equation, developed for transitional flow, with Harris's equation derived for flocculation in laminar regions, appears to be contradictory. However, the experiments were performed in a lower region of transitional flow (Re based on permeability in a range 1 to 10) where the effects of nonlinearity were less visible and results are consistent with the presented theory.

In this study, Richter's development was followed primarily to find the applicability range of Harris's equation and because of the lack of kinetic equations developed specifically for flocculation in transitional regions.

The net rate of decrease of primary particles N_o/N_m, also called the "performance parameter", is useful in char-

acterizing experimental performance as a function of residence time, mixing intensity and media and suspension characteristics. The simplified form of Harris's equation (2.18), solved for an infinite number of reactors is:

$$\frac{N_o}{N_m} = \exp\ (\ K_1 G N_o T\ ) \qquad (2.63)$$

The velocity gradient, G, (Eq. 2.5) is a function of power dissipated per unit volume described by Eq. (2.4). For the flow through porous media, the volume of liquid V_v = nAL, therefore Eq. (2.4) becomes:

$$\phi_m = \frac{W}{V_v} = \frac{H\rho gQ}{nAL} \qquad (2.64)$$

Substituting Eqs. (2.62) and (2.64) into Eq (2.5) results in:

$$G = \left[\frac{\rho gQ}{nAL}\ (\ h_o L + K \int_0^L \sigma_o dL)\right]^{1/2} \qquad (2.65)$$

where h_o = initial headloss per unit depth, calculated from Forchheimer's formula (Eq. 2.35):

$$h_o = aV + bV^2 \qquad (2.66)$$

Equations (2.63), (2.65) and (2.66), solved simultaneously, yield:

$$\frac{N_o}{N_m} = \exp\left\{ K_1 N_o T \left\{ \frac{\rho g Q}{n A L} \left(\left(a\left(\frac{-}{A}\right) + b\left(\frac{-}{A}\right)^2\right] + K \int_o^L \sigma_o dL \right\}\right)^{1/2}\right\} \qquad (2.67)$$

The complexity of the processes governing flocculation of colloidal particles in a nonlinear laminar flow regime makes the task of finding a universal equation extremely difficult. A large number of variables characterize porous media, turbidity causing particles and water and coagulant interactions; some of these are still undefined which further complicates the issue.

For the above reasons, Eq. (2.67) was used as a guideline or starting point, instead of as a ready formula, to monitor the whole process.

Chapter III

EXPERIMENTAL METHODS

3.1 Work Organization

Experimental studies were conducted at a pilot plant scale, thus avoiding some scaling effects and producing more representative results.

The experiments were conducted to test the application of theories based on Richter's (1977) findings, on flocculation in higher Re ranges. Richter conducted flocculation tests in a 2.1 m high bed, using as a medium uniform gravel with an average diameter of 6.7 mm and porosity, n, of 0.33.

Flocculation was performed using apparent velocities ranging from 0.19 to 0.83 cm/s. These flow conditions produced Reynold's numbers ($R_k = (Vk^{1/2})/\nu$) in a range of 0.18 to 0.80, and a flocculation time of approximately 1.4 to 6.0 minutes.

The experiments were divided into three series of replicate runs with corresponding media diameters of 32, 20, and 14 mm respectively. The flocculation unit in each series was operated with initial hydraulic rates of 0.195, 0.422, 0.650, 0.844, 1.039 and 1.234 cm/s, respectively, and monitored for a period of 4 to 8 hours after steady conditions were reached. These conditions allowed the

behaviour of the flocculator to be monitored in a range of Reynold's numbers from 1.7 to 76.7, and flocculation times between 1.4 and 14 minutes.

A constant head tank served as head control and maintained the declining flow rate regime during the flocculation runs. Furthermore, it was assumed steady conditions were reached when effluent pH 6.6 $\pm$ 0.1 was maintained for a period of 2 hours. The model was built and tested in the Hydraulics Laboratory at the Department of Civil Engineering of the University of Ottawa. The air temperature during this investigation varied from 20° to 24°C. For each of the media arrangements, the following tests were performed on a periodic basis: turbidity, alkalinity, and pH.

3.2 Experimental Apparatus.

The model is shown in Figs. 2, 3, and 4. Two 3,210 L tanks, each equipped with air mixers, were used to prepare and store the water suspension of kaolin. Air mixers were built of 10 mm (3/8 in) copper tubing in the form of grates laid on the bottom of the tanks. The air flow rate was adjusted to a level sufficient to keep the particles in suspension.

Kaolin suspension was pumped from holding tanks through a 25 mm (1 in) PVC pipe to the constant head tank, equipped with a mixer and flow rate control valve. The constant head tank had a 120 L capacity and was equipped with a propeller

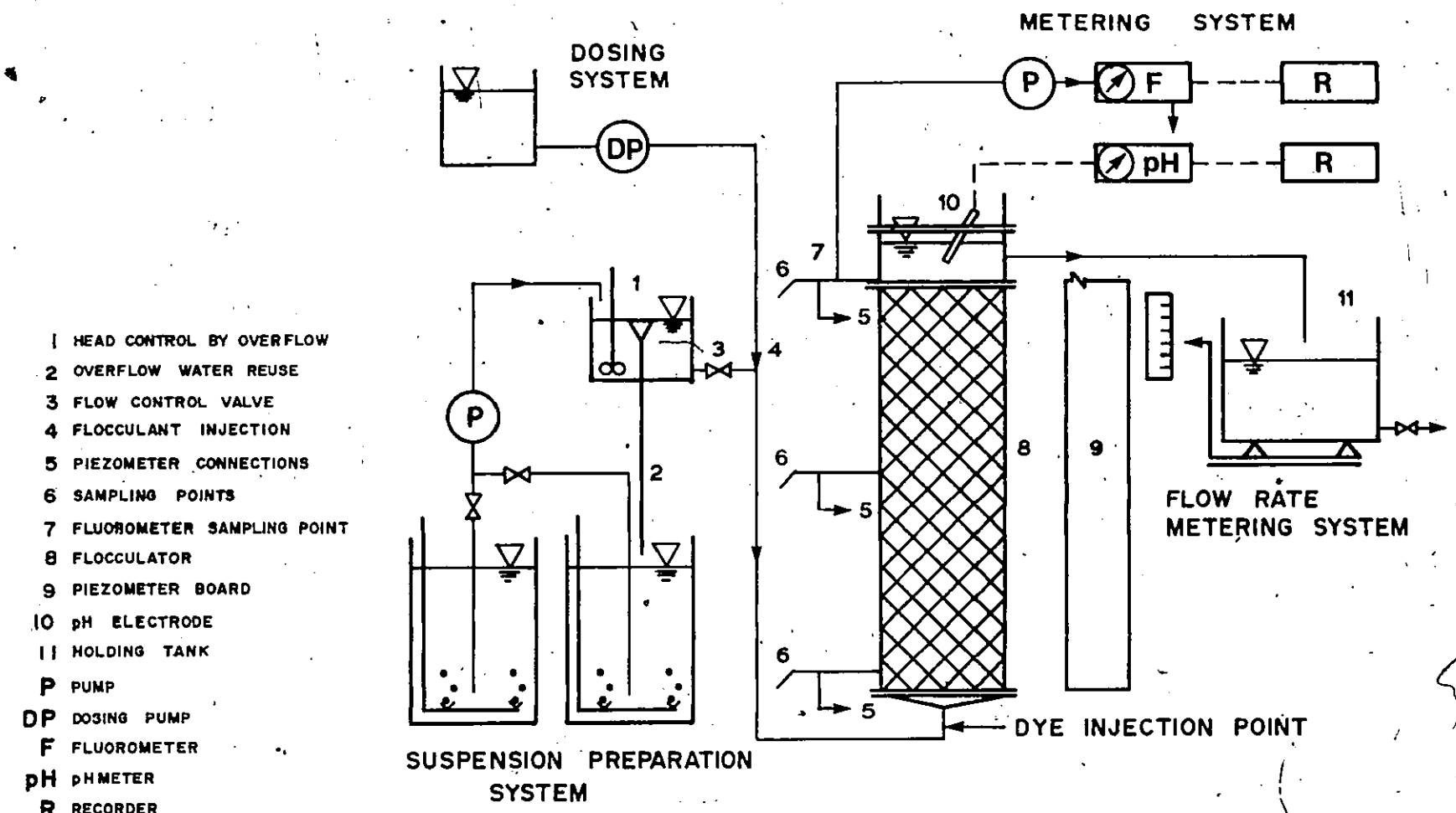

Figure 2 : GRANULAR MEDIA FLOCCULATION SYSTEM SCHEMATIC

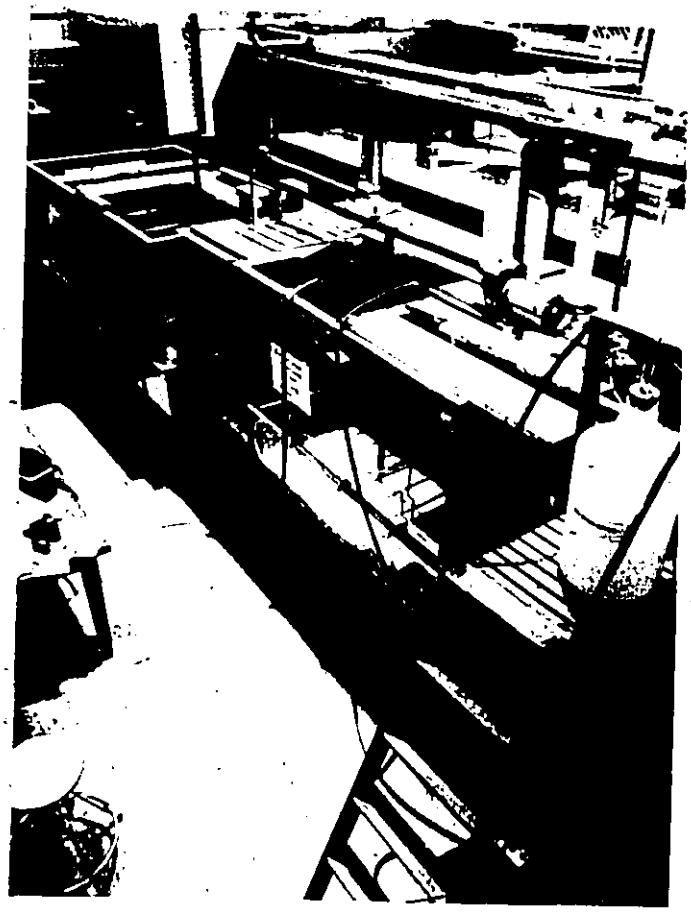

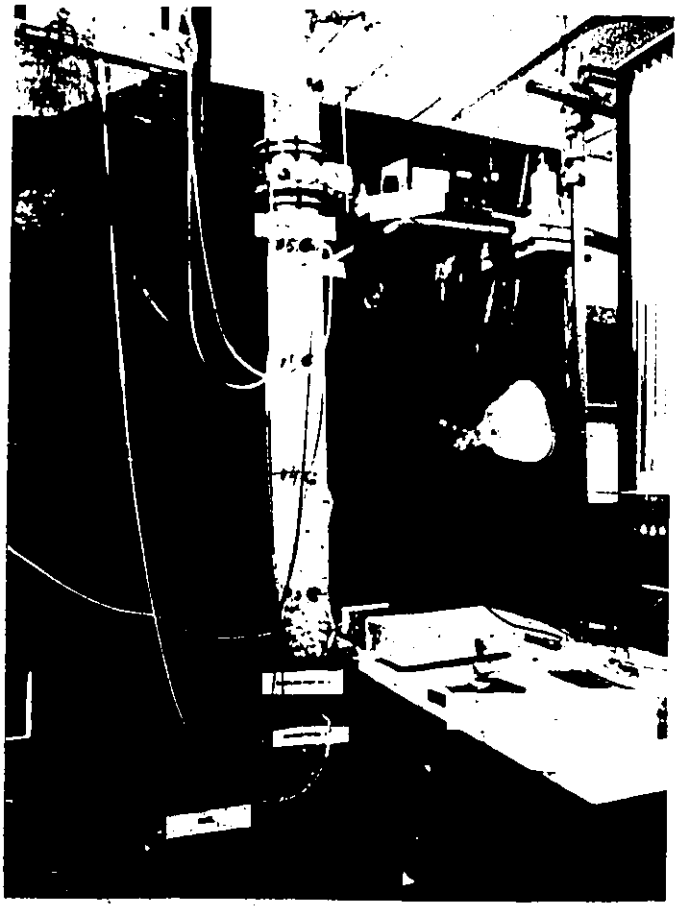

A - PUMPS AND CONTROLS

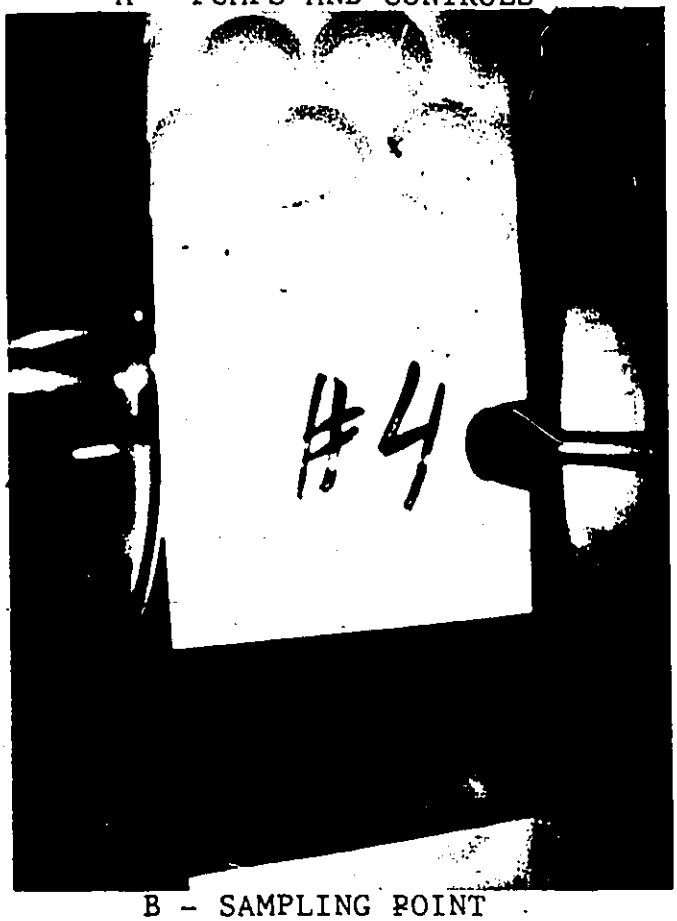

B - SAMPLING POINT

Figure 4 : FLOCCULATION SYSTEM

mixer, keeping the solution agitated without introducing air bubbles. The solution wasted from the constant head tank was returned through a 75 mm (3 in) PVC pipe to the holding tank. The feed solution was transferred by gravity through a 50 mm (2 in) PVC pipe from the head tank to the flocculation column.

The vertical part of the pipe was equipped with an inlet port to supply the required amount of coagulant. Alum coagulant was pumped from a 20 l plastic container through 5 mm diameter acrylic tubing to the flocculator supply pipe. Influent suspension was mixed with alum in the supply tubing. The mixing period ranged from 20 to 150 s, depending on the flow rate.

The flocculator consisted of a plexiglass cylinder 188 cm long and 14 cm ID filled with a granular medium. The media used were: hollow polypropylene balls in two diameters - 38 mm and 20 mm - and glass beads (marbles) 14 mm in diameter.

Provisions were made for sampling water at different points in the column and for measuring the piezometric heads at various depths. The flocculator had six available sampling points, numbered in ascending order from 1 to 6. Preliminary experiments indicated that a distance of 60 cm between neighbouring sampling points must be maintained to avoid interference during sampling. Therefore, sampling points 2, 4 and 6 were chosen. These points were located at 30.5, 91.5 and 188.0 cm heights, respectively, above the

bottom of the bed. The water levels in the piezometers were measured using Cathetometer model M911 (Gaertner Scientific Corporation). The sampling ports consisted of plastic tubing 3 mm (1/8 in) ID that protruded into the centre of the bed through rubber stoppers mounted in the column wall (Fig. 4B).

The column was initially washed for 20 minutes with clean tap water to remove any particles present in it. The suspension was then allowed to flow through the column for 20 minutes to establish the desired flow rate and uniform flow conditions. The clean water that remained in the column from washing was purged during this 20 minute period.

Flocs deposited in granular media can be easily redispersed during sampling, which influences sample turbidity. To avoid this phenomenon, the following sampling procedure was established: the first sample was taken from the top of the column, the second sample from the middle of the column and last sample from the bottom of the column. Samples of 0.5 L volume were siphoned periodically from these sampling points and after a 60 minute sedimentation period, turbidity was measured. A complete description of the turbidity measuring technique is in Section 3.6.

A mixture of the kaolin solution and alum solution ascended through the column to the outlet leaving the flocculator through the 50 mm (2 in) PVC tubing to the collection tank. Flow rates were measured by monitoring the time

to collect a given volume of effluent in the collection tank.

An electrode was placed in the column (above the medium) to determine the pH of the effluent leaving the flocculator. Measurements of pH were made in accordance with Section 423 of Standard Methods. The pH of the solution was not corrected during the experiments but was monitored continuously using a Fisher Accumet Model 140 A pH-meter connected to a Model Coleman 165 recorder (Perkin-Elmer). The apparatus was calibrated prior to each testing with commercially available buffers of known pH.

3.3 Packing of Model

The random nature of pores makes it practically impossible to obtain reproducibility of packing mode. Scheidegger (1960) found that for a given mode of packing, the porosity of the bed is independent of the sphere size and varies from 0.26 to 0.88. This is applicable when the linear dimensions of the vessel containing the spherical particles are greater than ten times the value of the diameter of the spheres (Morcom, 1946). Purchas (1978) proposed an even greater ratio, 1 to 50, to avoid wall effects. To obtain a random packing, the model was frequently shaken while the spheres were poured into the column at a slow steady rate. After packing was completed, the column was filled with a detergent solution which was frequently agitated, using compressed air. One hour later,

the medium was rinsed with tap water, maintaining air agitation for about 30 min. This procedure allowed the removal of impurities.

The model was packed by a known number of spheres of known size; thus, it was possible to find porosity by means of simple mathematical calculations:

$$n = \frac{V_v}{V_m} = \frac{V_m - V_s}{V_m} \qquad (3.1)$$

where: V_s = volume of solids within V_m

Substituting in Eq. (3.1) for

$$V_s = N \frac{4}{3} \pi r^3 \qquad (3.2)$$

and

$$V_m = L \pi R^2 \qquad (3.3)$$

the following is obtained:

$$n = 1 - \frac{N_s 4/3 \pi r^3}{L \pi R^2} \qquad (3.4)$$

where N_s = number of spheres with V_s
R = radius of column
L = depth of bed

Table 3 reports the results of these calculations.

Table 3. Porosity Measurements

Size of the media mm	Number of spheres	Porosity
32.0	430	0.745
20.0	3466	0.498
14.0	9125	0.547

3.4 Preparation of the Suspension

The composition of synthetic water used in this study was based on experiments conducted by Andreu-Villegas and Letterman (1976); however, for economic reasons, kaolin and sodium bicarbonate content was reduced by 50 %. The suspension consisted of 50 mg/L of laboratory grade colloidal kaolin powder in a solution of 84 mg/L of reagent grade sodium bicarbonate (1 meq/L of alkalinity) in tap water. At the time of preparation, this solution was stirred vigorously for 10 minutes and then stirred gently for 24 hours to allow the solution to reach room temperature and equilibrium with carbon dioxide in the atmosphere. The pH of this solution was 8.2 $\pm$ 0.1. Periodic analyses of the synthetic water were conducted to assure its constant quality. Turbidity measurements were used to assess concentrations of suspended solids in synthetic water. The calibration of turbidity measurements for increasing concentrations of kaolin are presented in Fig. 5. The characteristics of the tap water used during the experiments were on average as follows: alkalinity (as $CaCO_3$) - 24 mg/L; chlorides (as Cl^{-1}) - 4 mg/L, hardness (as $CaCO_3$) - 52.1 mg/L, turbidity 0.4 NTU and pH-8.6.

3.5 Preparation of Coagulant

The alum coagulant stock solution was prepared in 20 L volumes for each run by dissolving 1.2344 g of reagent grade

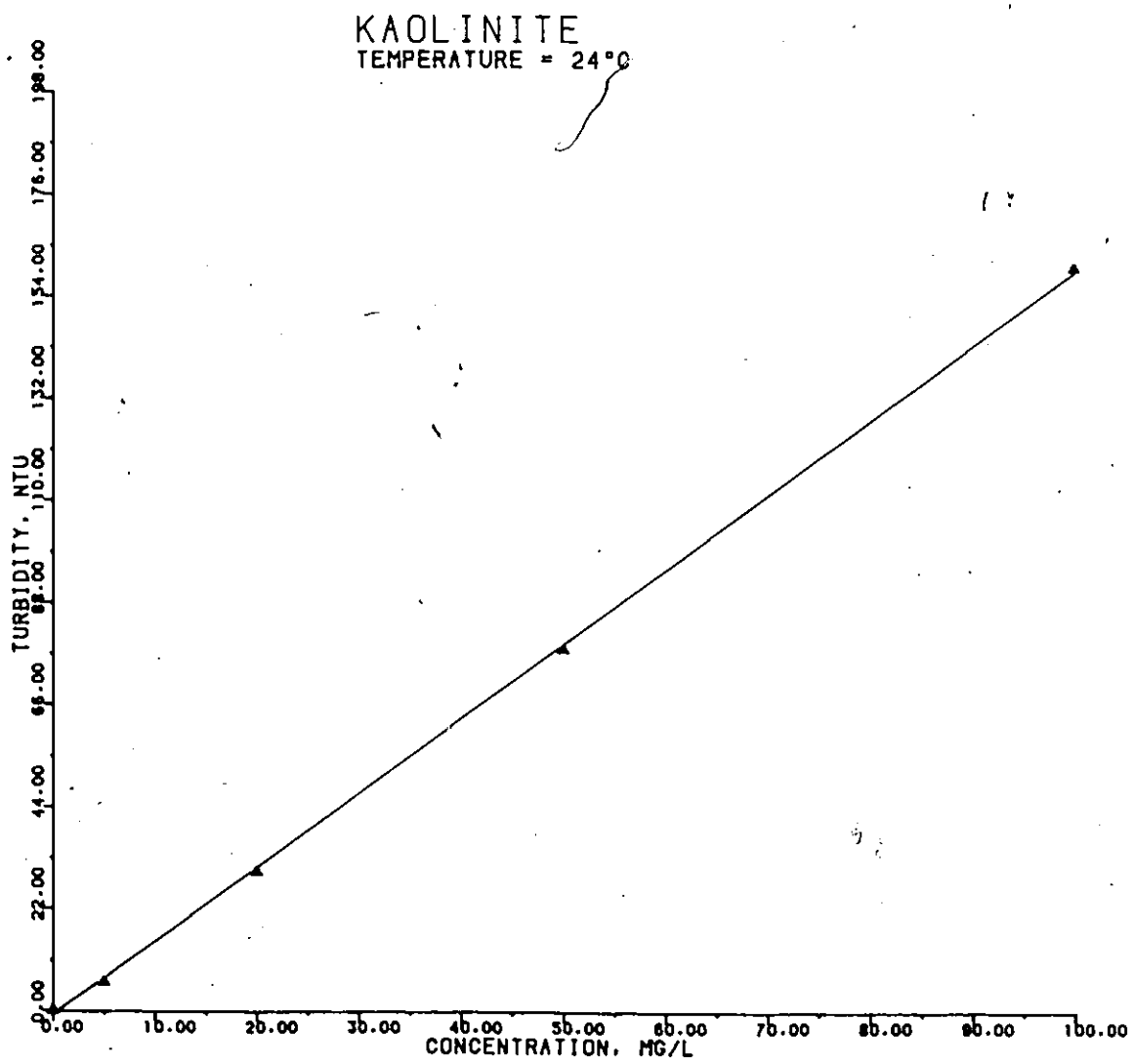

Figure 5: TURBIDITY VS SOLIDS CONCENTRATION FOR KAOLIN

$Al_2(SO_4)_3*18H_2O$ crystals in 1 L of tap water (this corresponds to 0.1 g/L as metal ion or 0.12%). The alum stock solution was never diluted prior to addition to the flocculation reactor.

3.6 Method of Flocculation Parameter Determination

The complex nature of the components causing turbidity in natural waters severely hampers the application of theoretical stoichiometric equations to everyday treatment practices.

The most common method used for determining flocculation parameters is the jar test. This test is usually conducted on a commercially available, variable speed jar tester which allows simultaneous variation of the speed of all its mixing paddles. The Phipps-Bird jar tester Model 300 with six 25 mm (1 in) by 75 mm (3 in) paddles was used.

The procedure used in this investigation involved an adaptation of Bratby's (1980), Sank's (1978), and TeKippe and Ham's (1970) optimization techniques:

1. Six 1 L pyrex beakers were filled with 1.0 L of the water to be tested and placed under the stirrer.
2. The stirrer was turned to its maximum speed.
3. The various coagulant doses were added to each beaker and stirring was continued for 1 min and then paddle rpm was lowered to 40.

4. Stirring was continued for 18 min and turned off. The stirrers were then pulled out from the solution and the samples were allowed to settle for 15 min.

5. A 100 ml sample was taken at a depth of 30 mm and analyzed for residual turbidity.

This sample was acidified to pH 2.5 by adding concentrated reagent grade hydrochloric acid, after which it was shaken to dissolve any residual hydroxide precipitate and then turbidity was measured.

Turbidity measurement was done in accordance with Section 214A of Standard Methods, using a light scattering turbidimeter, Fisher Scientific Model DRT 100, calibrated using standard formazin suspension supplied by the manufacturer.

Figure 6 reports the cumulative results of the jar tests, which revealed the optimum coagulant dosage, which is in the range of 1.5 to 2.0 mg/L. Later, during the flocculation runs, the alum dose ranged from 3.5 to 4.0 mg/L, yielding satisfactory results.

The difference between the optimum dose of coagulant indicated by the jar test and the applied dose was due to different mixing conditions and temperature oscillation of treated water. However, Fig. 6 indicates that further increases in coagulant dose do not result in meaningful increases of residual turbidity. An analysis of flocculation curves presented by numerous researchers flocculating kaolin

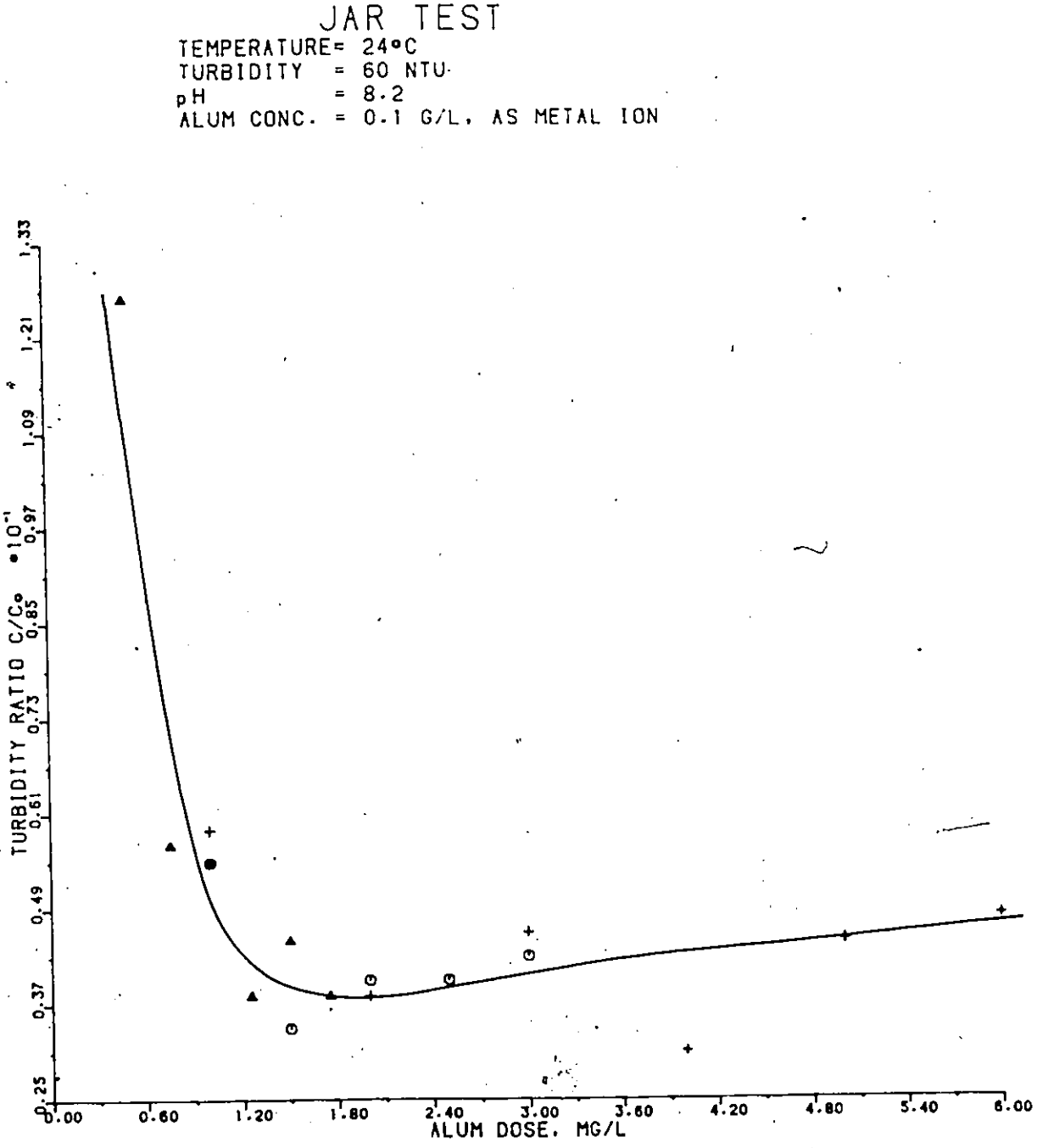

Figure 6: JAR TEST

suspension with alum yield similar conclusions (Andreu-Villegas and Letterman, 1976; Argaman, 1971; Tambo and Watanabe, 1979).

3.7 Evaluation of Flocculator Properties

A test was also conducted to determine the response of the granular medium flocculator to an interruption in coagulant feed and to a sudden change in flow rate. To investigate the influence of coagulant feed on the flocculator, 20 mm spheres and a flow velocity of 0.195 cm/s were chosen. This size of media performed well during flocculation runs and the low flow velocity allowed for the collection of required data.

The procedure used in this test was as follows: After 1 hour of continuous flocculation, the pump dosing alum into the feed kaolin suspension was shut off. As a result, the kaolin solution without coagulant formed a slug, flowing through the bed.

At the end of a 5 minute shut-off period, the previous coagulant feed rate was restored. The flocculator's response to this shut-off period was monitored by continuous pH measurements and periodic sampling.

The effect of a sudden change in flow rate was tested using 14 mm medium subjected to an initial flow velocity of 0.422 cm/s with a stop-and-start period after 9 hours of continuous run. At the end of a 6 hour idle period the flow was restored and flocculation was continued for a period of

15 hours. Data were collected by periodic sampling, flow rate measurements, head loss monitoring and photographs.

3.8 Dispersion Analysis

The determination of the dispersion coefficient was performed utilizing the relation between dispersion number and variance of the breakthrough curve. An outline of this method was given by Levenspiel and Smith (1957), they modified the variance (Eq. 2.48) of the time-concentration formula (Eq. 2.46) by replacing the integrals with finite sums and the theoretical function of Eq. (2.45) by the observed concentration readings:

$$\sigma^2_L = \frac{\Sigma\, t^2 f}{\Sigma f} - \left(\frac{\Sigma\, tf}{\Sigma f}\right)^2 \qquad (3.5)$$

where f is proportional to C/C_o and summation is taken over all the uniformly spaced readings.

The value of σ^2_L from Eq. (3.5) divided by detention time, T, results in:

$$\sigma^2 = \frac{\sigma_L^2}{T^2} \qquad (3.6)$$

where σ^2 = variance of time concentration formula

Consequently, by substituting σ, obtained from Eq. (3.6) into Eq. (2.50), the coefficient of dispersion is found. Neither the quantity of the tracer nor the actual outlet concentration are required.

The breakthrough curve was obtained by measuring the level of fluorescent tracer in water sampled continuously

from the top of the bed. The slug of the tracer (Rhodamine WT) was injected into the water supply tubing using a hypodermic syringe. Plastic tubing of 0.2 mm i.d. attached to a hypodermic needle, permitted the injection of dye into the centre of the water supply pipe.

Samples of water were continuously taken from the sampling point at the top of the column located 188 cm from the bottom of the media and pumped into the fluorometer, where the level of fluorescence was measured.

The level of fluorescence was measured by a photoelectric cell colorimeter Model III (G.K. Turner Associates) connected to a recorder. A detailed arrangement of this apparatus is presented in Fig. 2. The apparatus was calibrated prior to each test with samples of known concentration (Fig. 7).

The absorption properties of the media were tested using the static absorption test (Gupta, 1972). Samples of the media were submerged for a period of 24 hours in water of known tracer concentration. The solutions were frequently analyzed, and there was no significant change in the fluorescence level, regardless of the dye concentration used.

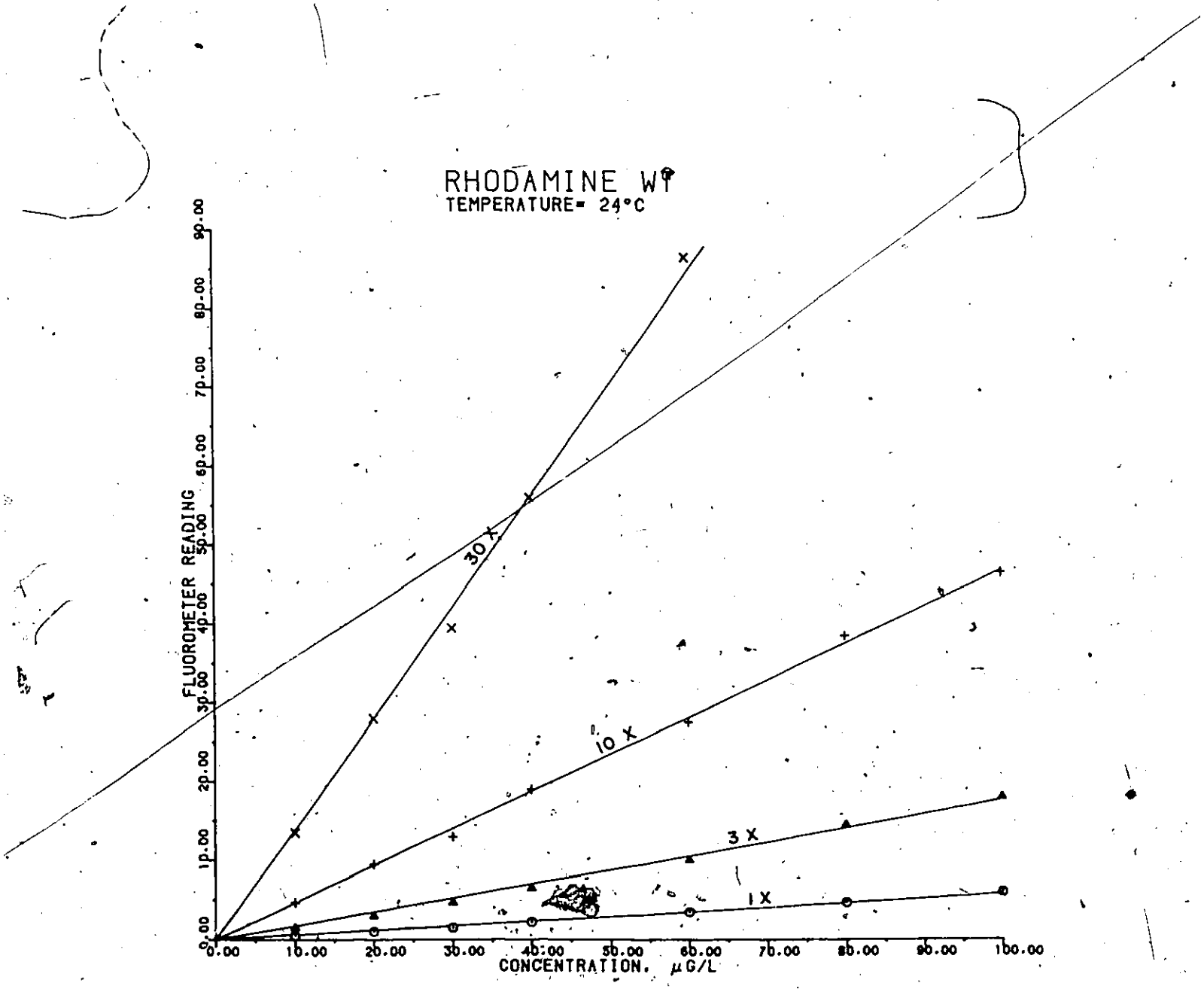

Figure 7: FLUOROMETER CALIBRATION

Chapter IV

ANALYSIS AND DISCUSSION OF EXPERIMENTAL RESULTS

4.1 Evaluation of Permeability and Reynold's Number Calculation Techniques

Calculations using five different permeability formulas were made to find the one most applicable to this study. Table B.4 (Appendix B) contains data together with k calculated using the Ward formula. Due to experimental error some measurements were rejected. Table 4 presents values of k calculated using some of the better known formulas. As expected, attempts to use Darcy's law failed; values in Table 4, also presented later in this chapter showing the correlation between J and V, indicate the flow was in the transitional range, where Darcy's law no longer applies.

The porosities and media sizes used in this study indicate that permeability values calculated by means of Harleman's and Bear's empirical formulas are too small.

Examination of available literature (Bear, 1972; Freeze and Cherry, 1979), suggests that the most reliable values are those described by Carman-Kozeny's and Ward's formulas. These two formulas produced similar results that fall in the range given by the above references. In this investigation, Carman-Kozeny's formula was utilized for simplicity and its proven results for flow in porous media (Hudson, 1981).

Table 4. Permeability , k, Calculated By Representative Formula

Formula	Units	media size, [cm] 3.2	2.0	1.4
Carman-Kozeny $k=(d^2/180)n^3/(1-n^2)$	k [cm^2] d [cm]	0.3617	0.0109	0.0087
Ward $k=((0.5\rho V^2+(0.302\rho^2V^4+4\mu VJ)^{1/2})/2J)^2$	all in [CGS]	0.1350	0.0066	0.0025
Empirical (Bear, 1976) $k=0.617\times10^{-4}\ d^2$	k [cm^2] d [μm]	0.0063	0.0025	0.0012
Harleman *et al.*, 1963 $k=6.54\times10^{-4}\ d^2$	k [cm^2] d [cm]	0.0067	0.0026	0.0013
Darcy law $k=\mu v/J\rho g$	k [cm^2]	0.0216	0.0002	0.0039

Parameter interpretations and an assessment of the value of Reynold's number presented in Chapter II were also examined. Table 5 contains Reynold's numbers values obtained using different length dimension parameters.

Respective values of Re were calculated using this same apparent velocity and kinematic viscosity. Careful analysis of R_K indicates that experiments were performed in the lower end of the transition zone (Reynold's number less then 100). However, values of Re suggests that a greater number of the runs was done in the upper range of transitional flow. This finding disagrees with observations presented in Section 4.4, where the left part of the hydraulic gradient curves yields similar results, indicating proximity of laminar flow range. In this range all nonlinear flow equations produce results analogous to those obtained from Darcy's formula.

Further analysis indicates that including the porosity in R_k does not influence its value to a large degree.

Table 5. Reynold's Numbers

Apparent velocity $\times 10^{-2}$ m/s	ν $\times 10^{-6}$ m²/s	Re $(Vk^{1/2})/\nu$	$(Vd_m)/\nu$	$(V(k/n)^{1/2})/\nu$
media size 32 mm, n=0.745, k*=0.3617 cm²				
0.195	0.918	12.68	68	14.80
0.435	0.918	28.33	147	32.03
0.650	0.946	41.32	220	47.88
0.844	0.963	52.48	280	61.07
1.052	0.963	65.39	345	75.18
1.234	0.963	76.70	410	89.28
media size 20 mm, n=0.498, k*=0.0109 cm²				
0.195	1.057	2.51	37	2.73
0.435	1.007	5.76	84	6.20
0.650	1.007	8.87	129	9.55
0.844	1.007	11.52	168	12.40
1.052	1.034	13.74	201	14.87
1.234	1.034	16.32	239	17.66
media size 14 mm, n=0.547, k*=0.0087 cm²				
0.201	1.120	1.67	24	2.20
0.422	1.120	3.51	53	4.75
0.650	1.120	5.41	81	7.31
0.844	1.120	7.03	106	9.50
1.039	1.120	8.65	130	11.70
1.234	1.120	10.28	154	13.90

* permeability calculated using Carman-Kozeny formula

These observations confirm the results of other investigators, who recommended using $k^{1/2}$ as a length dimension parameter (Greenkorn, 1964; Gupta, 1972; Ward, 1964). As a consequence, the value of square root of permeability in this study was used to calculate R_k.

4.2 Evaluation of Dispersion Parameters

Tracer tests were conducted in three series, using six different flow velocities for 32 mm spheres, and seven velocities for 20 and 14 mm media, respectively. Results of 3 runs were averaged and are presented in Figs. B to 10 and B1 to B17 (Appendix B), where C/C_o represents the ratio of tracer passing through the column to the total mass of the tracer; t/T is a ratio of the tracer passing time to the detention time; FLOW VEL. is apparent flow velocity and DISP. COEFF. is equal to dispersion coefficient calculated by means of the method presented in Section 3.8.

Skewness to the left in the dispersion curves indicates existence of PF conditions in the pebble flocculator. Furthermore the single strong peak implies absence of short circuiting. The peak, occurring at reduced time significantly less than 1.0, and the long tail suggest presence of dead space. The comparison of the dispersion curves reveal that the volume of dead space remains constant during all test runs. This dead space can be attributed to voids retaining tracer particles and to the imperfection of the sampling device. The early appearance of the dispersion curve could also indicate channelling of the fluid in voids adjacent to the walls of the vessel. This deficiency can be corrected by placing flow breaking rings inside the column (Purchas, 1978). A summary of results obtained from the dispersion tests together with calculated R_K is presented in Tables 6-8.

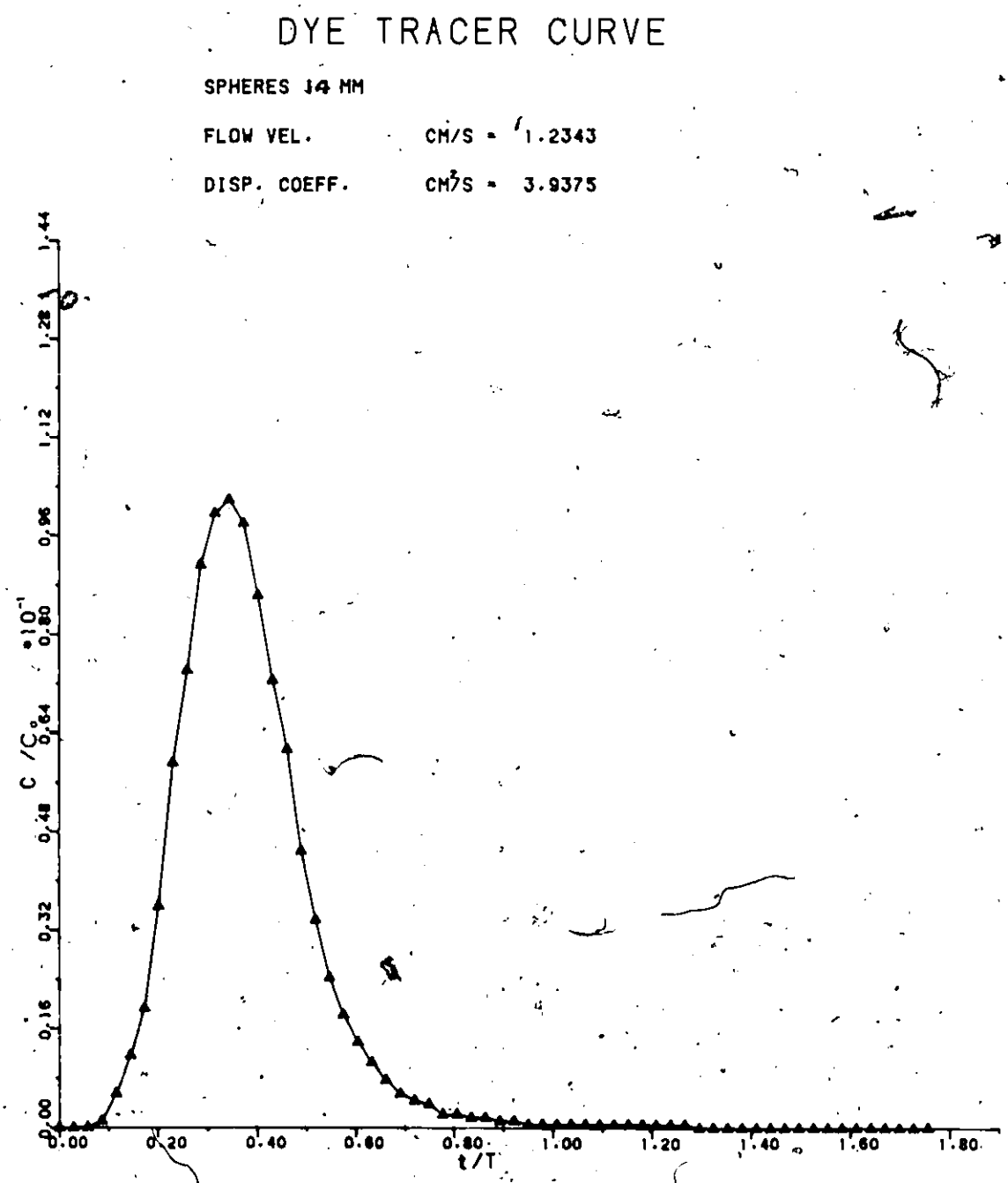

Figure 8: TRACER TEST

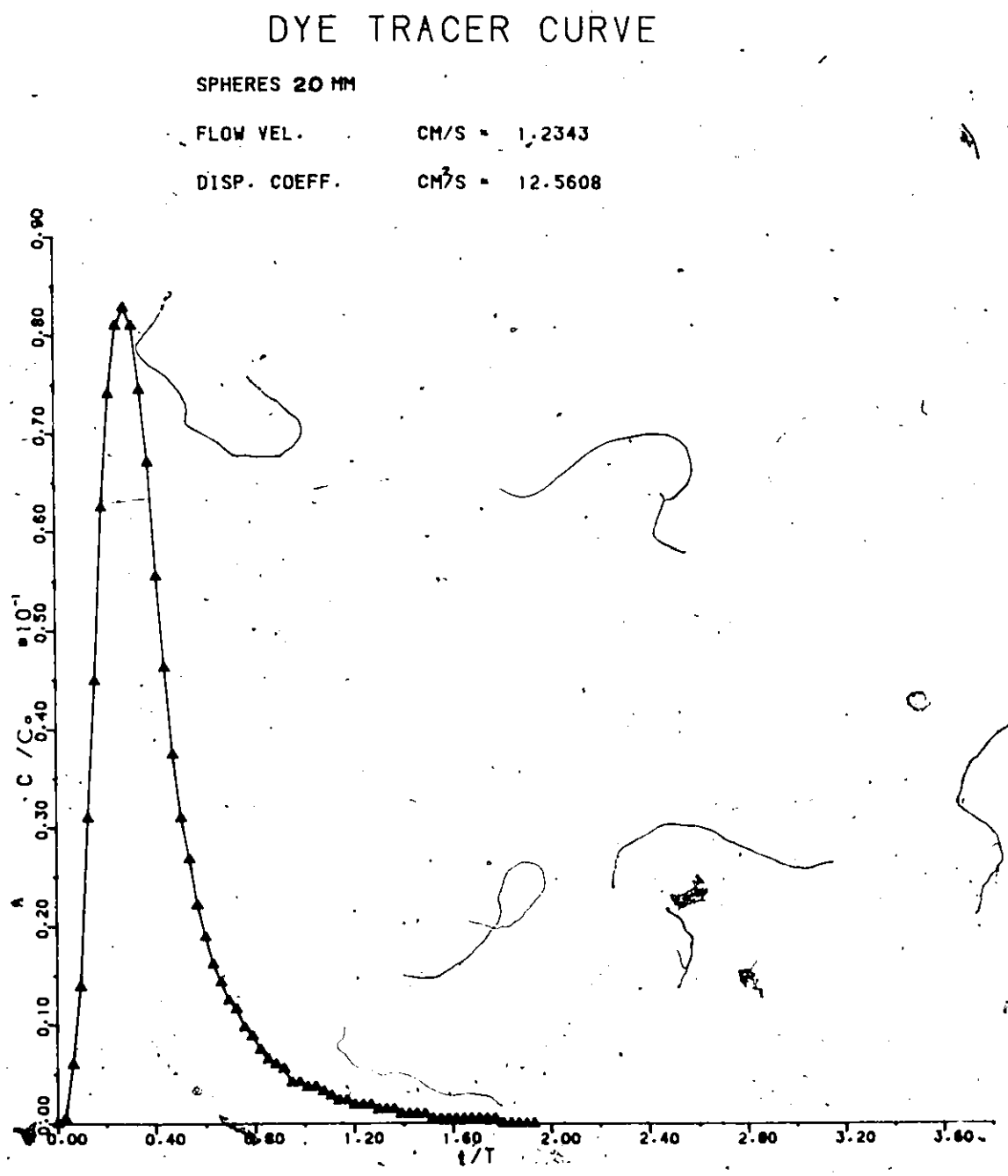

Figure 9: TRACER TEST

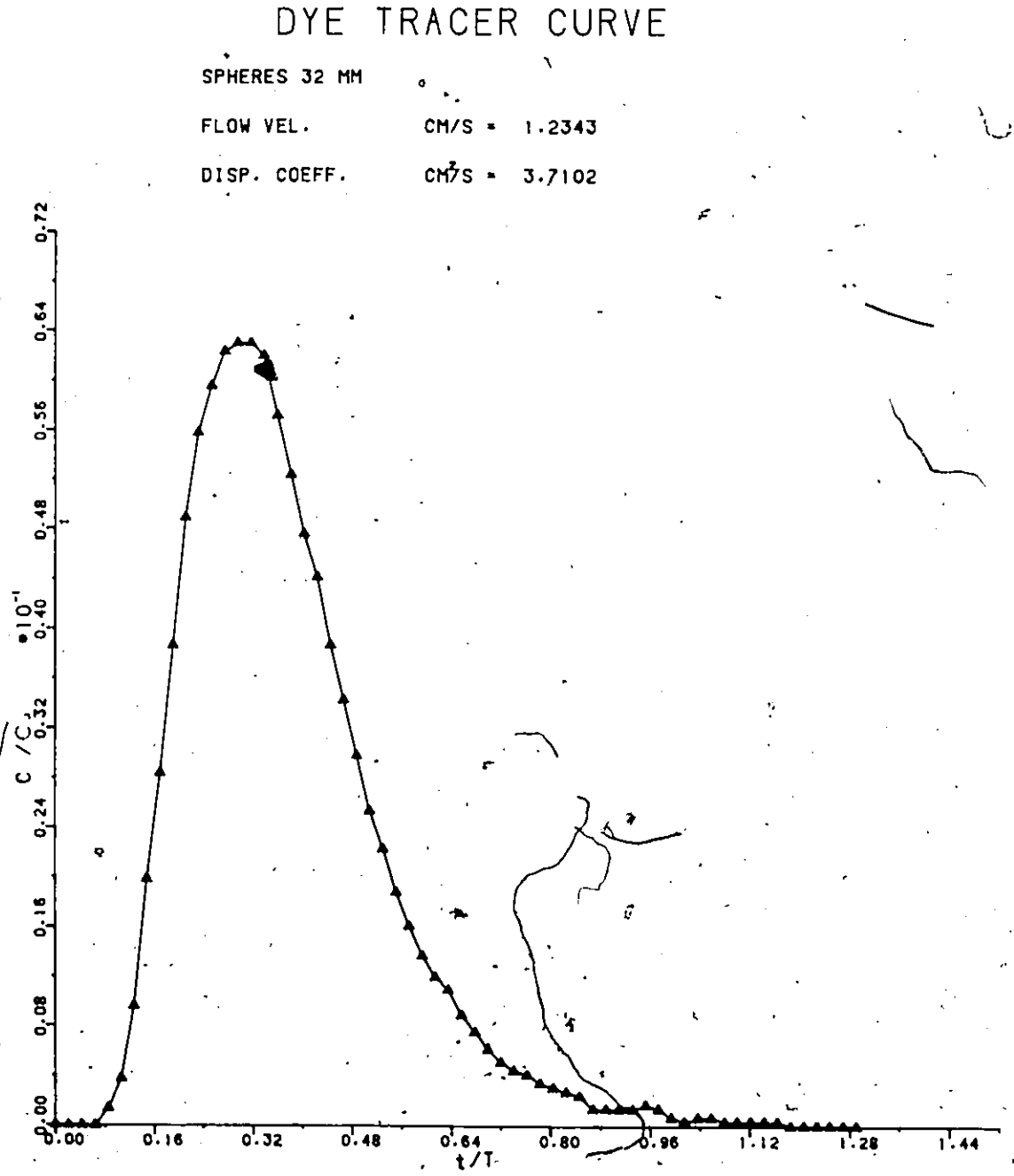

Figure 10: TRACER TEST

Table 6. Dispersion Test Data
media size 32 mm, n = 0.745, k = 0.3617 cm²

Flow x10⁻³ m³/s	Apparent Velocity x10⁻²m/s	Temp. °C	Det. Time s	Dispersion Number	Dispersion Coefficient D, cm²/s	D/ν	R_K
0.030	0.195	24	718	0.0182	0.8974	97.13	12.68
0.067	0.435	24	321	0.0170	1.8724	202.66	28.33
0.100	0.650	23	215	0.0141	2.3145	244.76	41.32
0.130	0.844	22	166	0.0137	2.9276	302.47	52.48
0.162	1.052	22	133	0.0133	3.5425	365.99	65.39
0.190	1.234	22	114	0.0119	3.7102	383.32	76.70

Table 7. Dispersion Test Data
media size 20 mm, n = 0.498, k = 0.0109 cm²

Flow x10⁻³ m³/s	Apparent Velocity x10⁻²m/s	Temp. °C	Det. Time s	Dispersion Number	Dispersion Coefficient D, cm²/s	D/ν	R_K
0.030	0.195	18	480	0.0378	2.7773	260.58	2.51
0.045	0.292	20	321	0.0313	3.4521	342.81	3.99
0.067	0.435	20	215	0.0288	4.5905	455.86	5.76
0.100	0.650	20	144	0.0290	7.1239	707.44	8.87
0.130	0.844	20	111	0.0274	8.7203	865.97	11.52
0.162	1.052	19	89	0.0234	9.1710	910.72	13.74
0.190	1.234	19	76	0.0270	12.5608	1208.12	16.32

Table 8: Dispersion Test Data
media size 14 mm, n = 0.547, k = 0.0087 cm²

Flow x10⁻³ m³/s	Apparent Velocity x10⁻²m/s	Temp. °C	Det. Time s	Dispersion Number	Dispersion Coefficient D, cm²/s	D/ν	R_K
0.031	0.201	16	512	0.0161	1.1148	99.55	1.67
0.045	0.202	16	509	0.0177	1.7749	158.50	2.43
0.065	0.422	16	244	0.0125	1.8099	161.63	3.51
0.100	0.650	16	158	0.0116	2.5843	230.78	5.41
0.130	0.844	16	122	0.0093	2.7104	242.04	7.03
0.160	1.039	16	99	0.0091	3.2660	291.66	8.65
0.190	1.234	16	83	0.0093	3.9375	351.62	10.28

4.2.1 Relationship Between Apparent Velocity and Dispersion Coefficient

Data from Tables 6, 7, and 8 were used to find a correlation between dispersion coefficient and apparent velocity. Figure 11 presents plots of dispersion coefficient *versus* apparent velocity, indicating curvilinear relationships between these two parameters.

Results of regression analysis presented in Table 9 and Figs. 12, 13 and 14 indicate that the value of coefficient b is well below 1.0, which is supposedly the lowest limit, according to Scheidegger (1960).

As expected, these results closely follow Eq. (2.52). An analysis of Table 9 and Fig. 11 indicates that other factors besides shape and medium size influence values of coefficients a and b. The most probable factor is the packing mode of the model, but more experiments are required to arrive at definite reasons for the variations observed in Fig. 11. Gupta (1972) found the value of b to range from 0.9 to 1.16 for grain diameter less than 1.0 mm, and flow velocities below 2.6×10^{-4} m/s.

Similar observations were reported by Greenkorn (1970) when testing grains ranging in size from 44 to 840 μm, and hydraulic loadings ranging from 0.04 to 0.075 cm/s.

Both authors noticed deviations from Scheidegger's theory; however, they did not give an explanation for these occurrences.

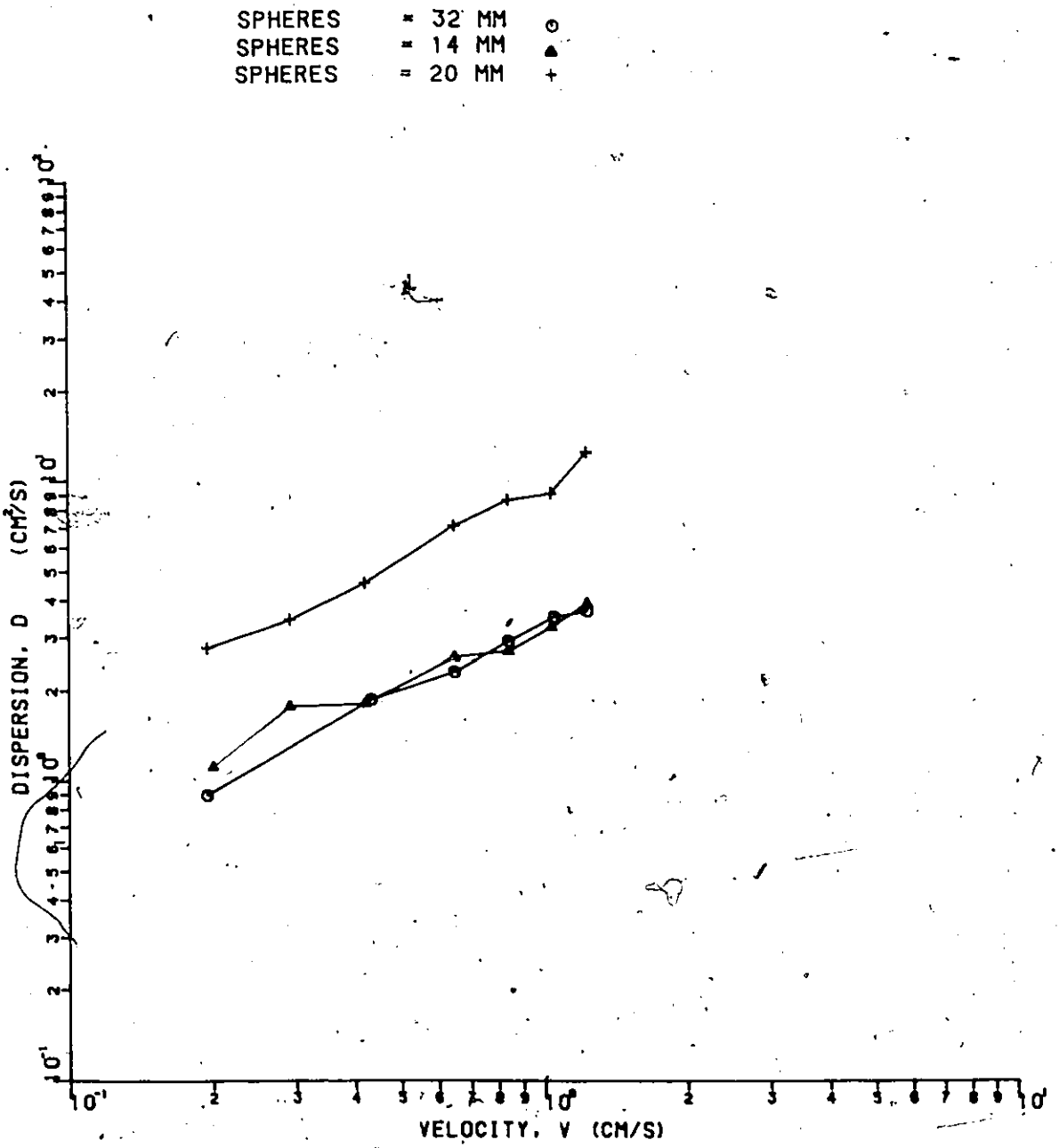

Figure 11: DISPERSION COEFFICIENT – VELOCITY

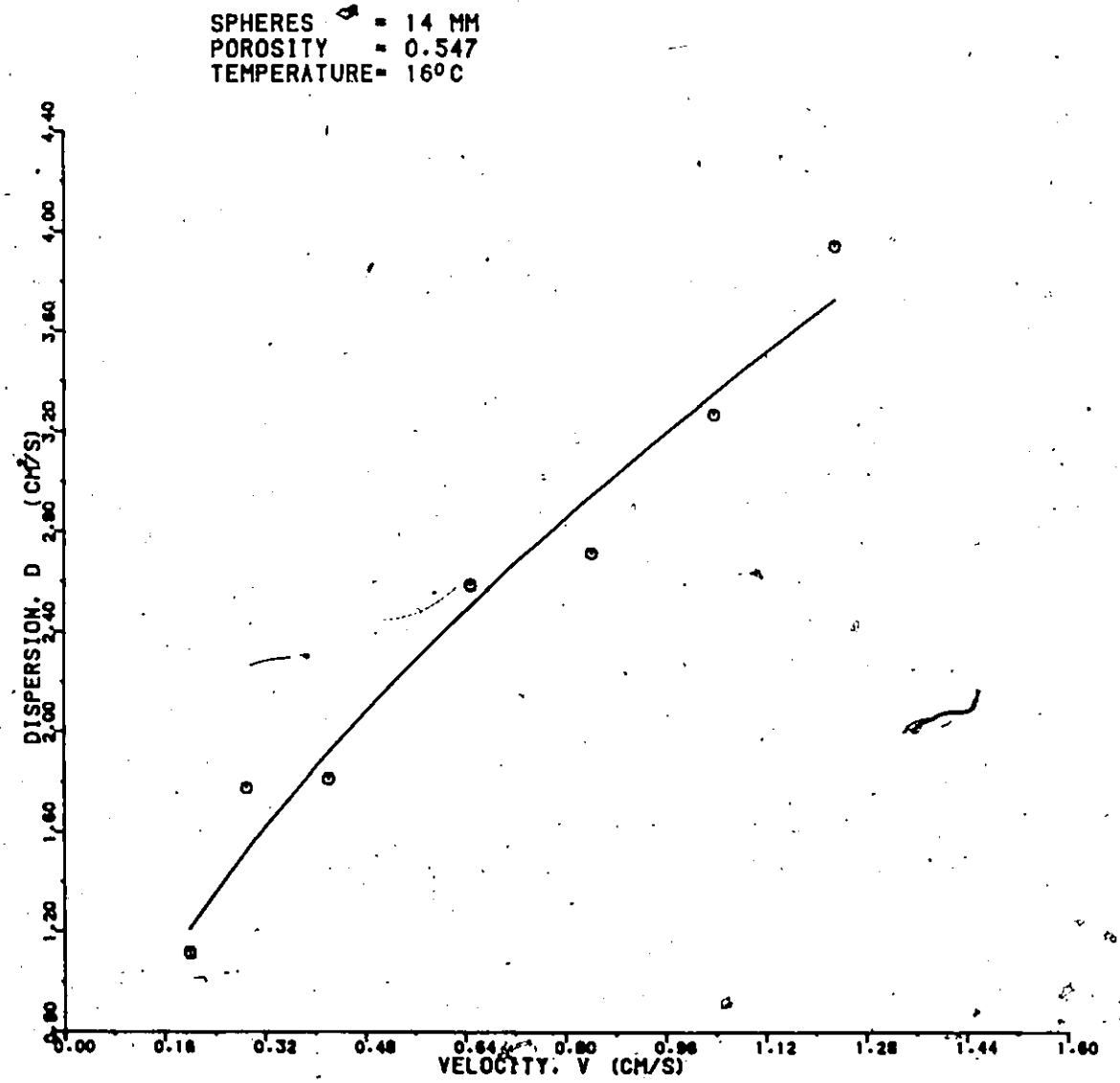

Figure 12: VELOCITY VERSUS DISPERSION COEFFICIENT, 14 MM. SPHERES

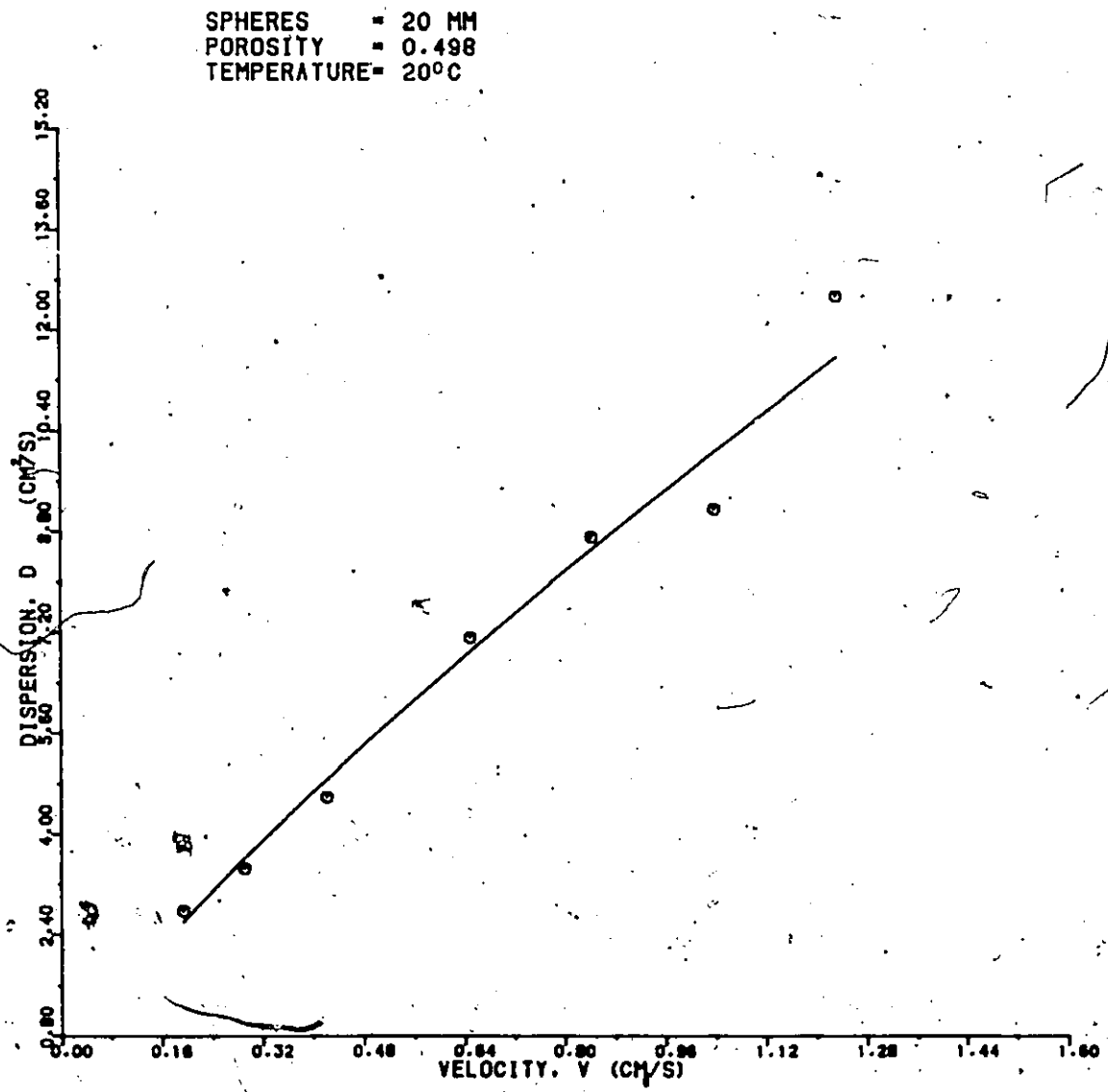

Figure 13: VELOCITY VERSUS DISPERSION COEFFICIENT, 20 MM SPHERES

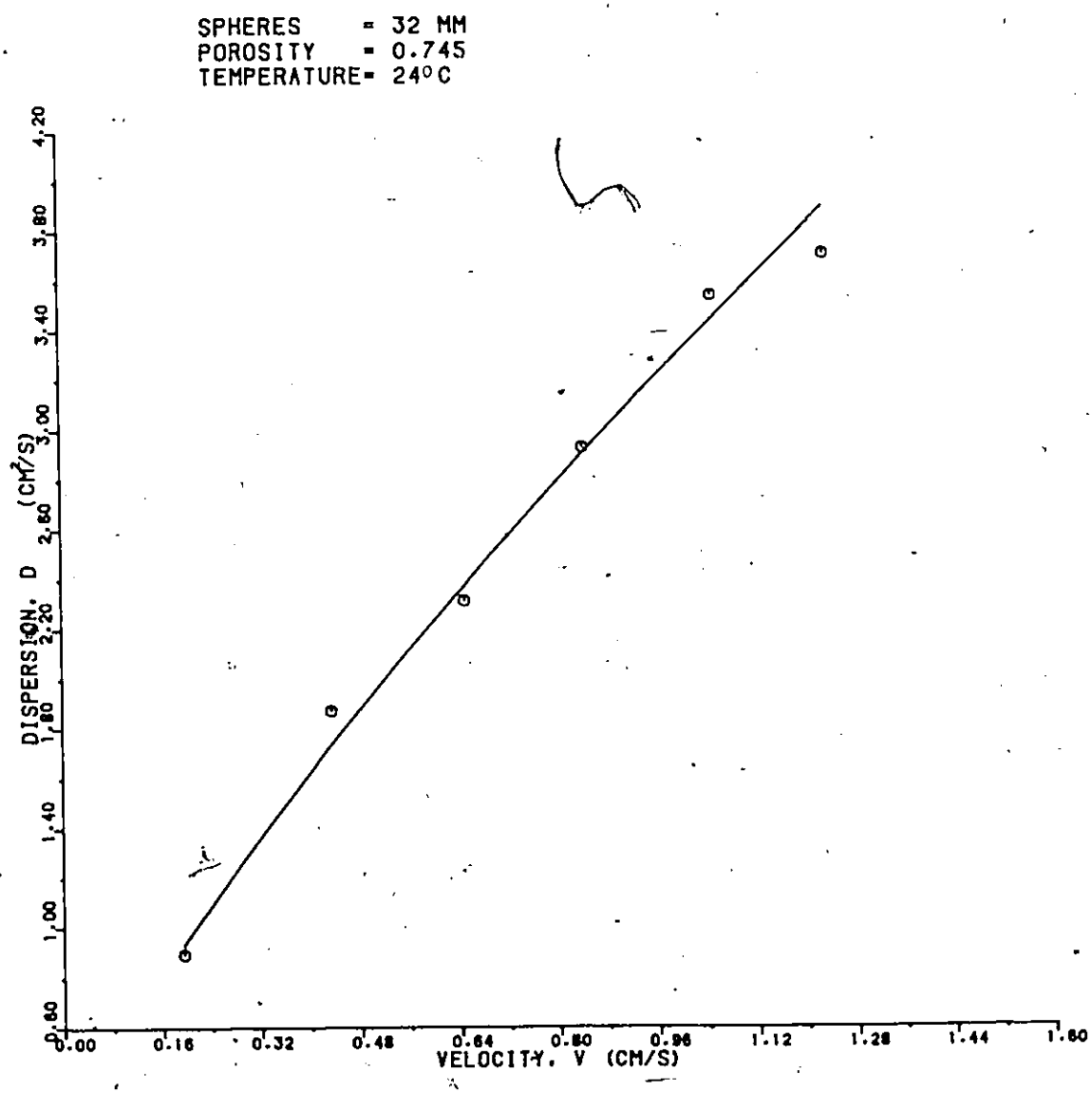

Figure 14: VELOCITY VERSUS DISPERSION COEFFICIENT, 32 MM SPHERES

There is insufficient information to give a definite explanation for this phenomenon; therefore it can only be assumed that the coefficient b is influenced by changing permeability from the significantly larger media sizes used in this study.

Table 9. Velocity and Dispersion Coefficients $D = av^b$

Size of the media	Coefficients a	b	Coefficient of Determination	Correlation	Standard Error
32 mm	3.3113	0.7752	0.9921	0.9961	0.0524
20 mm	9.7730	0.8080	0.9857	0.9928	0.0728
14 mm	3.2668	0.6198	0.9596	0.9796	0.0943

4.2.2 Relationship Between Reynold's Number and Dispersion Coefficient

It was remarked in Chapter II that dispersion properties of the media could be presented as a function of R_K (Eq. 2.54). Calculated values of D/V for various media sizes and over a wide range of velocities are plotted against R_K, in Fig. 15.

Data presented in this figure follows a curvilinear pattern following an exponential function (Eq. 2.54). As in the previous section, insufficient data hampered attempts to develop a universal equation relating dispersion to other media parameters.

Results of regression analysis are tabulated in Table 10 and plotted in Figs. 16-18.

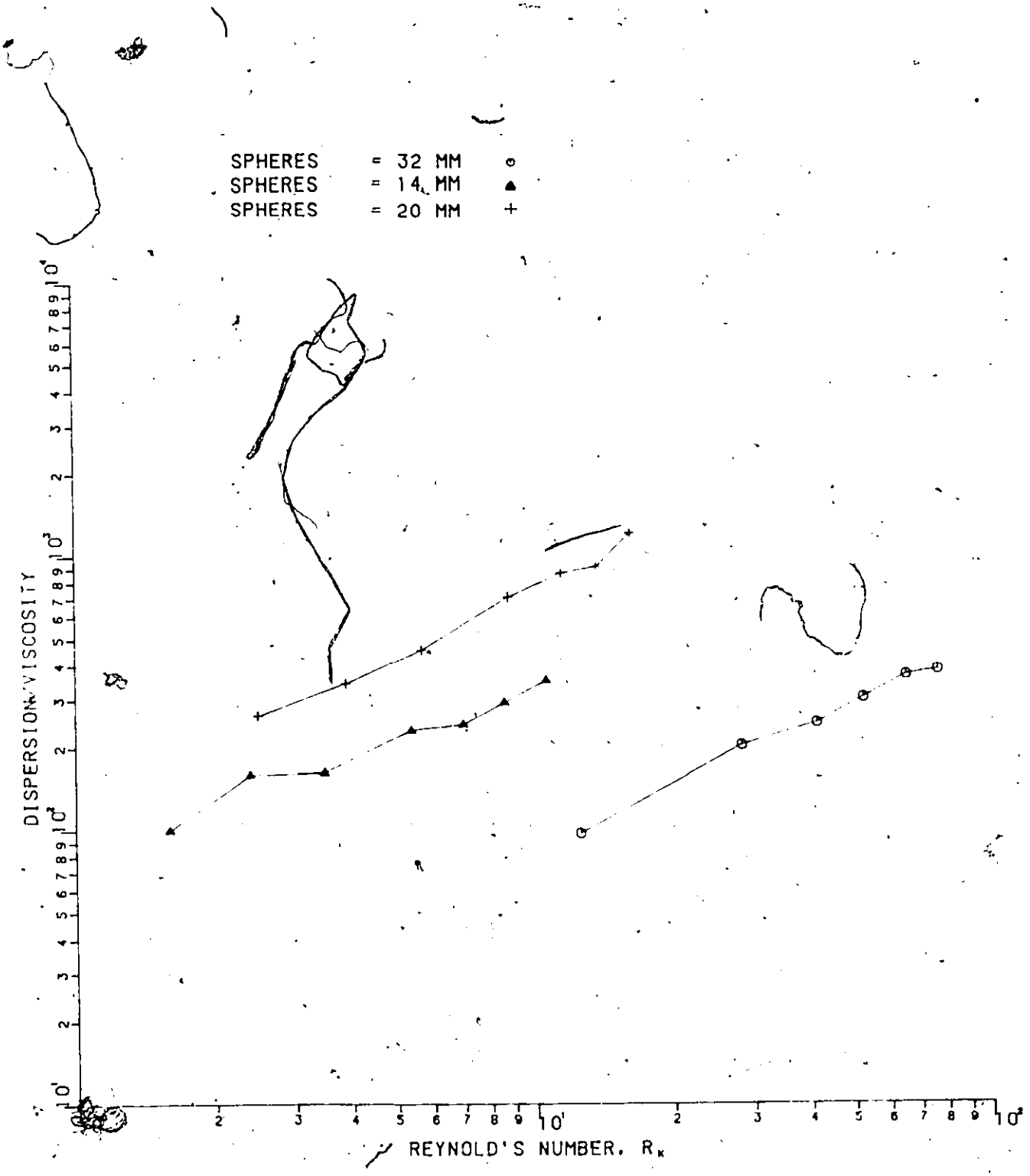

Figure 15: DISPERSION - R_K DATA

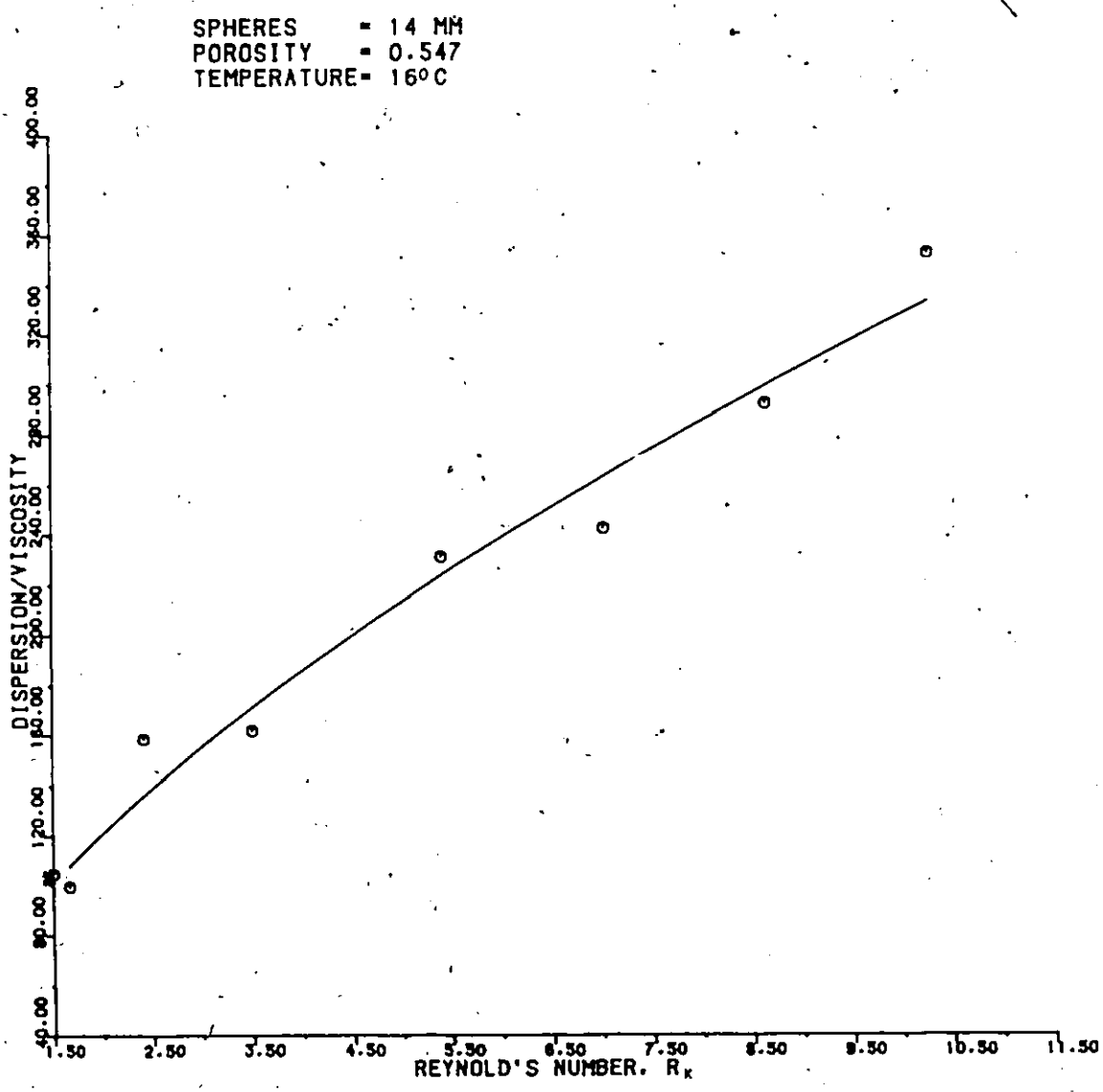

Figure 16: CORRELATION OF EXPERIMENTAL DATA AND GEOMETRIC REGRESSION, 14 MM SPHERES

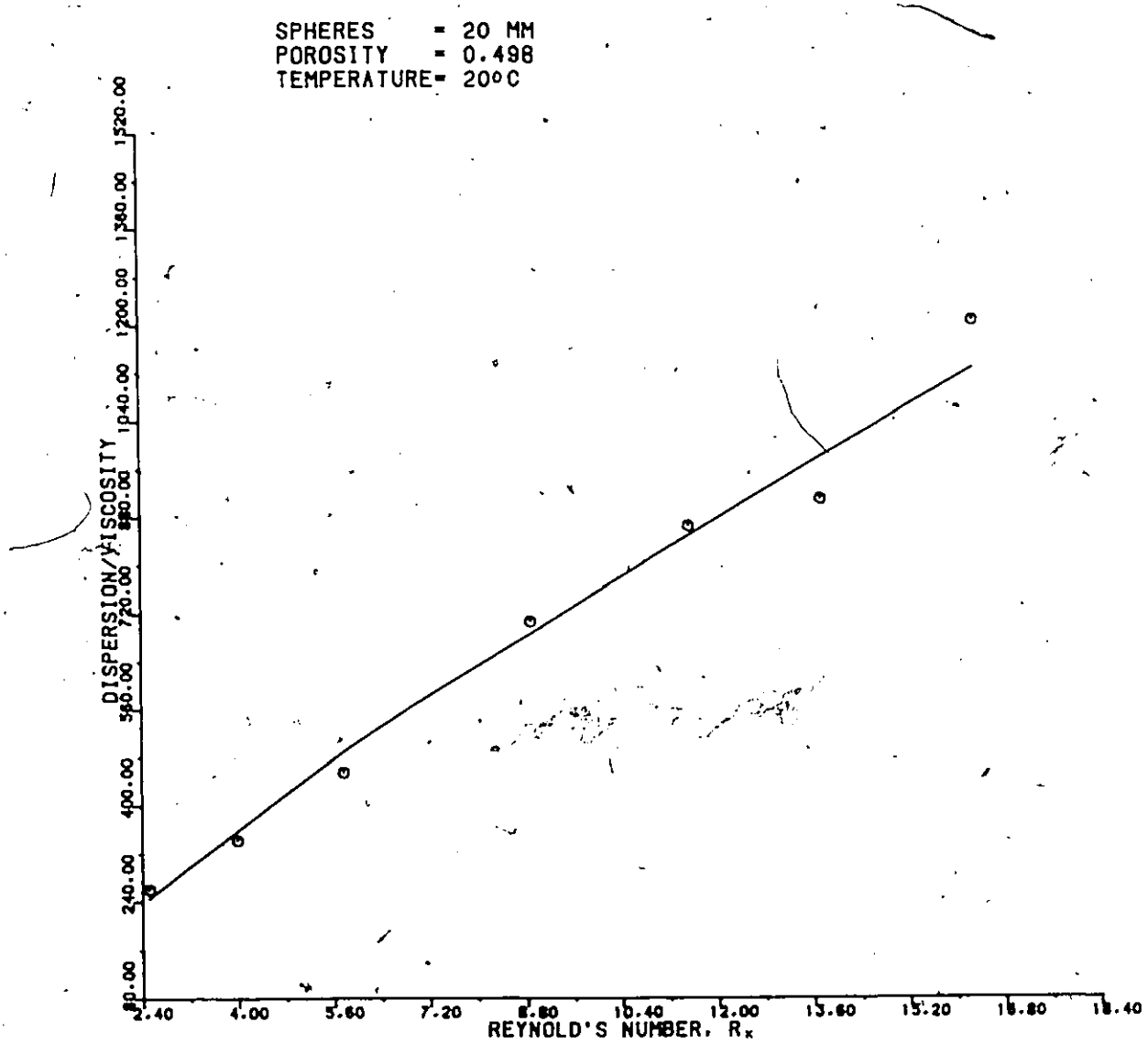

Figure 17: CORRELATION OF EXPERIMENTAL DATA AND GEOMETRIC REGRESSION, 20 MM SPHERES

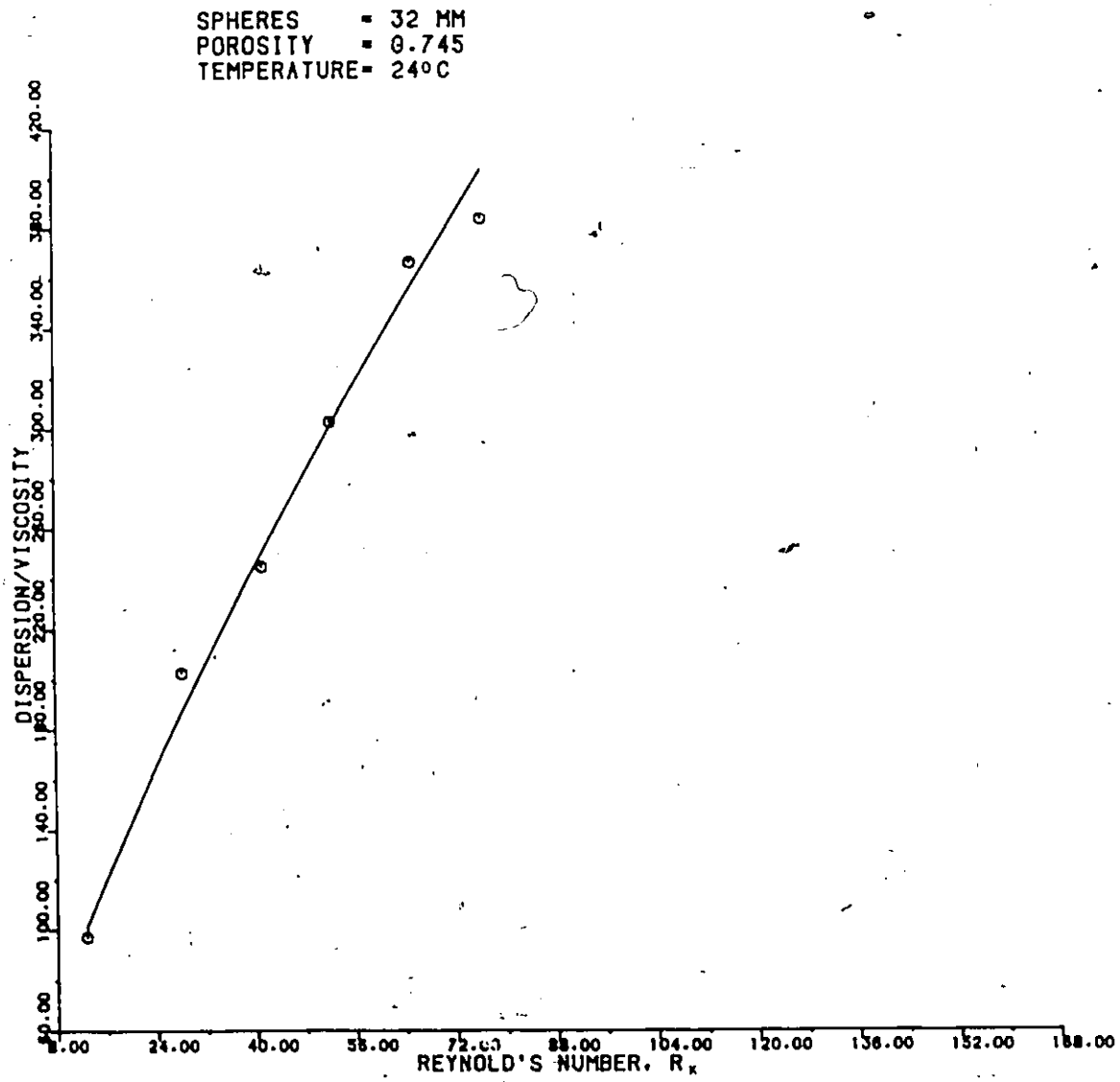

Figure 18: CORRELATION OF EXPERIMENTAL DATA AND GEOMETRIC REGRESSION, 32 MM SPHERES

It is also observed that values of coefficient b^1 (Table 10) are virtually the same as values of b in Table 9. This fact, mentioned by Gupta (1972), is a consequence of using Greenkorn's formula (Eq. 2.52) to develop Eq. (2.54) and the method he used to calculate k.

Table 10. Reynold's Number and Dispersion For $D/\nu = a' R_*^{b'}$

Size of the Media (mm)	Coefficients a'	Coefficients b'	Coefficients Determination	Correlation	Standard Error
32	14.35	0.77	0.9911	0.9955	0.0534
20	116.09	0.81	0.9894	0.9946	0.0636
14	78.53	0.62	0.9597	0.9796	0.0941

4.3 Turbidity Removal Data

Data in Fig. 19 demonstrate the normalized change in concentration obtained from port No. 6 (at the top of the bed) for three different filtration rates. Time 0.00 hr in these figures corresponds to the moment when uniform flow conditions were established and coagulant was introduced. The first samples were taken 30 min later when steady conditions had been established. The number of data points presented in this and other figures was limited for the purpose of clarity.

Data from three representative hydraulic loadings were chosen to demonstrate media performance under various conditions. Selected Flow rates represent upper, middle and lower ranges tested in this investigation.

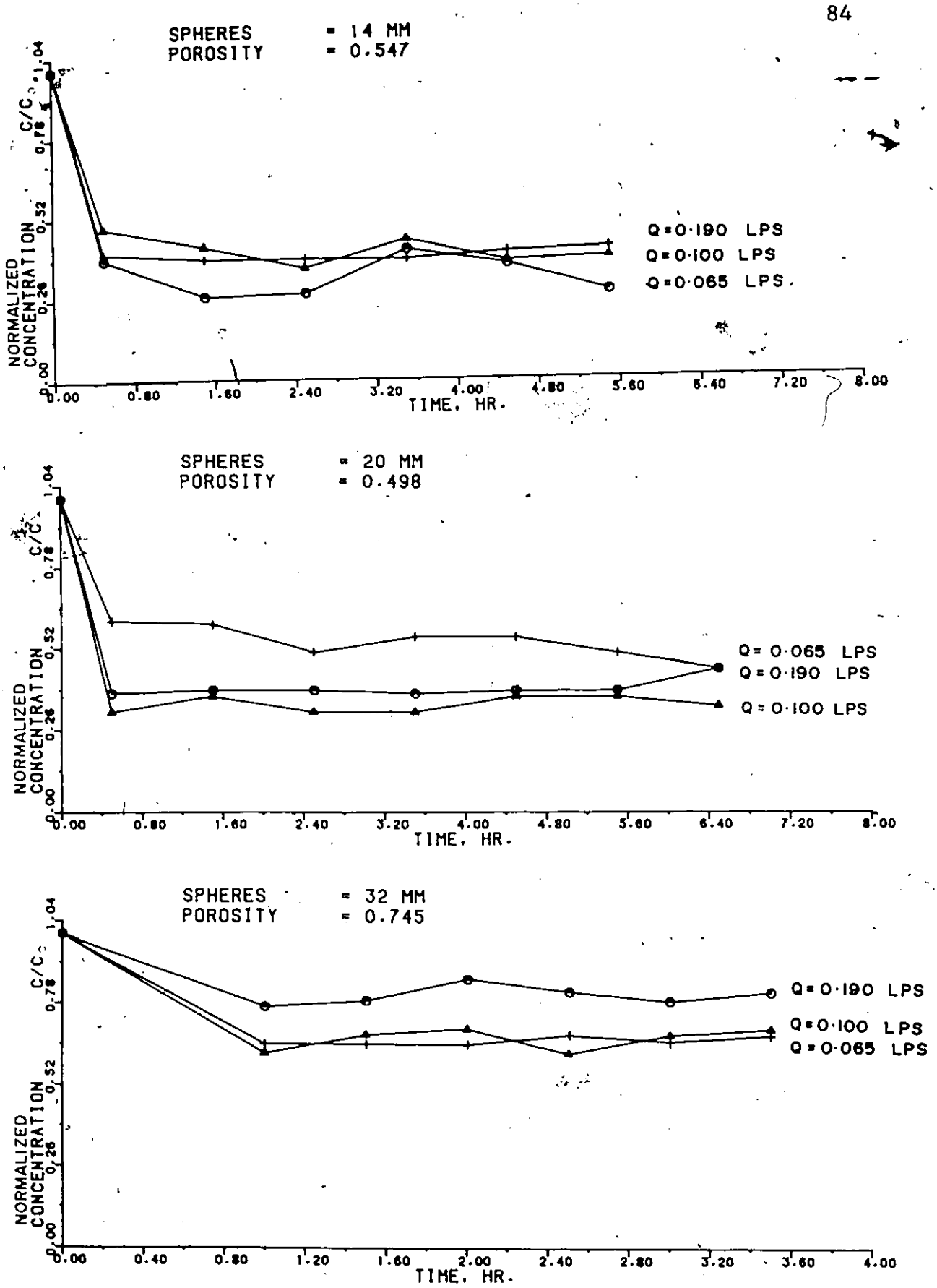

Figure 19: TURBIDITY REMOVED VERSUS TIME

Additional data presented in Appendix B followed the same pattern indicated by the representative curves. All turbidity measurements used in this chapter were made after a 1 hour settling period. A few tests were made on the removal of kaolin without coagulant addition: it was found that after 20 hrs only a maximum of 10% of the kaolin was settled (Table B.5, Appendix B).

Based on the shape of these curves it can be seen that normalized concentration (ratio of measured turbidity to turbidity of influent) does not vary significantly for a given medium size and flow rate with respect to time, and can therefore be averaged. The virtually constant flocculation efficiency can be attributed to a declining flow regime, allowing the flocculator to respond to progressive clogging.

The effect of time on the normalized change in concentration at a given depth of the bed can be evaluated from the series of curves presented in Figs. 20-22. These figures were developed using the same initial flow rate and data points corresponding to the normalized concentration at three sampling levels. Careful analysis of these figures shows that after an initial period (approximately 60 min), all three sampling points produce an effluent of basically constant quality. Periodic oscillations of normalized concentration in lower parts of the bed are probably caused by redispersion of deposit during sampling.

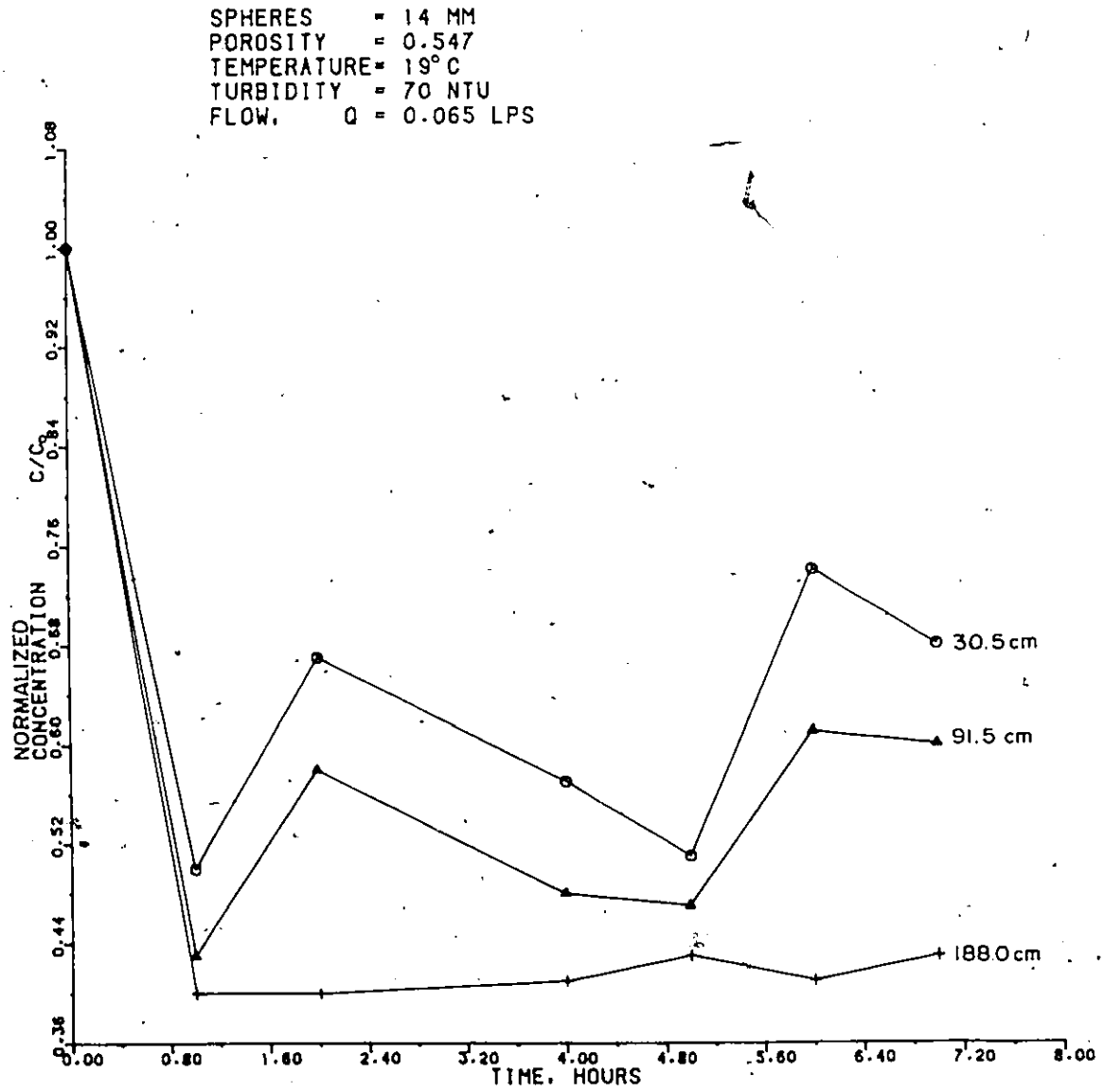

Figure 20: EFFECT OF TIME AND BED DEPTH ON ON FLOCCULATION EFFICIENCY, 14 MM SPHERES

SPHERES = 20 MM
POROSITY = 0.498
TEMP. = 17°C
CONC., C_o = 72 NTU
Q-FLOW = 0.065 LPS

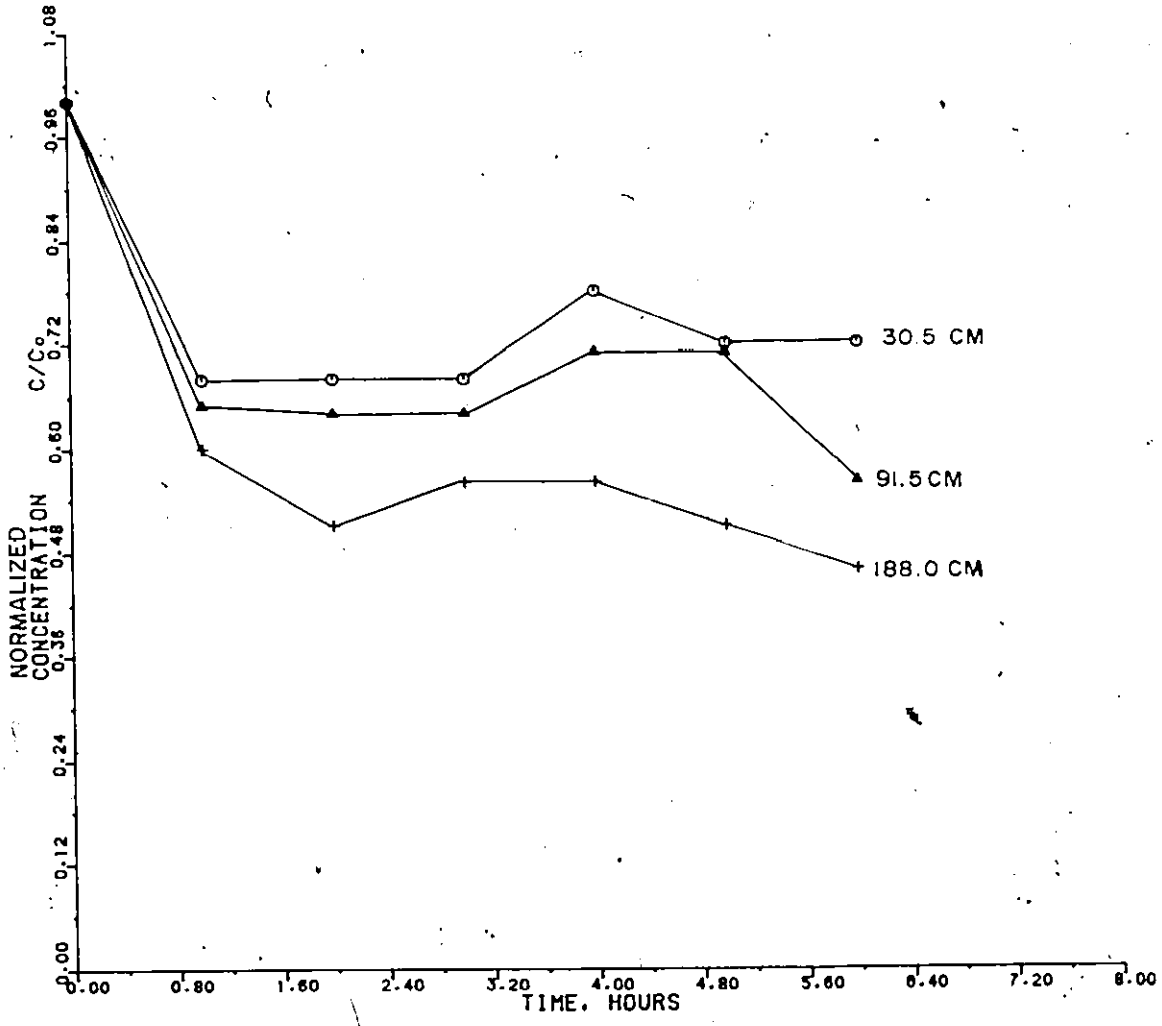

Figure 21: EFFECT OF TIME AND BED DEPTHS ON FLOCCULATION EFFICIENCY, 20 MM SPHERES

SPHERES = 32 MM
POROSITY = 0.745
TEMP. = 21° C
CONC., C_o = 66 NTU
Q-FLOW = 0.065 LPS

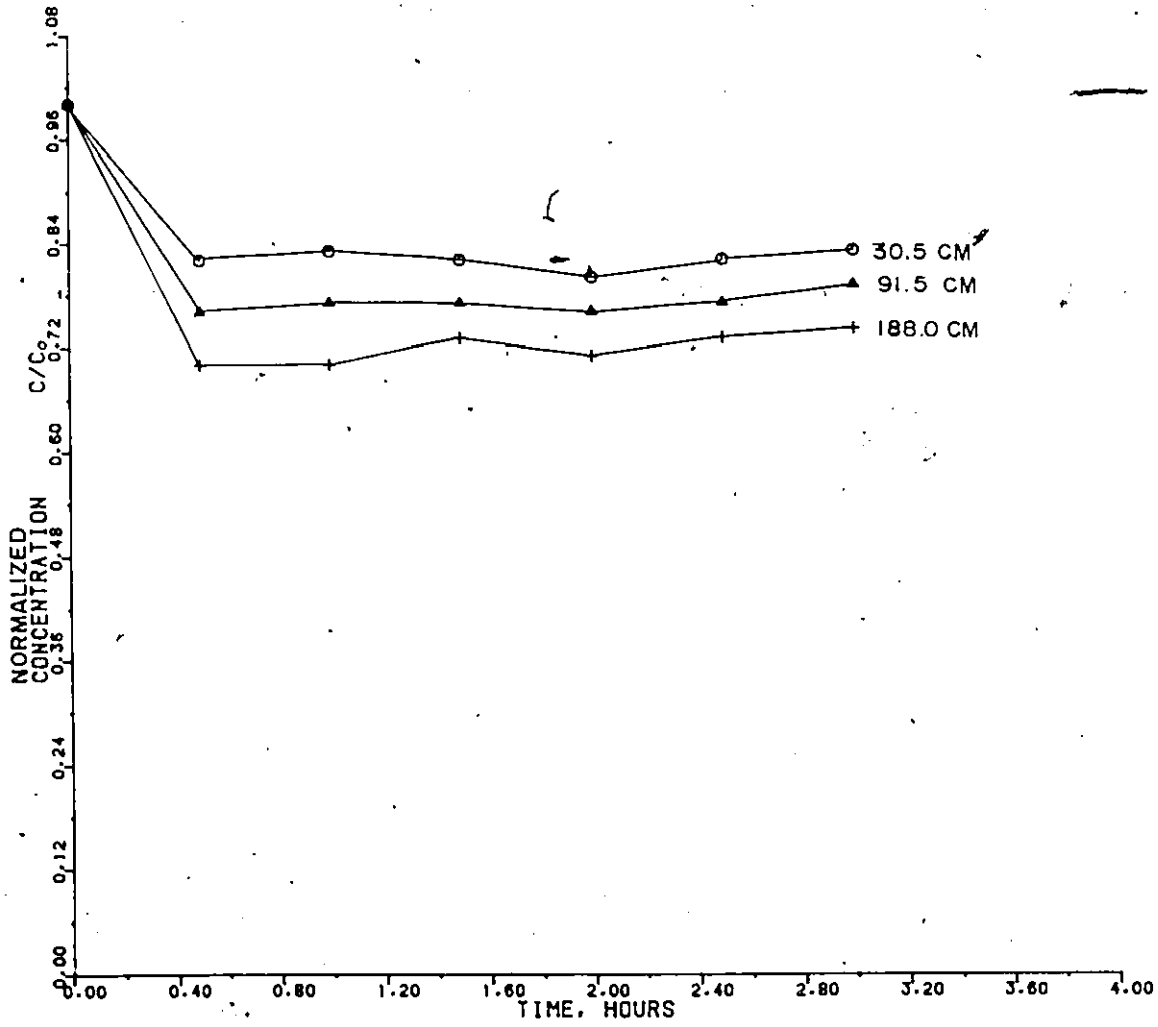

Figure 22: EFFECT OF TIME AND BED DEPTH ON FLOCCULATION EFFICIENCY, 32 MM SPHERES

Also, for each medium, samples were taken from the bottom of the column after coagulant had been introduced and from the top of the medium to determine if there was a significant change in turbidity due to removal in the column. Turbidity was measured without the usual settling period. It was found that the difference between raw water turbidity (70-71 NTU) and turbidity of the sample was less than 2 NTU.

These effects are greater in a medium consisting of spheres of smaller sizes, since interstitial velocities are greater and there are more particle retention sites available. As indicated by the curves, the flocculation process is developed mainly in a relatively thin layer of the bed. This phenomenon, also observed by Kradile (1983), greatly influences the design of pebble flocculators, minimizing required media depth.

4.3.1 Effect of Flow Rate on Flocculation Efficiency

Chapter II has stressed the importance of the relationship between media and initial flow velocity. The effect of flow rate on removal efficiency was investigated by controlling all of the process variables except the flow rate.

Data resulting from these experiments for three different sizes of spheres and three different flow rates are presented in Fig. 23. The curves presented in Fig. 23 consist of the normalized changes in concentration achieved with depth for three different initial filtration rates, for a given media size.

The declining flow regime utilized in this study resulted in a change of the flow rate as clogging developed. Consequently the initial filtration rate was used to classify the flow range and not to represent flow conditions during the whole run. Velocity change during a run is discussed in Section 4.3.3.

Data reported in these figures are averaged, since it was found that the normalized concentration did not change significantly during the testing period (Figs. 19-22).

Analysis of Fig. 23 reveals a noticeable effect of flow velocity on flocculation efficiency in the smaller medium. However, change in velocity does not consistently affect flocculator efficiency. Therefore flow velocity is not the main parameter governing the process.

4.3.2 Effect of Size of Media Particles on Flocculation Efficiency

Data from Fig. 23 were replotted as shown in Fig. 24 to illustrate the effect of media grain size on flocculation efficiency.

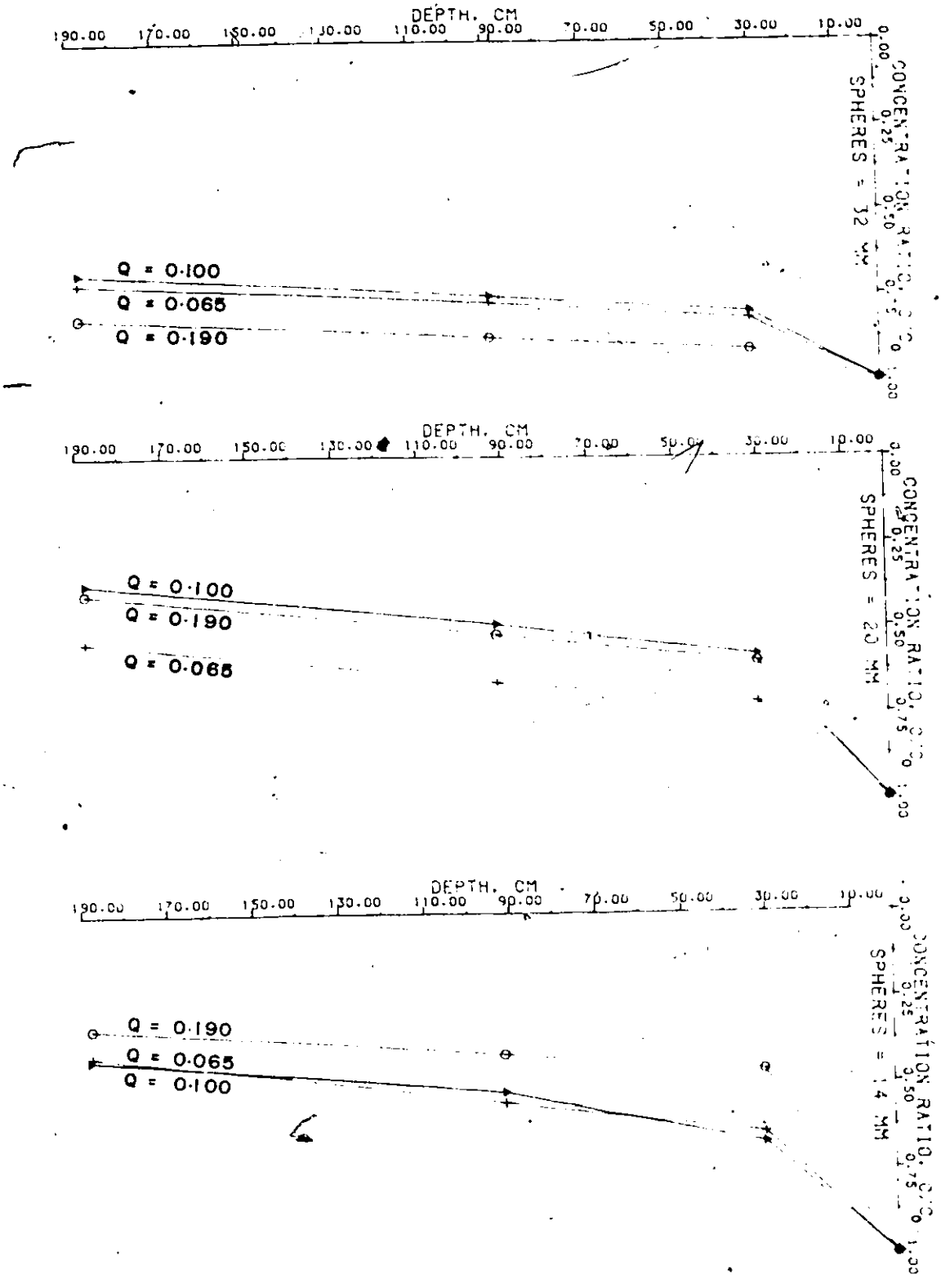

Figure 23: EFFECT OF FLOW RATE ON FLOCCULATION EFFICIENCY

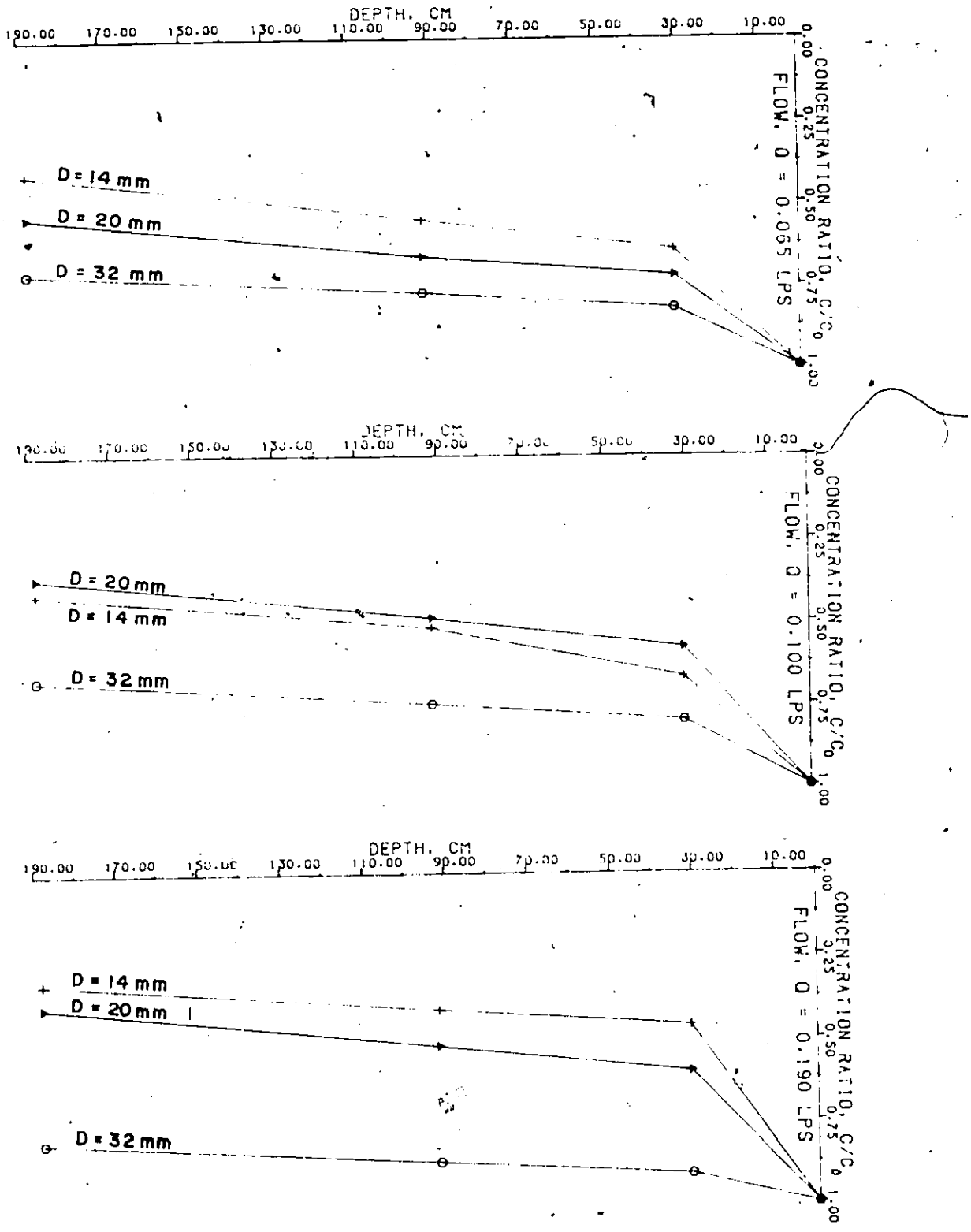

Figure 24: EFFECT OF MEDIA SIZE ON FLOCCULATION EFFICIENCY

Comparing Figs. 23 and 24, it is evident that media size has a greater effect on flocculation efficiency than does the flow rate. The effects are more visible from curves representing efficiency in higher hydraulic loadings and indicate superior performance of smaller media. Analysis of Fig. 24 confirmed earlier observations regarding the occurrence of most of the removal in a relatively small bottom layer of the media.

4.3.3 Flow Rate and Headloss Development Versus Time

Typical data on the change of normalized flow rate (the ratio of measured to initial flow rate) are presented in Figs. 25-27 and Table 11. The curves indicate increasingly pronounced effects of clogging on flow rate with decreasing size of the media. The distribution of points indicates that after the initial period of rapid decrease in flow rate, changes become less dramatic.

This phenomenon may be attributed to changes in the way particles are deposited in the porous media. At first flocs fill up all available dead spaces and begin to constrict flow channels within a bed. This results in a decrease of porosity, an increase of interstitial velocity, and an increase of headloss (Figs. 28-30). If the bed were operated in a constant flow rate regime, the interstitial velocities would soon reach the critical velocity and the scouring process would begin.

Table 11. Normalized Output Rate Variation With Time

Initial Flow Rate, Lps	Time, hours			
	2	3	4	End of Run
media size 14 mm				
0.193	0.95	0.98	0.99	1.00
0.165	0.97	0.96	0.96	0.95
0.135	0.98	0.93	0.90	0.83
0.103	0.96	0.95	0.95	0.94
0.067	0.76	0.75	0.73	0.45
0.029	0.90	0.86	0.83	0.72
media size 20 mm				
0.197	0.98	0.98	0.98	0.96
0.165	0.98	0.97	0.97	0.95
0.137	0.87	0.87	0.86	0.85
0.104	0.98	0.98	0.98	0.99
0.066	0.91	0.89	0.88	0.88
0.030	0.90	0.90	0.87	0.83
media size 32 mm				
0.191	0.99	0.99	–	0.99
0.172	1.00	–	–	1.00
0.138	0.79	–	–	0.79
0.098	0.98	0.97	–	0.97
0.065	0.97	0.92	–	0.92
0.032	0.97	0.97	0.94	0.94

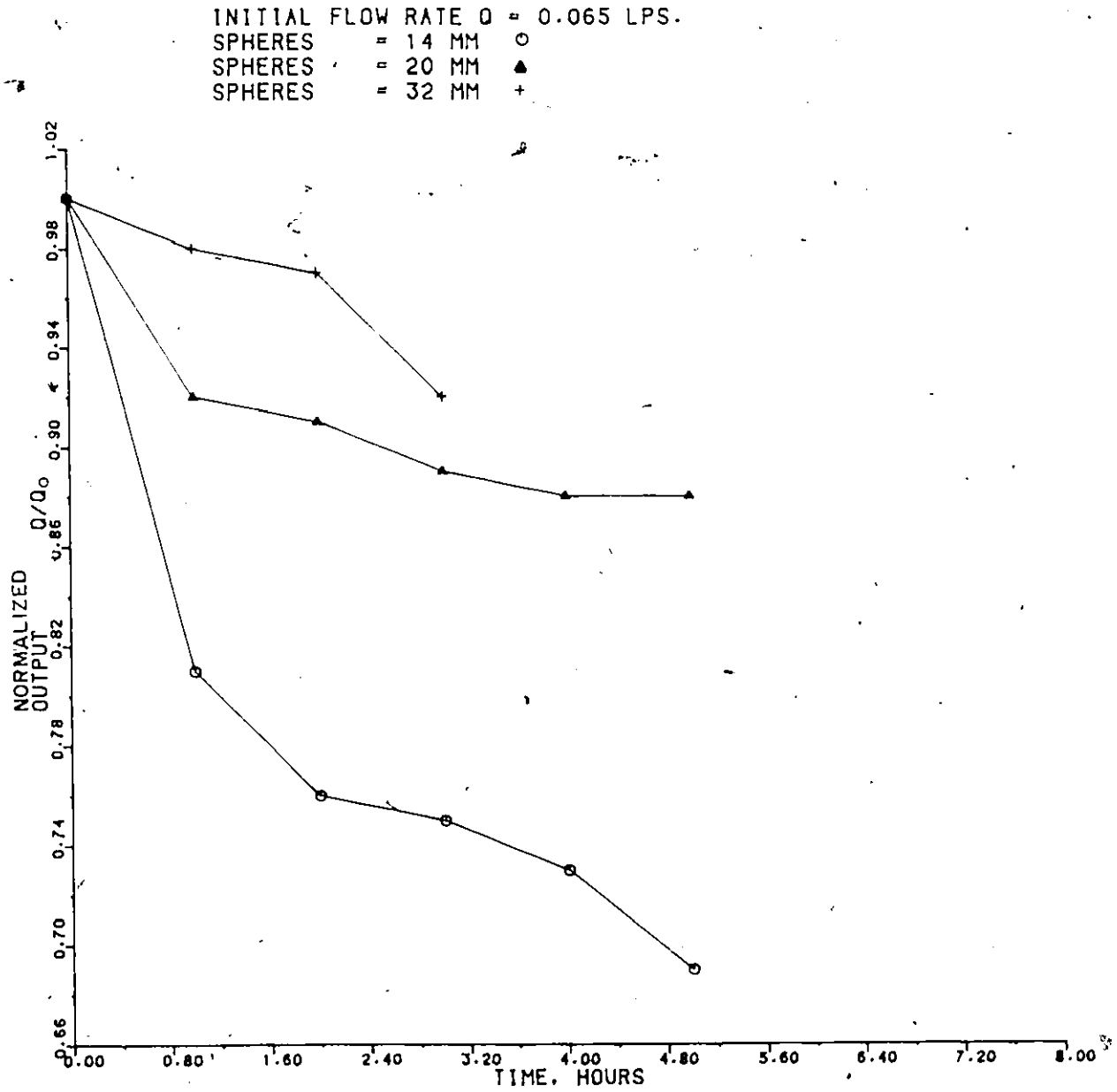

Figure 25: NORMALIZED OUTPUT RATE VERSUS RUN TIME, 0.065 Lps INITIAL FLOW RATE

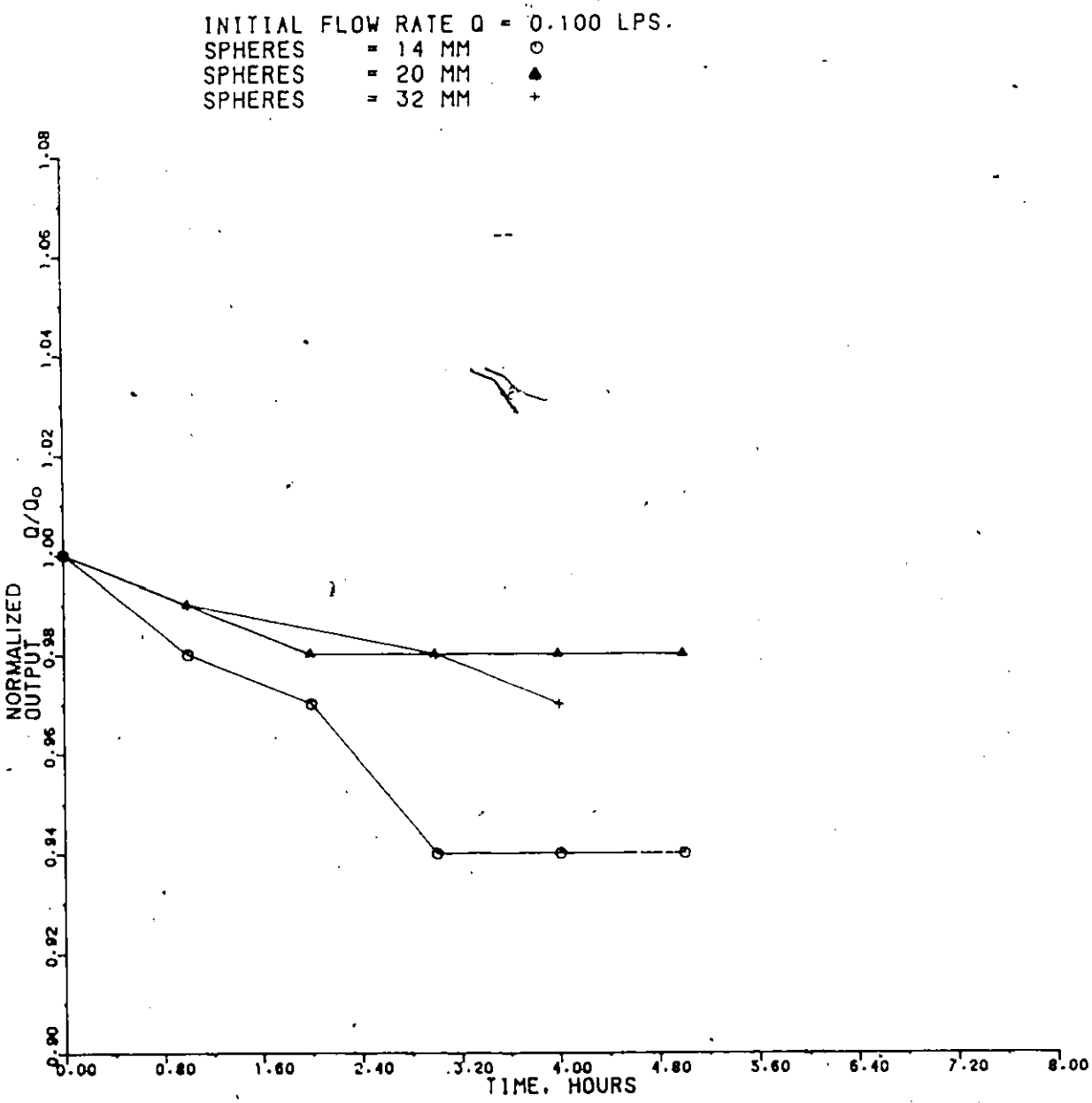

Figure 26: NORMALIZED OUTPUT RATE VERSUS RUN TIME, 0.100 Lps INITIAL FLOW RATE

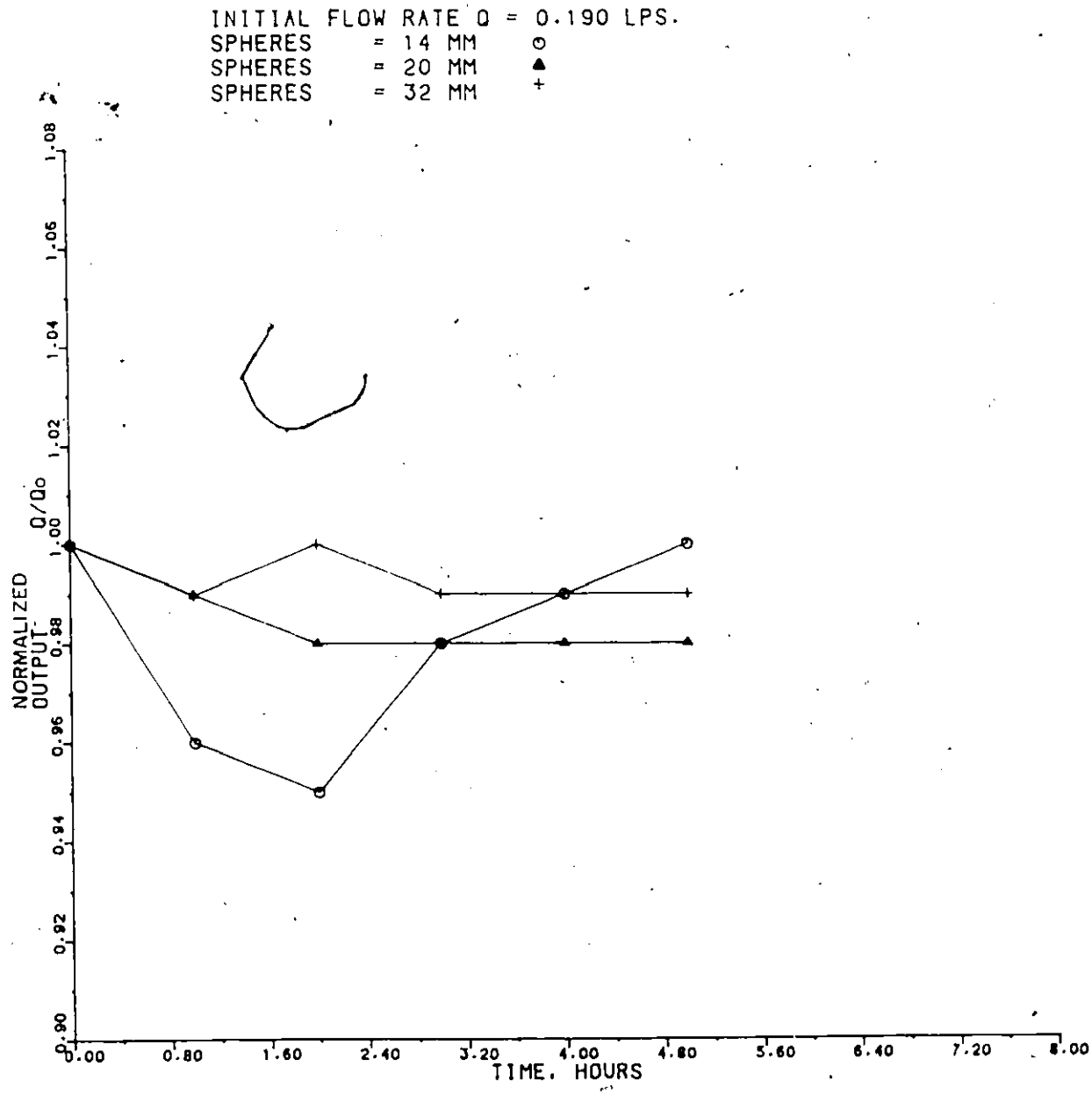

Figure 27: NORMALIZED OUTPUT RATE VERSUS RUN TIME, 0.19 Lps INITIAL FLOW RATE

Any further deposition would only be possible with compaction of deposited particles within a bed. In the declining flow regime used in this experiment, the increase of interstitial velocity and headloss is smaller. The system responds to the clogging process by decreasing flow rate, and minimizing scour of deposited material. However, floc strength is limited and declining interstitial velocity becomes critical and scour begins.

An analysis of Figs. 28-30 and Table 11 indicates that clogging strongly influences flow in 14 and 20 mm media; its effects are less visible for 32 mm medium. In addition, the influence of clogging on normalized flow rate seems to be less profound when initial flow rate decreases.

Comparing Figs. 25 and 27 for 14 mm medium and for flow rates higher than 0.1 Lps, it is observed that solids deposition affected headloss more than the flow rate.

The nearly linear relationship observed in Figs. 28-30 indicates simultaneous changes in flow rate, which is characteristic of beds working under declining flow regimes. The shape of these curves indicates that material which is retained in void spaces restricts flow channels, giving rise to headloss which results in decreased flow rate. An interesting observation can be made by comparing Figs. 28-30 with Figs. 25-27: headloss is increasing steadily even though change in flow rate becomes less dramatic.

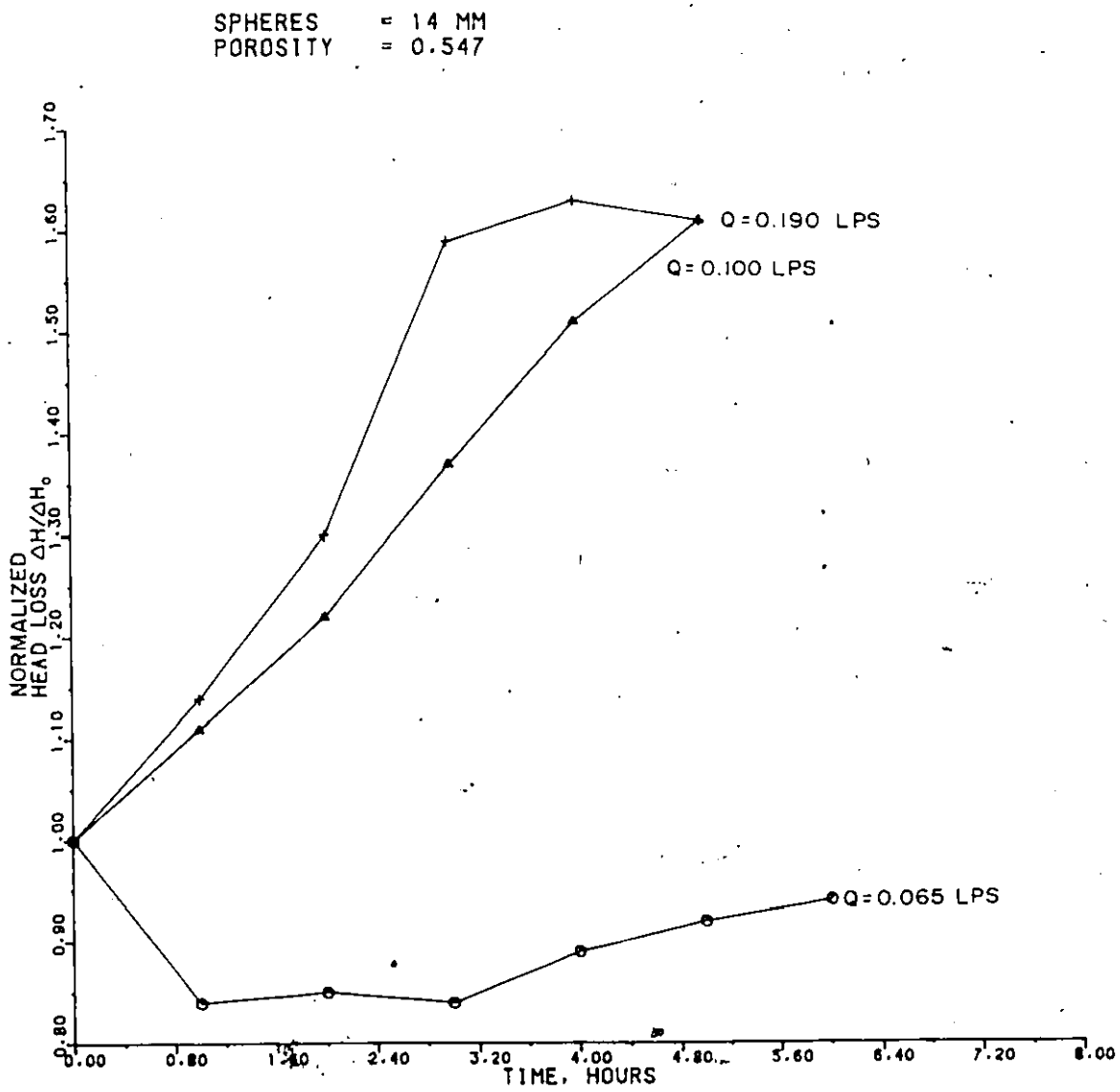

Figure 28: NORMALIZED HEADLOSS VERSUS RUN TIME, 14 MM SPHERES

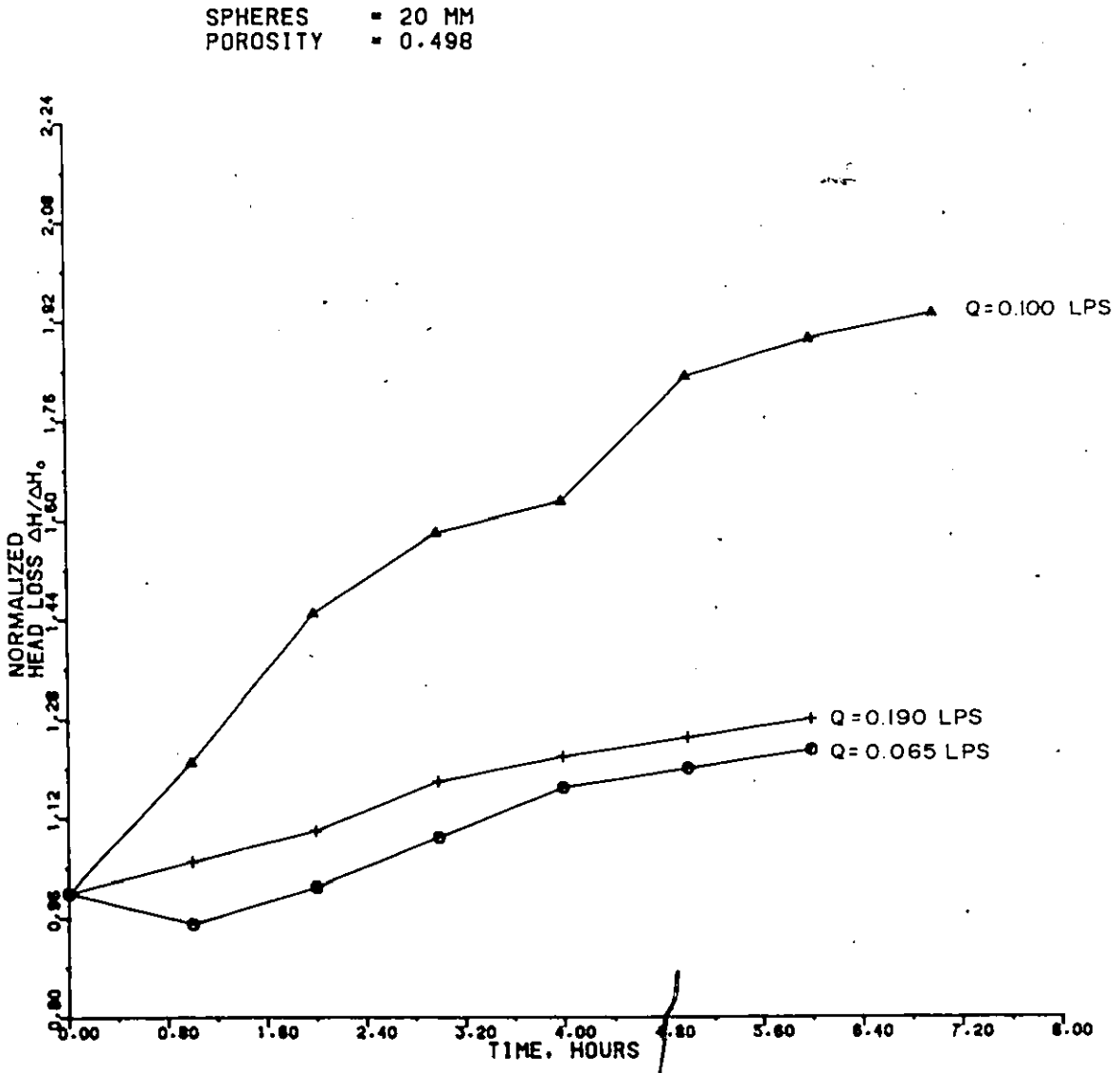

Figure 29: NORMALIZED HEADLOSS VERSUS RUN TIME, 20 MM SPHERES

SPHERES = 32 MM
POROSITY = 0.745
TEMP. = 22°C

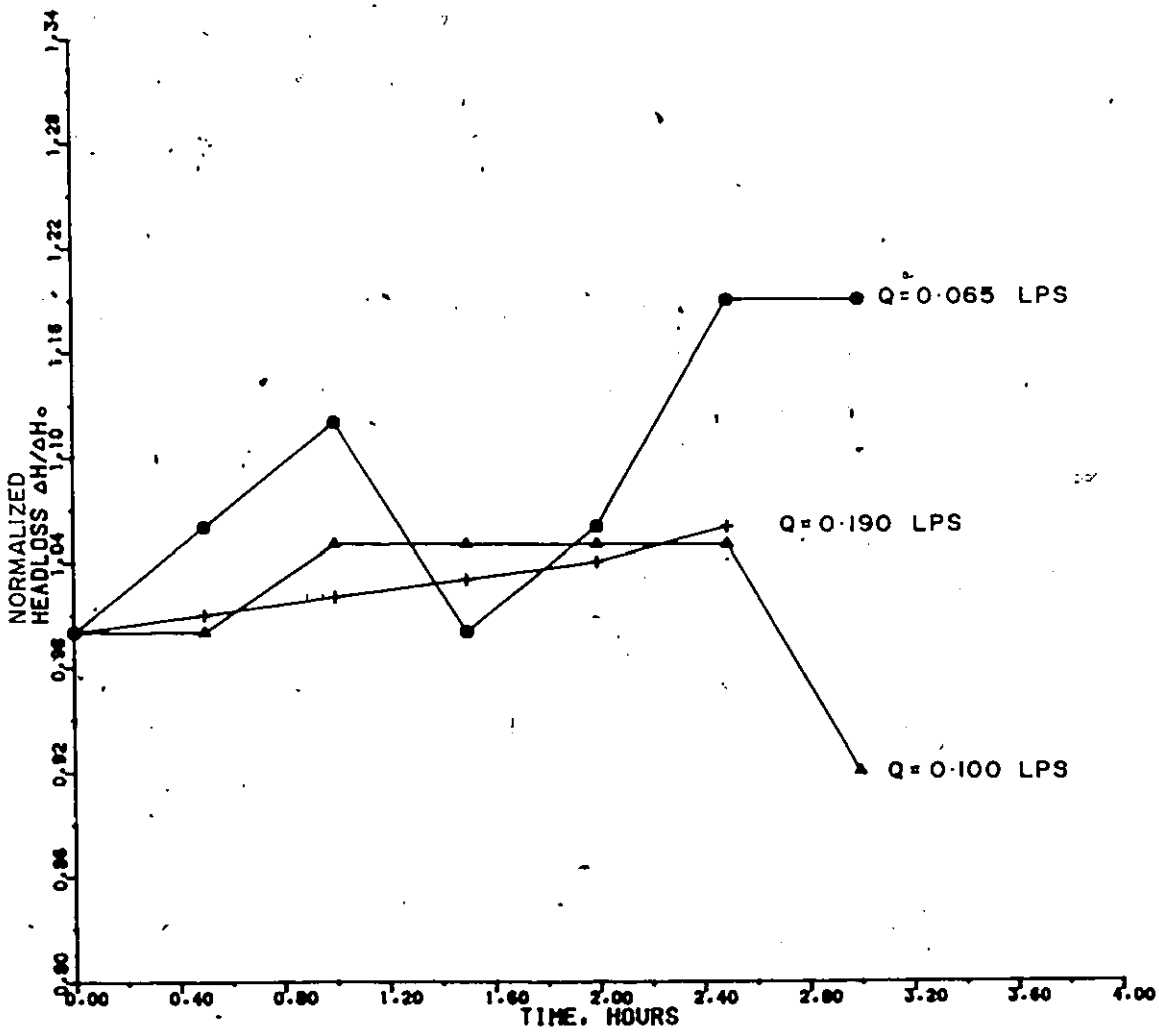

Figure 30: NORMALIZED HEADLOSS VERSUS RUN TIME, 32 MM SPHERES

This phenomenon indicates that the compaction process produces a significant increase in headloss. The normalized headloss of clear water passing through the filter is represented by the intercept on the ordinate. The decrease in headloss for 0.065 Lps in Fig. 28 can be attributed to a reading error. This assumption is confirmed by the distribution of other points indicating steady increase of normalized headloss.

4.3.4 Effect of Coagulant Feed Loss on Flocculator Performance

The effect of coagulant deficiency on flocculator performance was investigated using a flow rate of 0.03 Lps and medium size spheres. The chosen flow rate provided ample information and facilitated sample collection. The response of the bed working under high flow rates would not have allowed the collection of an adequate number of meaningful samples.

The data in Fig. 31 represent changes in normalized concentration measured at the bottom and middle sections of the bed. The effect of a coagulant deficiency can be noted by the sharp increase of turbidity measured in a settled sample. The time difference between loss of coagulant feed and turbidity increase is equal to the time required for a slug of the solution to flow through the system.

Short periods of coagulant deficiency does not completely shut off flocculation abilities of the bed, after an initial breaking in period is completed.

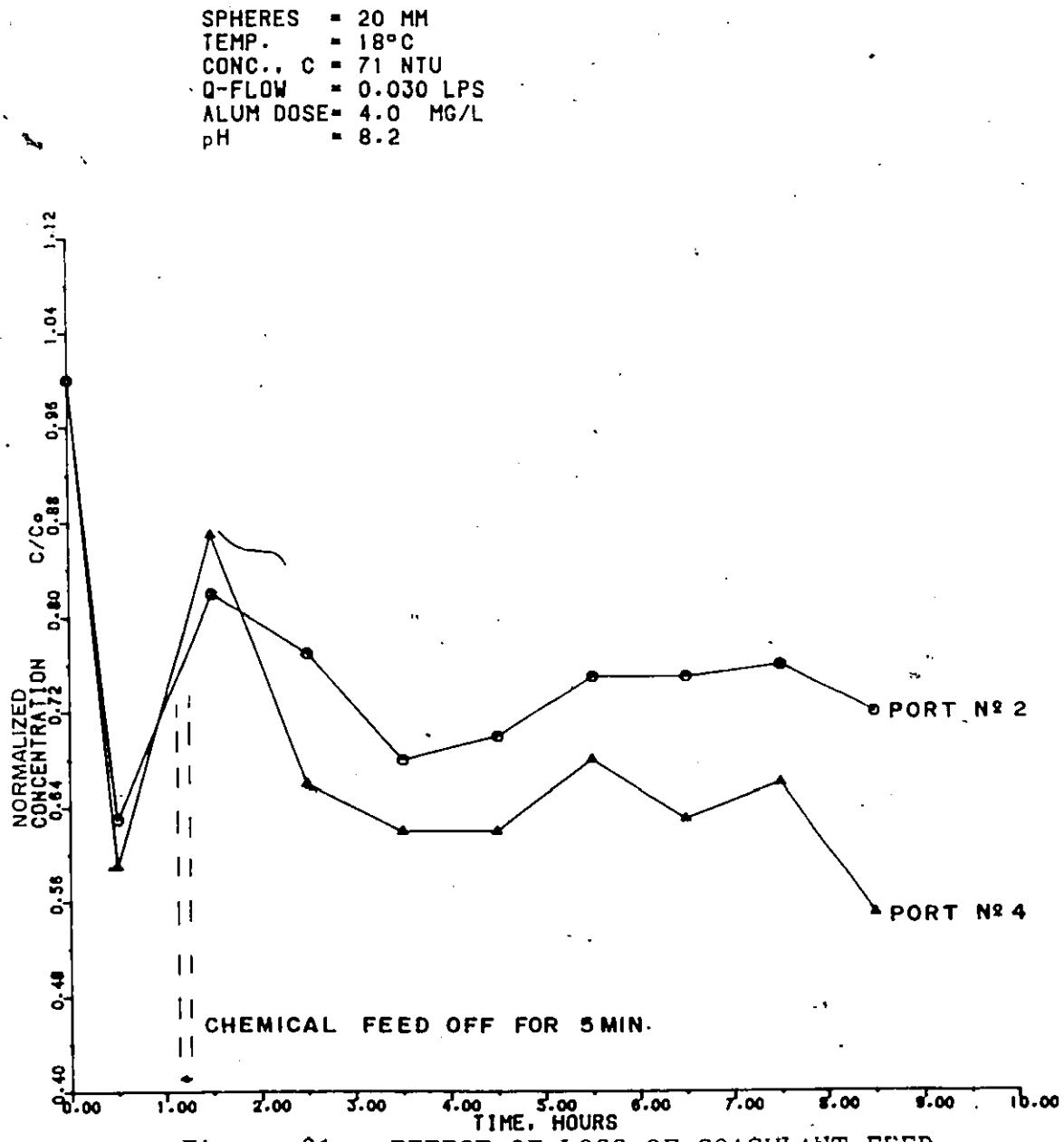

Figure 31: EFFECT OF LOSS OF COAGULANT FEED ON FLOCCULATOR PERFORMANCE

The effect of loss of coagulant feed on pH is shown in Fig. 32. As indicated by the curve, the loss of coagulant results in an increase of pH. When initial conditions are restored, pH returns to its previous level. The general shape of the pH curve (Fig. 32) also demonstrates the PF nature of the system.

The intercept on the ordinate represents pH of the suspension before coagulant is introduced. These observations introduce the possibility of using pH value to monitor coagulant dosage during the flocculation process.

4.3.5 Effect of Sudden Rate Increases

Sudden increases of the flow rate on a partially clogged bed tends to disrupt the equilibrium between attachment forces retaining solids in a bed and hydraulic shear forces. As a result particles move deeper into the bed and into the effluent. Analysis of Figs. 25-30 indicated that clogging affects mainly 14 mm medium working under low flow rates (0.065 Lps). For higher flow rates and coarser media, effects of deposition are not as evident. For this reason, a 24 hr test was performed, using 14 mm medium subjected to an initial flow velocity of 0.42 cm/s (0.065 Lps) with a stop-and-start period after 9 hrs of continuous operation. Results of this test are presented in Figs. 33-34 together with photographs taken at various times in the runs in Figs. 35-37.

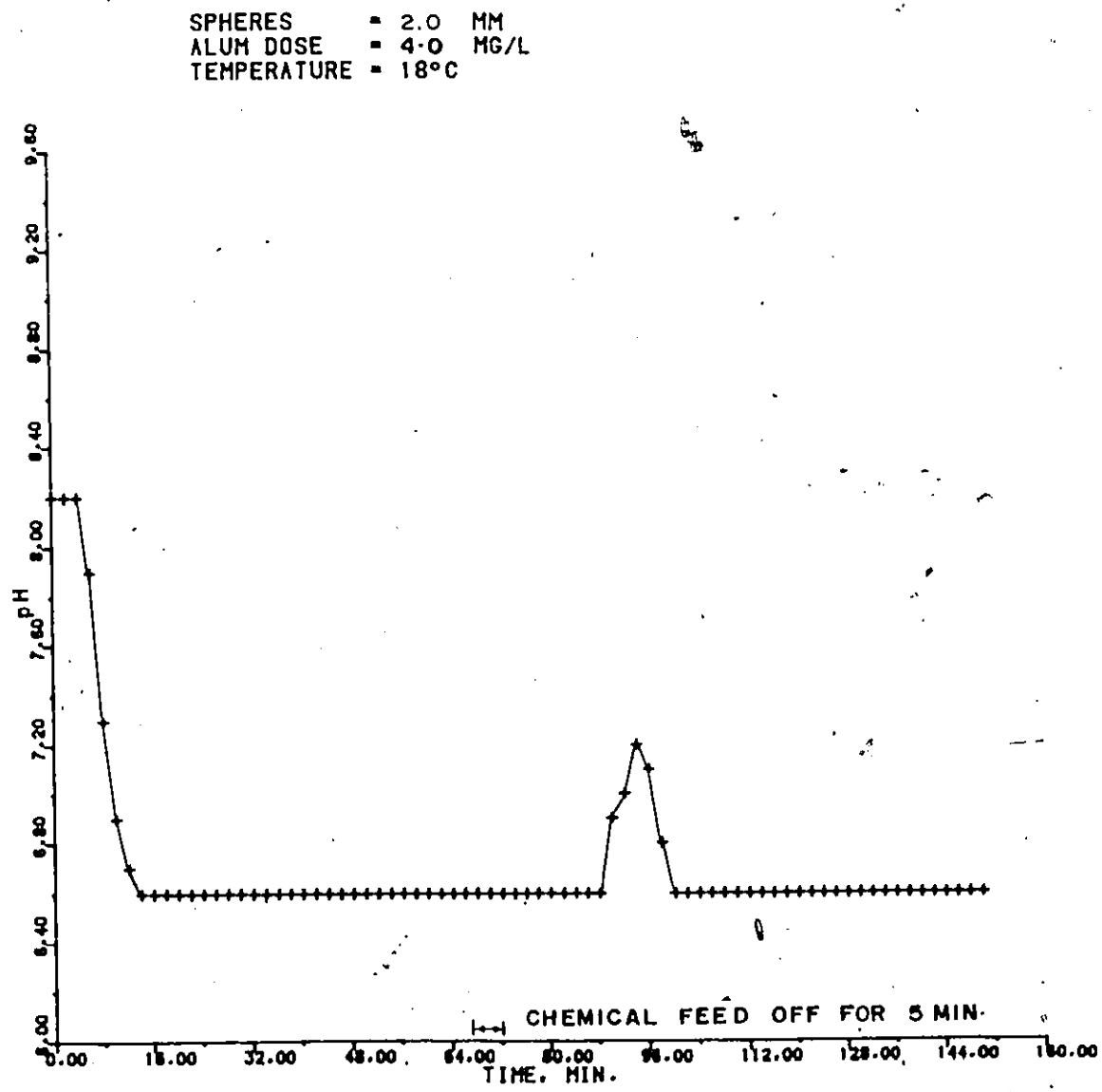

Figure 32: EFFECT OF LOSS OF COAGULANT FEED ON pH

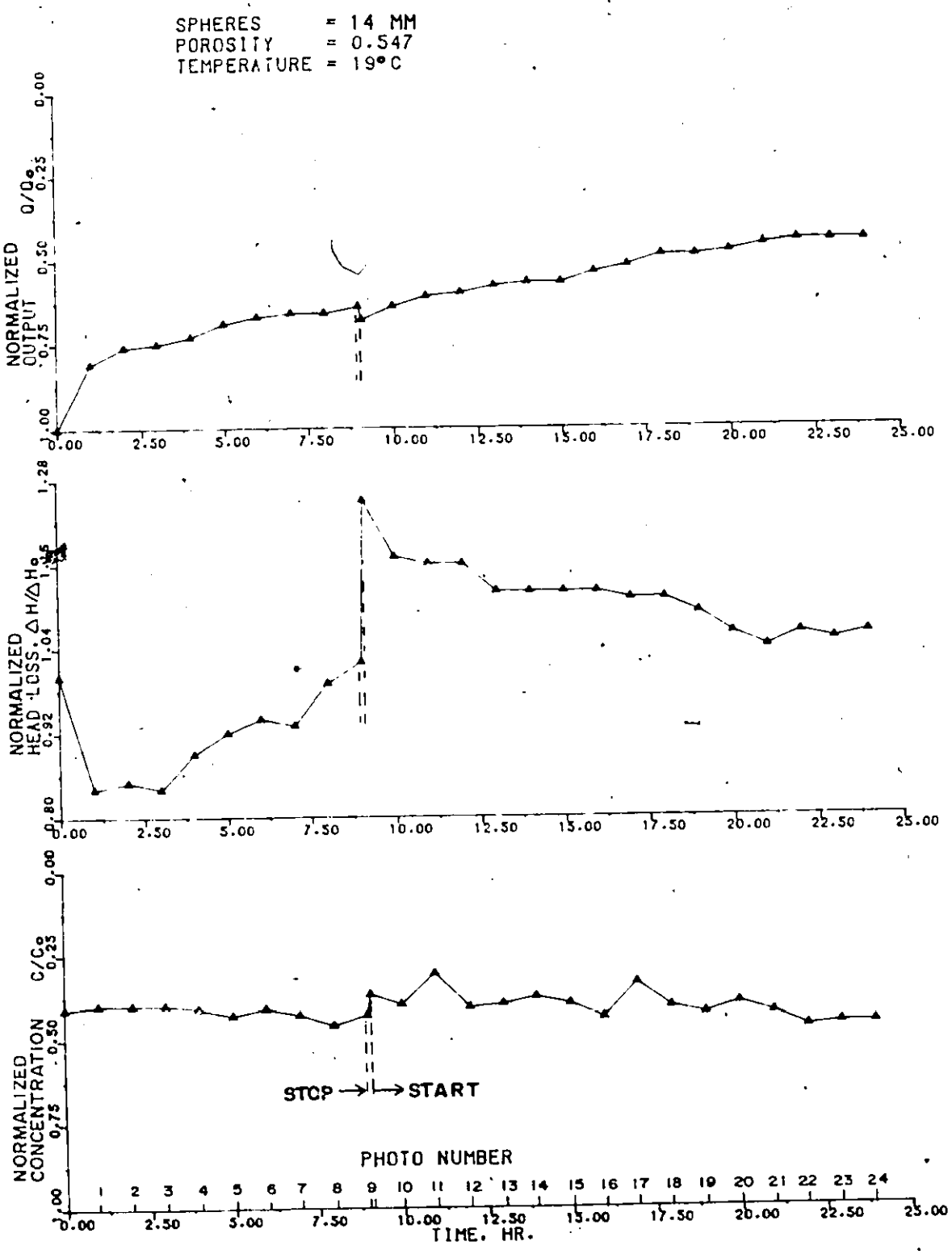

Figure 33: EFFECT OF SUDDEN RATE INCREASES

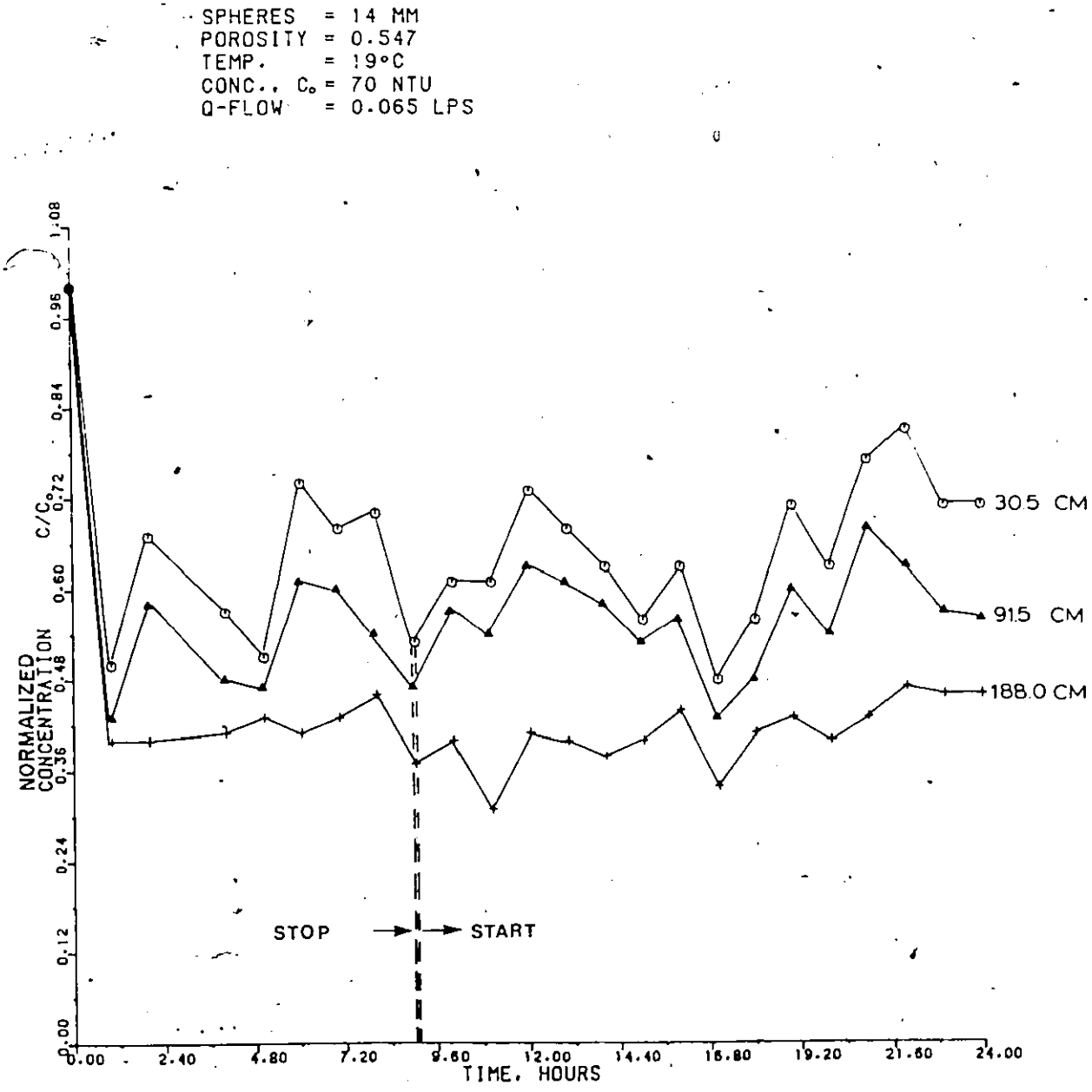

Figure 34: EFFECT OF SUDDEN RATE INCREASES

A - TIME 0:00 HR START OF FLOCCULATION

B - TIME 09:00 HR
JUST BEFORE STOP

Figure 35: INFLUENCE OF STOP-AND-START ON PERFORMANCE

A – TIME 09:00 HR
JUST BEFORE ON

B – TIME 09:00 HR
AFTER RESTORING FLOW RATE

Figure 36: INFLUENCE OF STOP-AND-START ON FLOCCULATION PERFORMANCE

A - TIME 17:00 HR

B - TIME 24:00 HR

Figure 37: INFLUENCE OF STOP-AND-START ON FLOCCULATION PERFORMANCE

As indicated by the data in Fig. 33, deposition of solids caused a steady decrease in the normalized flow rate and increased normalized headloss in a bed up to the "stop" period. At the end of 9 hrs continuous flocculation (Fig. 35B), flow was cut off and the bed stayed idle for a period of 6 hrs (Fig. 36A), after which flow was restored (Fig. 36B).

The idle period resulted in compaction of deposited flocs, causing an increase of normalized headloss and by actual decrease of apparent volume of deposited material, partial "restoration" of available void space. The latter, together with release of deposited material, resulted in an increase of normalized flow rate and normalized concentration, as represented in Figs. 33-34. These observations are similar to those obtained by Cleasby (1981) for impact of sudden rate increases on dirty filters. Photographs of the bed presented in Figs. 35-36 confirmed previously discussed findings showing definite changes in shape of deposited flocs during "stop-and-start" operation.

Another interesting observation is that after a short time all parameters follow an almost linear relationship and the progress of clogging (Fig. 36) does not affect effluent quality significantly (Fig. 34).

Figure 37 presents this same medium after 17 and 24 hours of continuous flocculation, illustrating further increase of clogging.

4.3.6 Solids Deposition Versus Media Size

Influence of media size on rate of bed clogging was indicated by the shape of the curves in Figs. 25-30 and a comparison of photographs presented in Figs. 35-37. Figure 38 presents photographs of the 20 mm medium working under a 0.42 cm/s initial flow velocity. The first photograph was taken at the beginning of the flocculation run. The second photograph presents this same media after six hours of continuous flocculation.

As indicated by Fig. 38, the amount of deposited material is negligible, especially when compared to the 14 mm medium working under identical flow velocity (Figs. 35A and 35B). This would indicate that clogging of the bed is primarily controlled by the size of the medium and effect of the flow rate is considerably smaller. Visual observations of other runs yielded similar results.

The above findings are also in agreement with observations discussed by Tchobanoglous (1970). Furthermore, analysis of Figs. 25-30 indicates that increase of flow rate and media size results in considerably smaller floc deposition.

4.3.7 Removal Ratio and Reynold's Number

Turbidity measurements produce the data on reduction of primary particles after a flocculation period, which can be related to flow velocity based on Eq. (2.67).

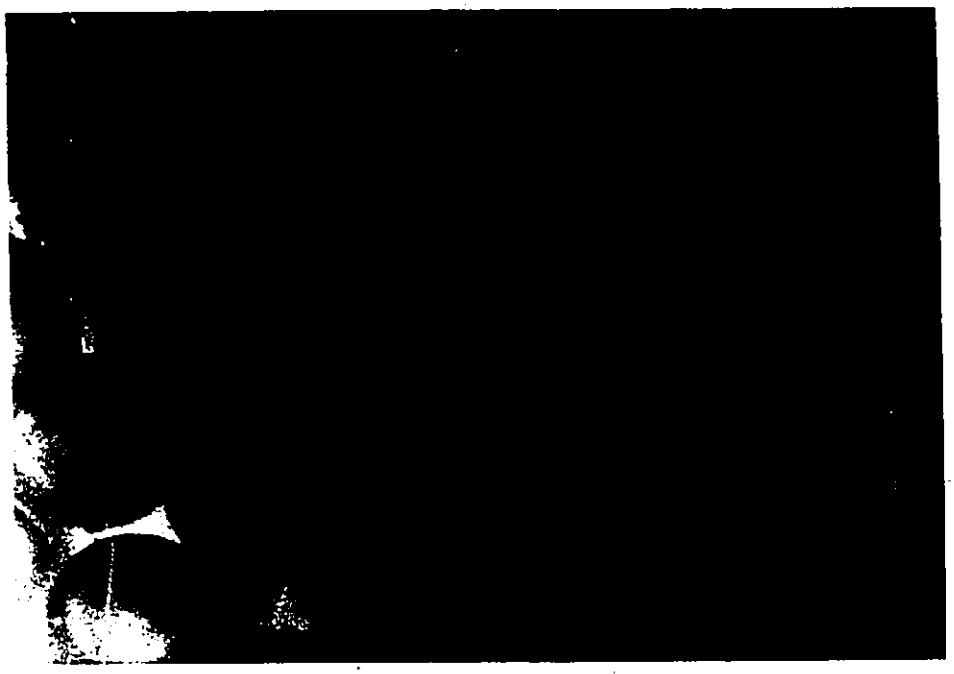

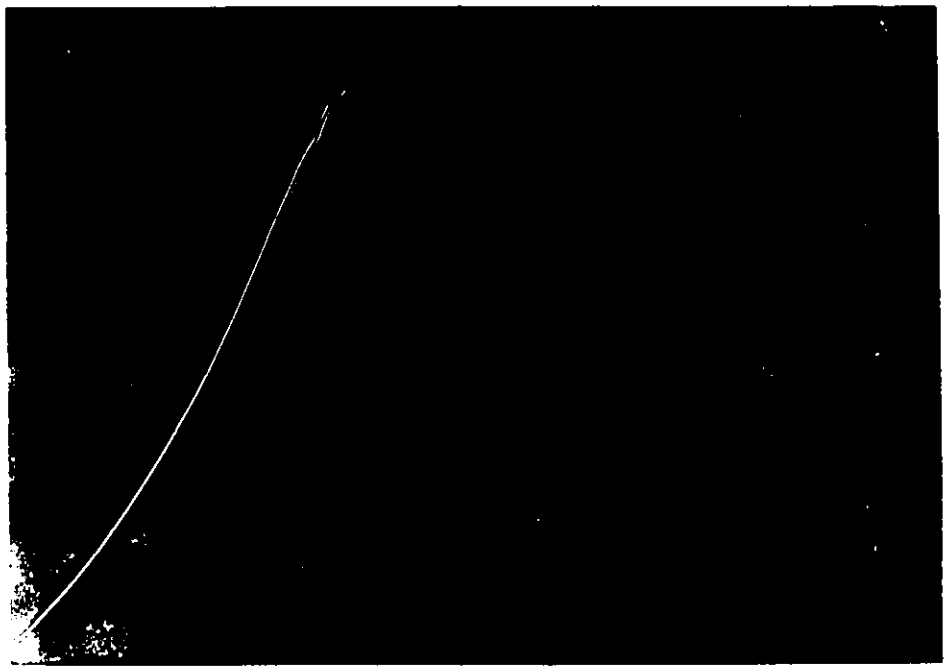

Figure 38: INFLUENCE OF MEDIA SIZE ON DEPOSITION OF SUSPENDED FLOCS
FLOC VELOCITY 0.36 cm/s
MEDIA SIZE 20 mm

The results of this correlation are presented in Figs. 39-41. A regression analysis of data presented in these figures is summarized in Tables A.4 and A.5, Appendix A. Figures 42-44 show flow velocity and R_K calculated for clean bed conditions. An attempt to find average values at the times greater than 0 were hampered by clogging, which continuously changed porosity and the corresponding velocity and permeability. Analysis of Figs. 39-41 and previous observations indicate that change in apparent flow velocity does not dramatically influence flocculation performance. Hence, the author suggests using Reynold's number as a parameter, since it represents both flow velocity and media properties.

These same data correlated with R_K (Figs. 42-44 and Table 12) allow more interesting observations to be made. These data indicate that there is an optimum range of R_K where flocculation is most efficient. Optimum conditions seem to develop for R_K from 7 to 40 and the lower limit applies to all three media sizes.

Analysis of Table 12 reveals that optimum contact time for media smaller then 32 mm is lower than 3 minutes. Also, there is noticeable influence of flow velocity on parameter K_1, which seems to increase with increasing flow velocity.

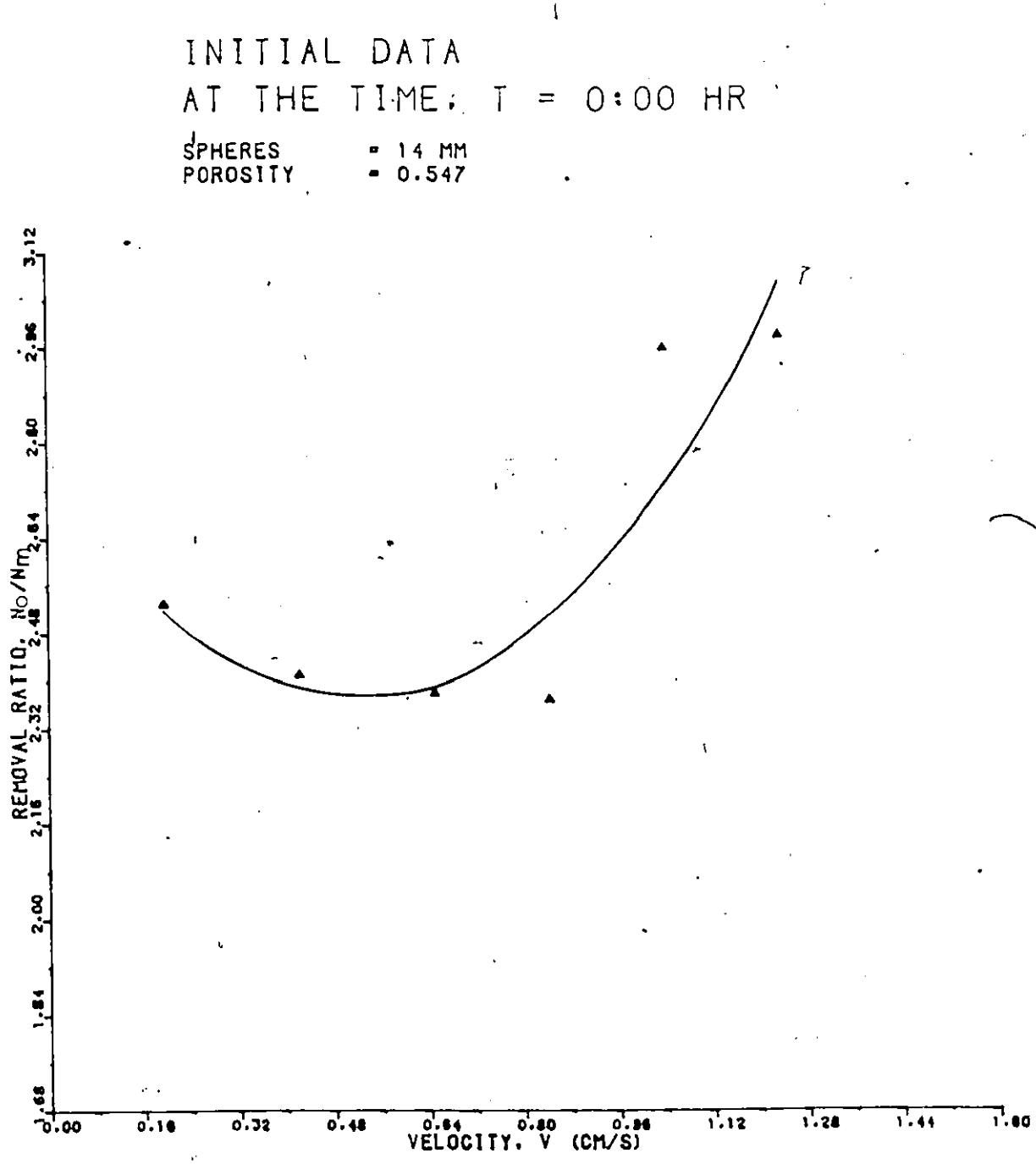

Figure 39: EFFECT OF VELOCITY ON FLOCCULATION PERFORMANCE, 14 MM SPHERES

INITIAL DATA
AT THE TIME, T = 0:00 HR

SPHERES = 20 MM
POROSITY = 0.498

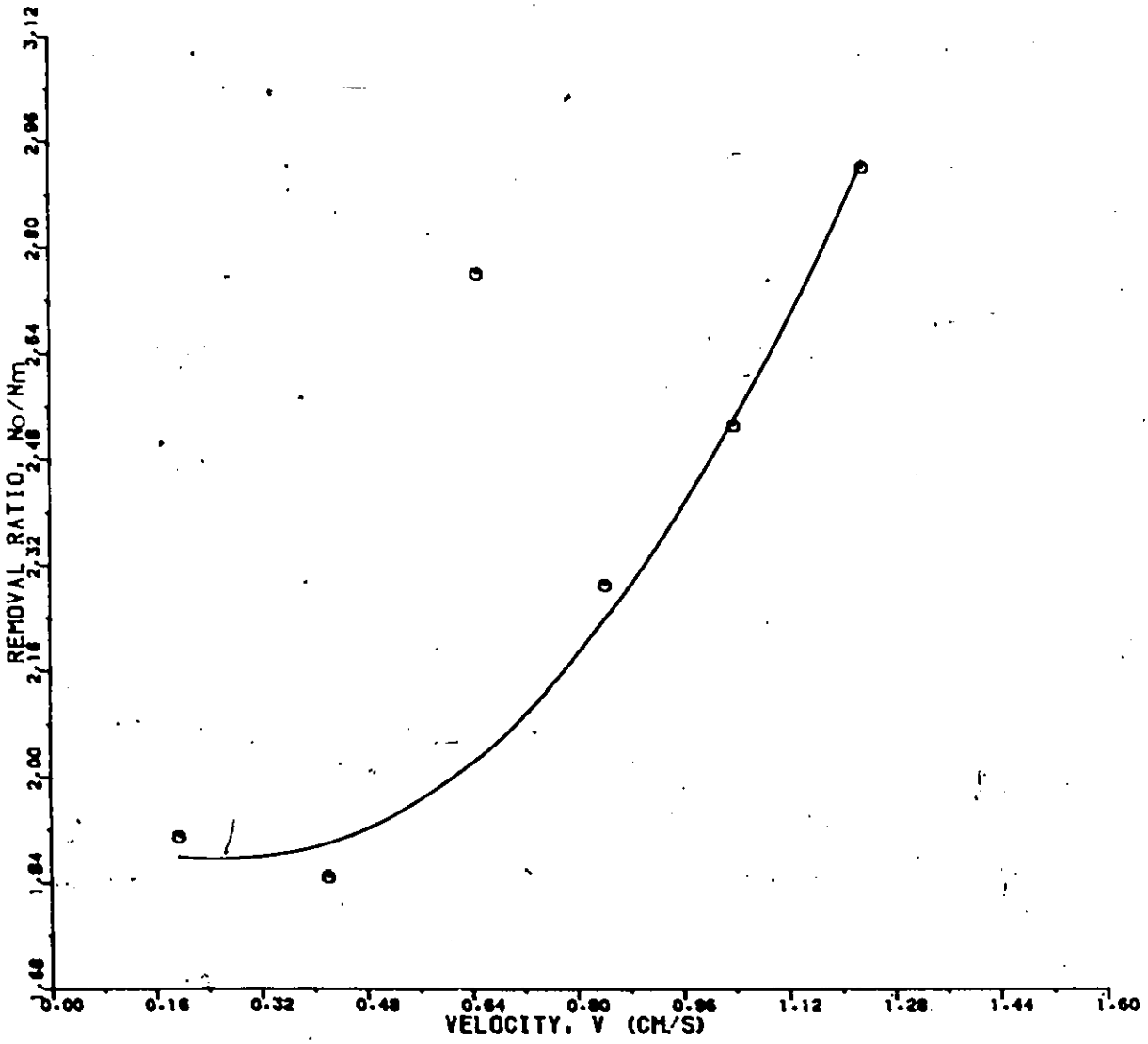

Figure 40: EFFECT OF VELOCITY ON FLOCCULATION PERFORMANCE, 20 MM SPHERES

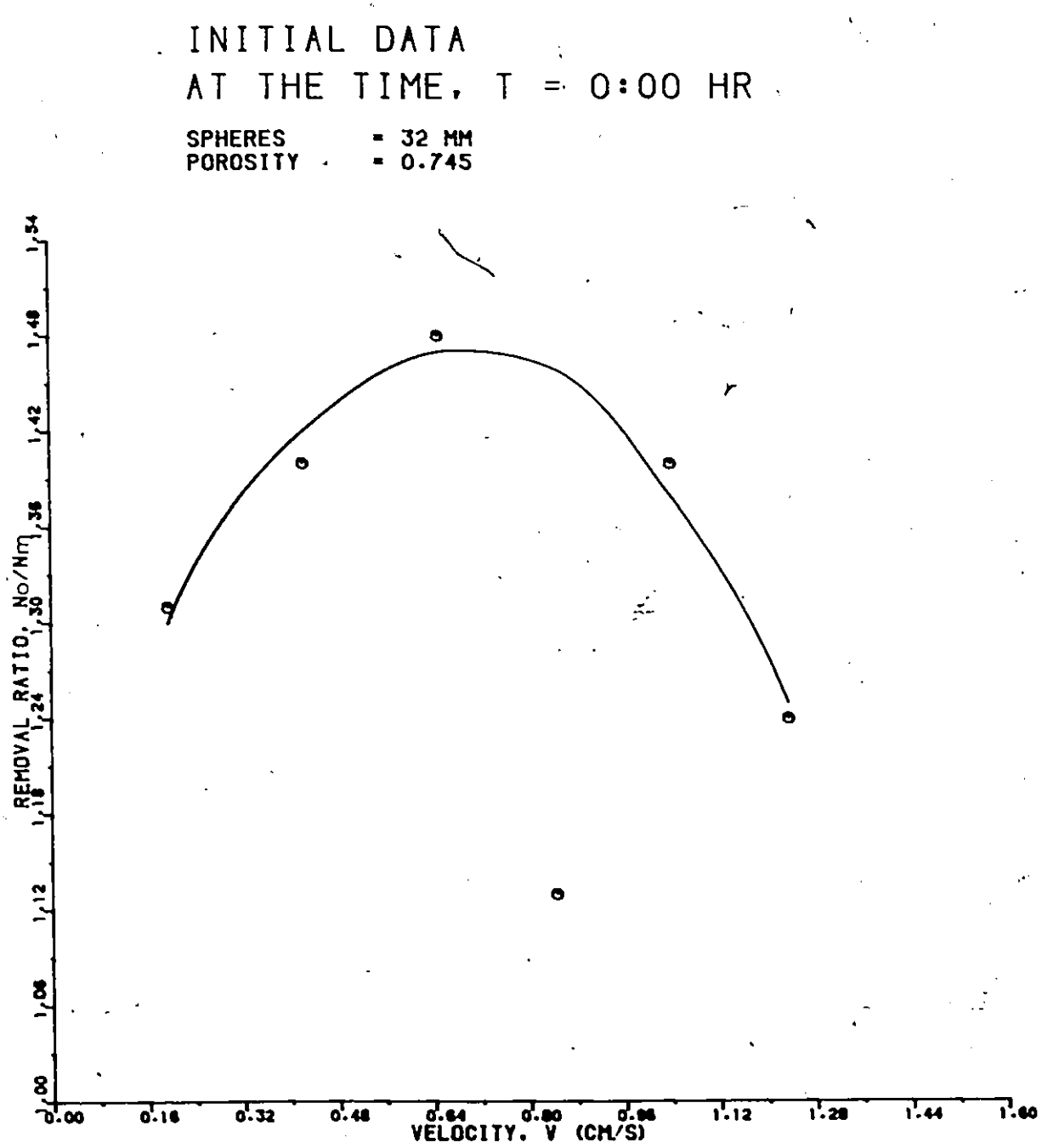

Figure 41: EFFECT OF VELOCITY ON FLOCCULATION PERFORMANCE, 32 MM SPHERES

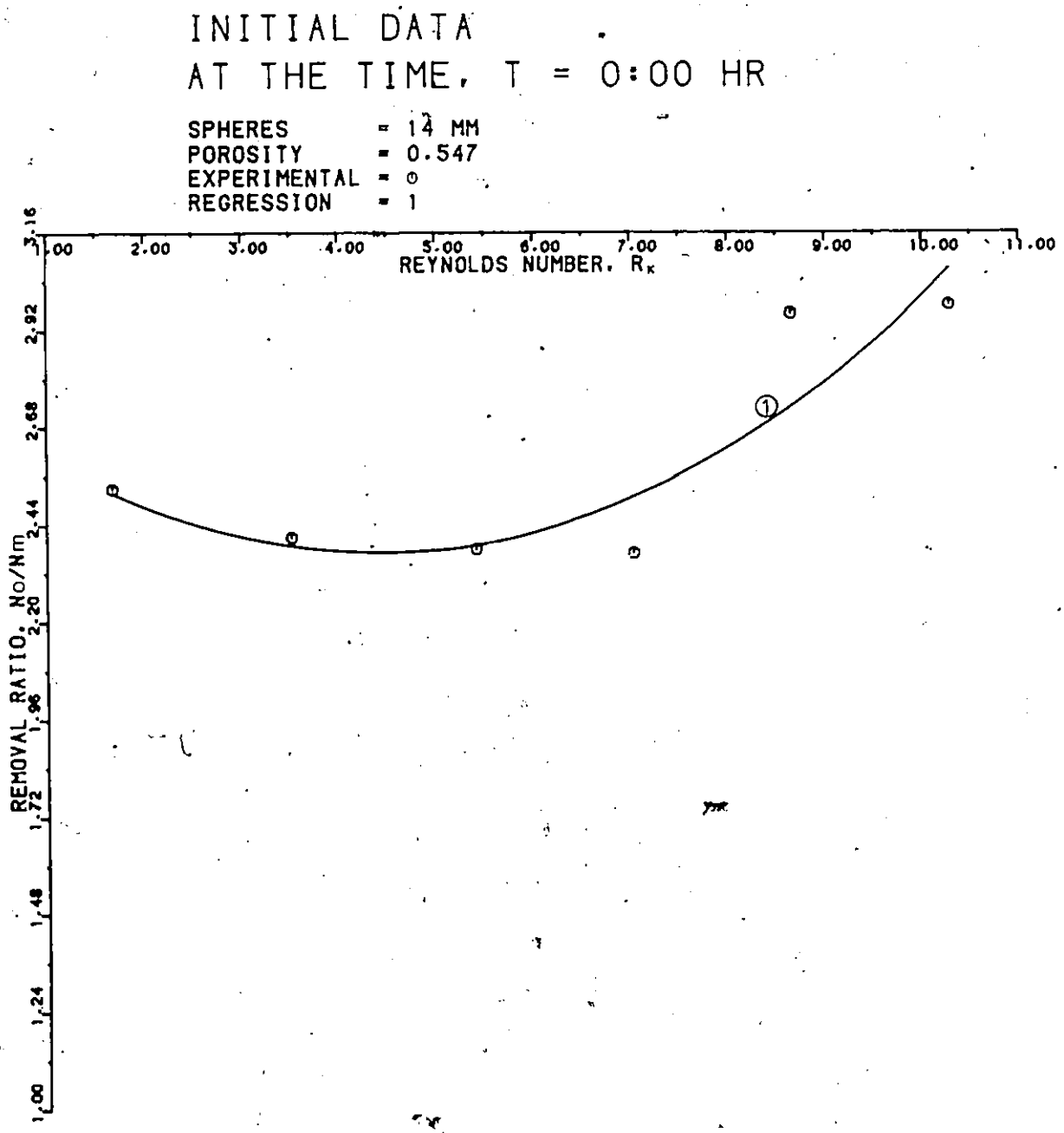

Figure 42: FLOCCULATION PERFORMANCE VERSUS R_K, 14 MM SPHERES

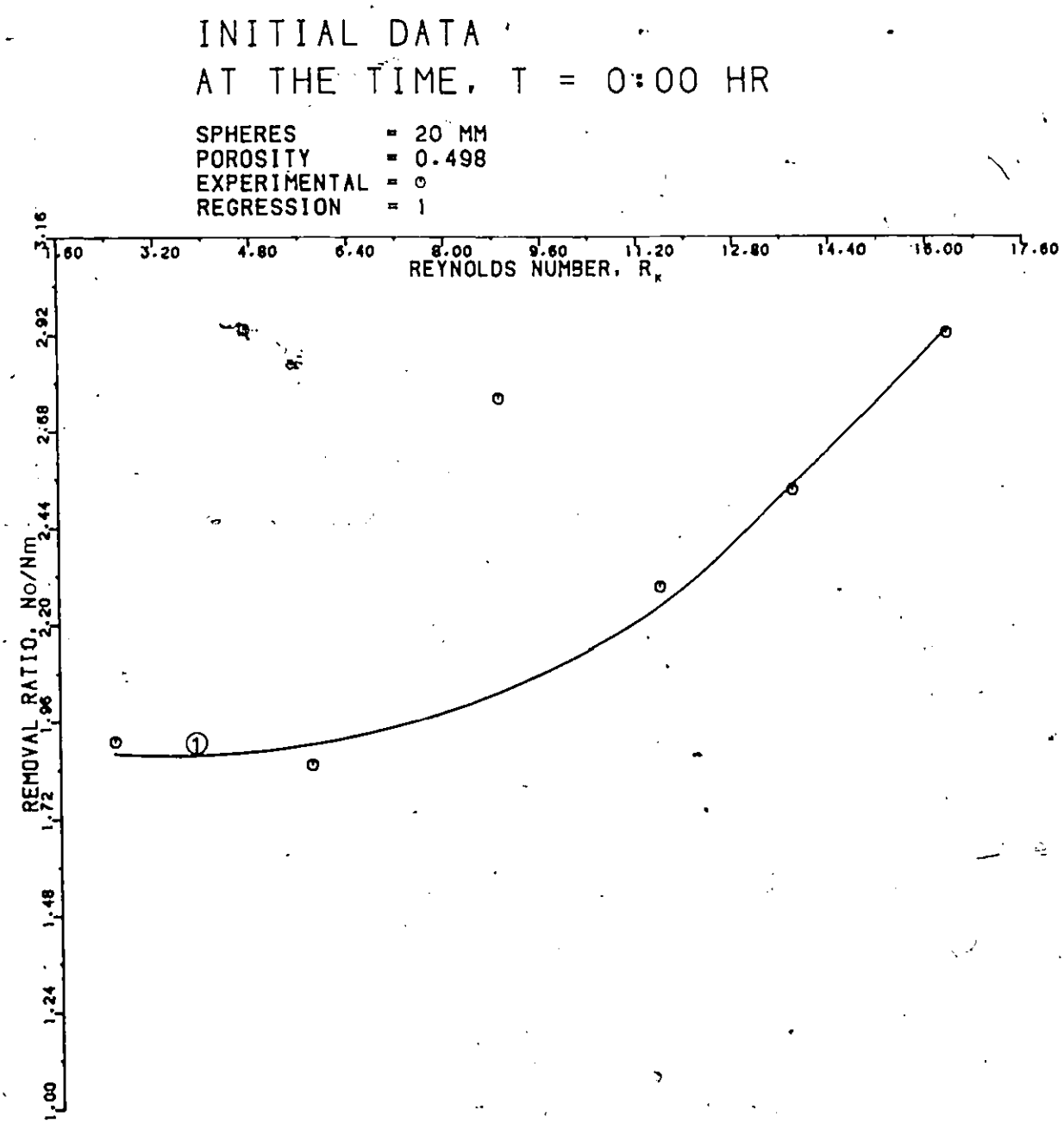

Figure 43: FLOCCULATION PERFORMANCE VERSUS R_K, 20 MM SPHERES

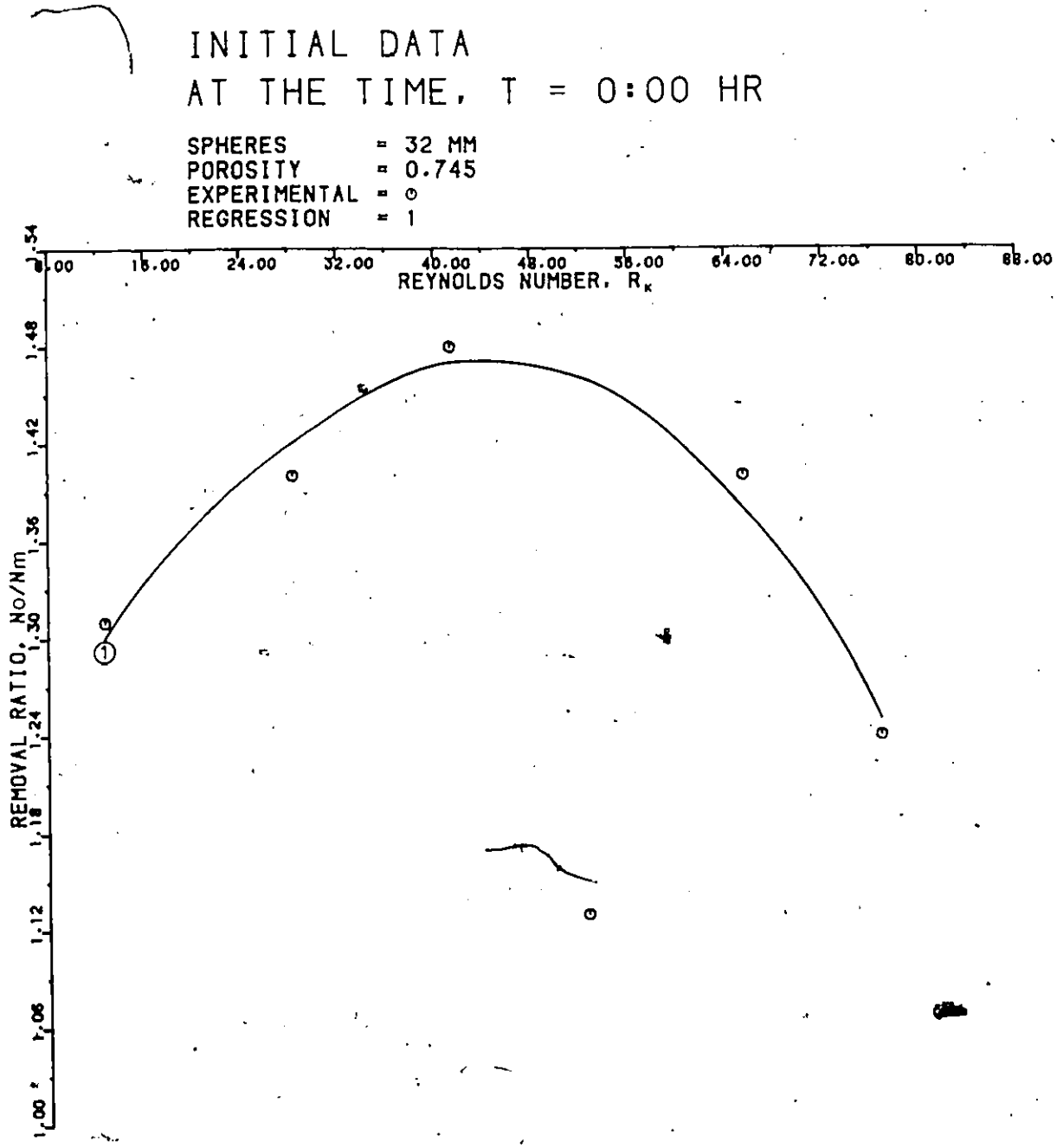

Figure 44: FLOCCULATION PERFORMANCE VERSUS R_K, 32 MM SPHERES

Table 12. Removal Ratio and Reynold's Number

Apparent Flow Velocity $x10^{-2}$ m/s	Flocculation Time s	G 1/s	R_K	N_o/N_m	K_1N_o $x10^{-4}$
media size 32 mm, n = 0.745					
0.195	718	2.79	12.68	1.31	1.167
0.422	332	2.68	28.33	1.40	3.304
0.650	215	5.81	41.32	1.48	2.732
0.844	166	9.72	52.48	1.13	0.662
1.039	135	13.23	65.39	1.40	1.641
1.234	114	15.92	76.70	1.24	1.039
media size 20 mm, n = 0.498					
0.195	480	3.71	2.51	1.91	3,148
0.422	222	8.19	5.76	1.85	2.957
0.650	144	12.90	8.87	2.76	4.770
0.844	111	19.27	11.52	2.29	3.385
1.039	90	25.73	13.74	2.53	3.502
1.234	76	32.98	16.32	2.92	3.735
media size 14 mm, n = 0.547					
0.195	527	2.84	1.67	2.53	5.376
0.422	244	10.37	3.51	2.41	3.040
0.650	158	17.28	5.41	2.38	2.757
0.844	122	23.72	7.03	2.37	2.598
1.039	99	31.99	8.65	2.96	2.976
1.234	83	39.67	10.28	2.98	2.867

Another interesting finding observed from the regression analysis is that the data follow a geometric function more closely than the exponential function represented by Eq. (2.67). These two observations indicate that there is no universal equation for removal and Eq. (2.63) suggested by Richter (1977) should be replaced by another form suitable for flocculation at higher Reynold's numbers. Difficulties lie in the lack of precise methods to measure changes in n, G and R_k. If it was possible to obtain continuous data on G and R_k, a more consistant relation may have been observed.

4.4 Comparison of Predicted and Experimental Data

The applicability of the equations developed and presented in Chapter II can be represented by comparing the measured headloss for clean water only in various media to that calculated using the Forchheimer type equations presented in Table 1.

Summary data for these calculations are presented in Table 13 and Figs. 45-47. Analysis of these figures indicates agreement between measured data and that computed using Eq. (2.66). The best correlation between experimental data and theoretical development was obtained using Ward's formula (Table 1). A similar formula developed by Schneebeli (Table 1) especially for spheres yields considerably higher results.

Table 13: Hydraulic Gradient and Velocity, Comparison of Calculated and Experimental Data
Time 00:00 HRS

media size 32 mm, n= 0.745

Apparent Flow Velocity $\times 10^{-2}$ m/s	Experimental $J \times 10^{-3}$	Regression $J \times 10^{-3}$	Theoretical Formulas: Ergun $J \times 10^{-3}$	Schneebeli $J \times 10^{-3}$	Carman $J \times 10^{-3}$	Ward $J \times 10^{-3}$	Irmay $J \times 10^{-3}$
0.195	0.452	0.380	0.017	0.352	0.018	0.041	0.010
0.422	0.425	0.475	0.071	1.140	0.066	0.178	0.033
0.650	0.558	0.777	0.159	2.270	0.138	0.410	0.067
0.845	1.356	1.199	0.266	3.690	0.226	0.690	0.109
1.040	1.941	1.771	0.396	5.260	0.326	1.040	0.156
1.230	2.367	2.496	0.553	7.170	0.446	1.460	0.214
		media size	20 mm, n = 0.498				
0.195	0.877	0.940	0.300	0.815	0.342	0.399	0.242
0.422	2.021	1.789	1.010	2.380	1.070	1.390	0.653
0.650	2.952	3.291	2.030	4.390	2.040	2.870	1.130
0.845	5.319	5.103	3.270	6.830	3.200	4.660	1.710
1.040	7.340	7.384	4.740	9.570	4.510	6.790	2.330
1.230	10.159	10.160	6.480	12.800	6.020	9.330	3.040
		media size	14 mm, n = 0.547				
0.195	0.480	0.464	0.323	1.440	0.372	0.455	0.273
0.422	3.080	2.988	1.060	4.070	1.150	1.590	0.731
0.650	5.560	5.744	2.150	7.550	2.240	3.330	1.300
0.845	8.060	8.305	3.380	11.300	3.410	5.320	1.890
1.040	11.600	11.029	4.840	15.500	4.750	7.740	2.550
1.230	13.700	13.949	6.490	19.800	6.170	10.500	3.180

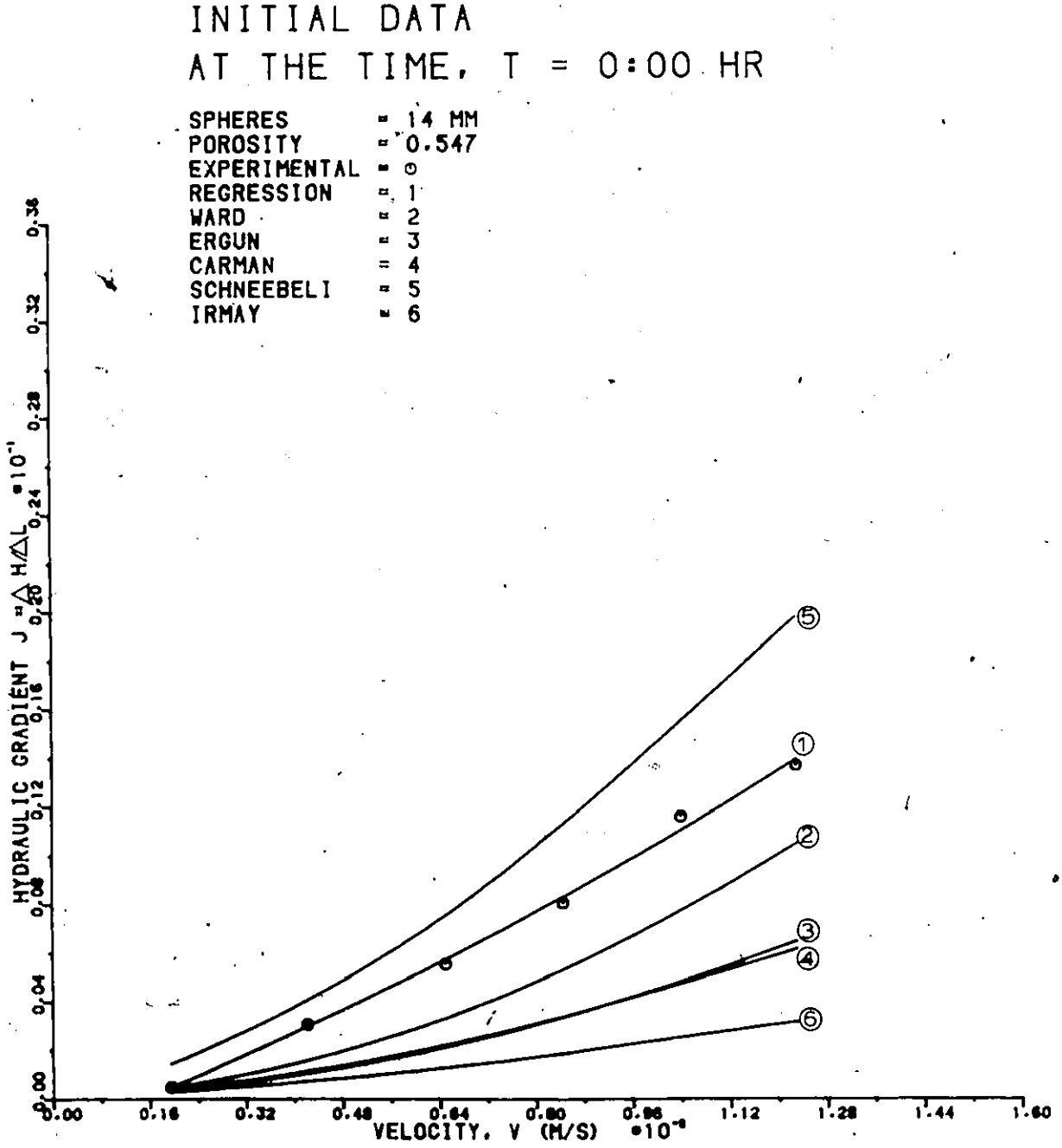

Figure 45: COMPARISON OF PREDICTED AND MEASURED HEADLOSS, 14 MM SPHERES

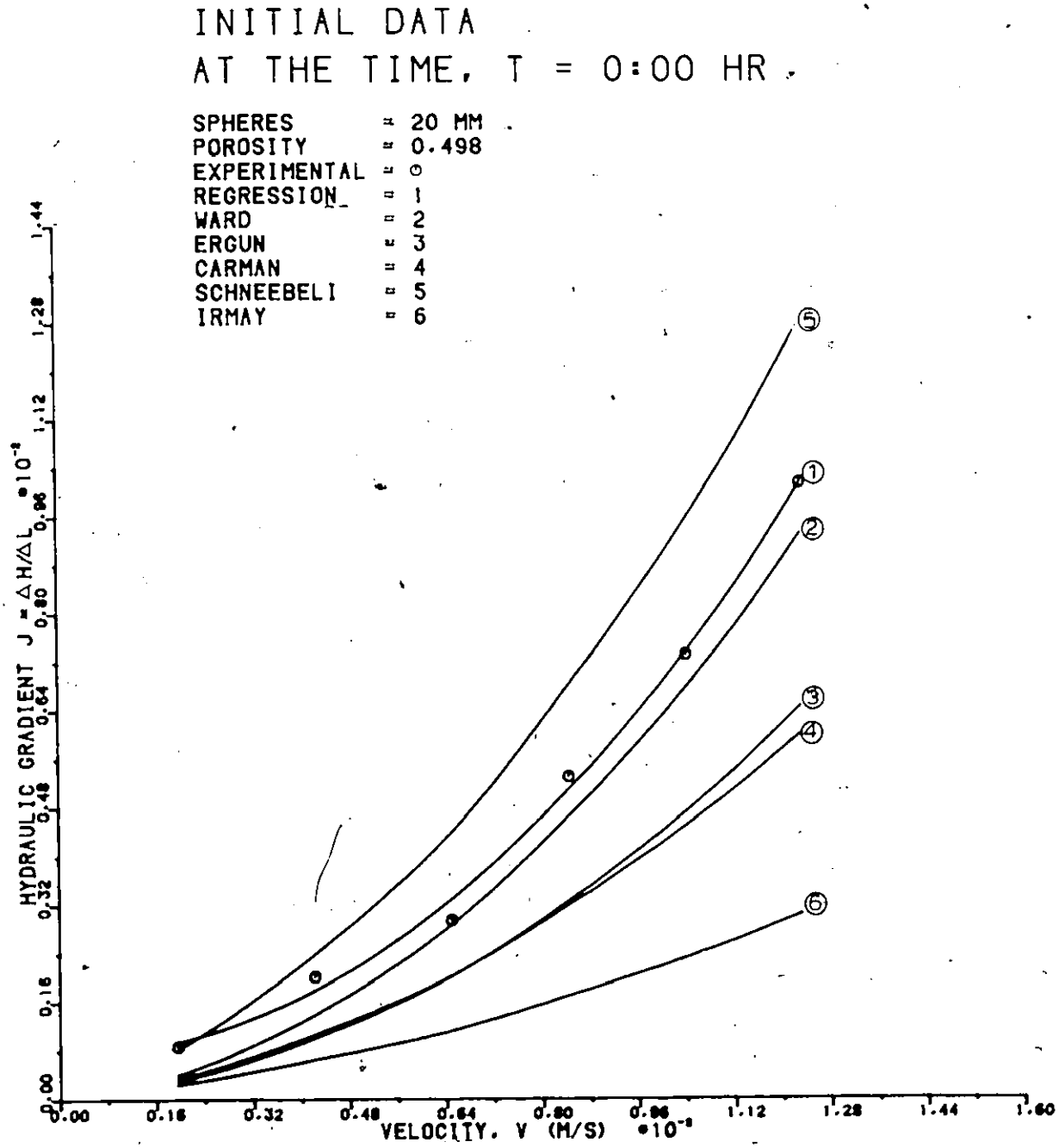

Figure 46: COMPARISON OF PREDICTED AND MEASURED HEADLOSS, 20 MM SPHERES

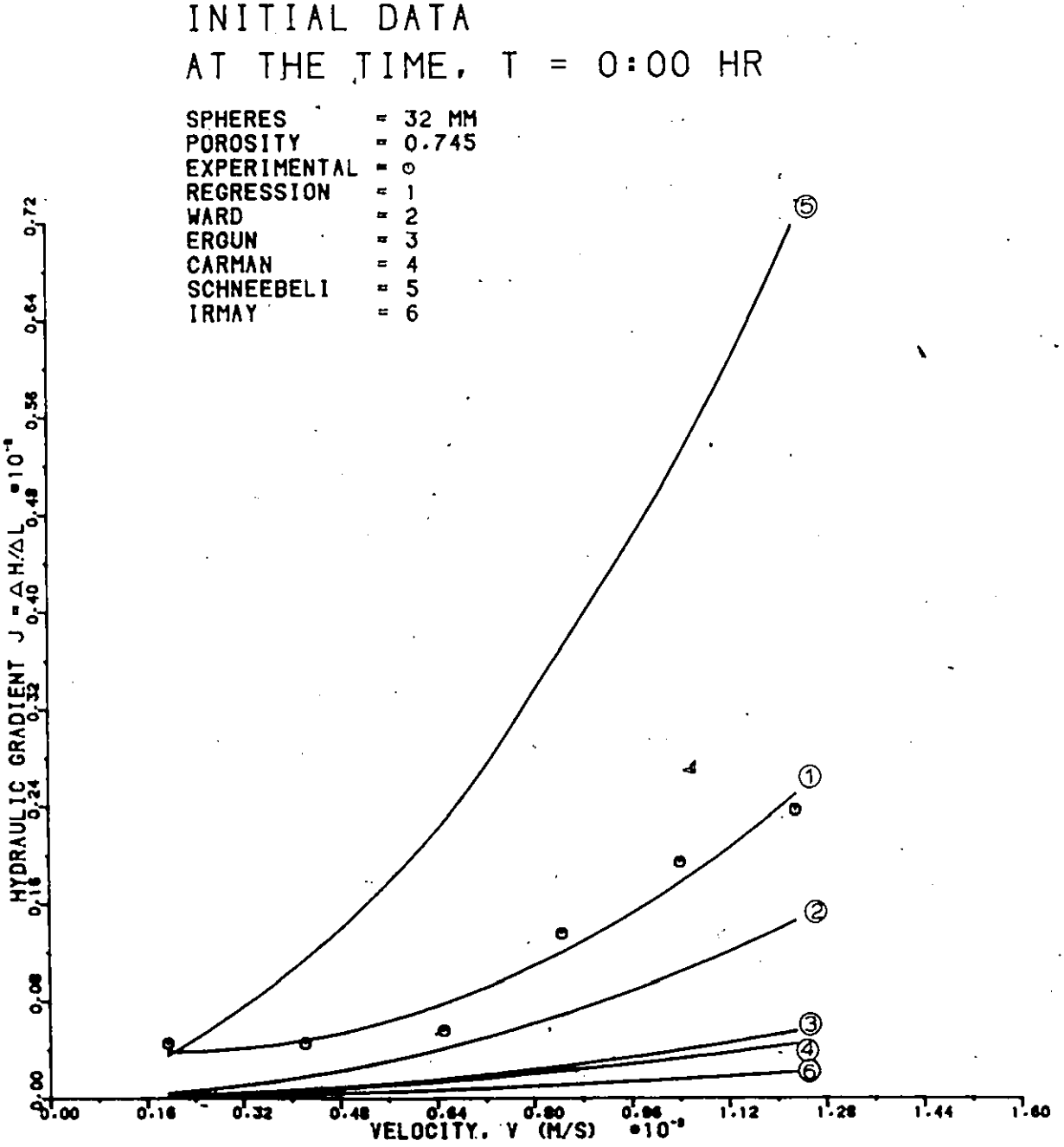

Figure 47: COMPARISON OF PREDICTED AND MEASURED HEADLOSS, 32 MM SPHERES

The observed deviation from measured values for 32 mm medium is caused by higher than usual porosity of the bed (0.745), where diameters of the spheres and column influence packing mode.

Other formulas produce more conservative values than Eq. (2.66), and probably could be better applied for smaller sizes and different shapes of media. It should be noted that these equations are applicable for the clear water headloss, and further use is hindered by difficulties of porosity estimation for various degrees of clogging.

Previous analyses indicated that for coarser media sizes and higher terminal flow velocities, clogging effects on the headloss become negligible (Figs. 26-30). Therefore the second term in Eq. (2.62) can be omitted, and Eq. (2.66) can be applied over approximately the first 2 hour period for flow in partially clogged beds. Further application is restricted by visible influence of clogging on flow rate and porosity.

These observations are also supported by analysis of the velocity gradients.

4.4.1 Velocity Gradients - Data

Determination of rms velocity gradient, G, was based on Eq. (2.65). Analysis of the experimental data allow the correlation of the G value with respect to increasing initial velocity and media sizes (Appendix A).

Data presented in Fig. 48 proved media size to be the main variable in granular flocculation. As would be expected from previously reported results, decreasing size of the media particles causes increase of G for a comparable flow velocity. Furthermore, Figs. 49-51 and Table 14 present a comparison of theoretical formulas developed based on Ward's equation with experimental data.

From the data on these plots one can notice a good correlation for small and intermediate media sizes. More discrepancy for the largest media (Fig. 51) results from the unusually high porosity.

The data presented in Figs. 52-54 and Table 14 represent effects of clogging on G values. After 2 hrs of continuous flocculation there is very little change in measured G values and both initial and final data follow the same pattern. Observation of constant G value over this period of time confirms continual flocculation efficiency of granular media.

Data for flocculation over a period longer than 2 hours were difficult to correlate, since calculation of G (Eq. 2.65) required knowledge of the porosity of the clogged bed. An attempt to utilize clean bed porosity, and flow rate after that time would produce considerably higher values of interstitial velocities than existed in the media. For this reason obtaining a correlation for flocculation over a period exceeding the initial 2 hour period was not done.

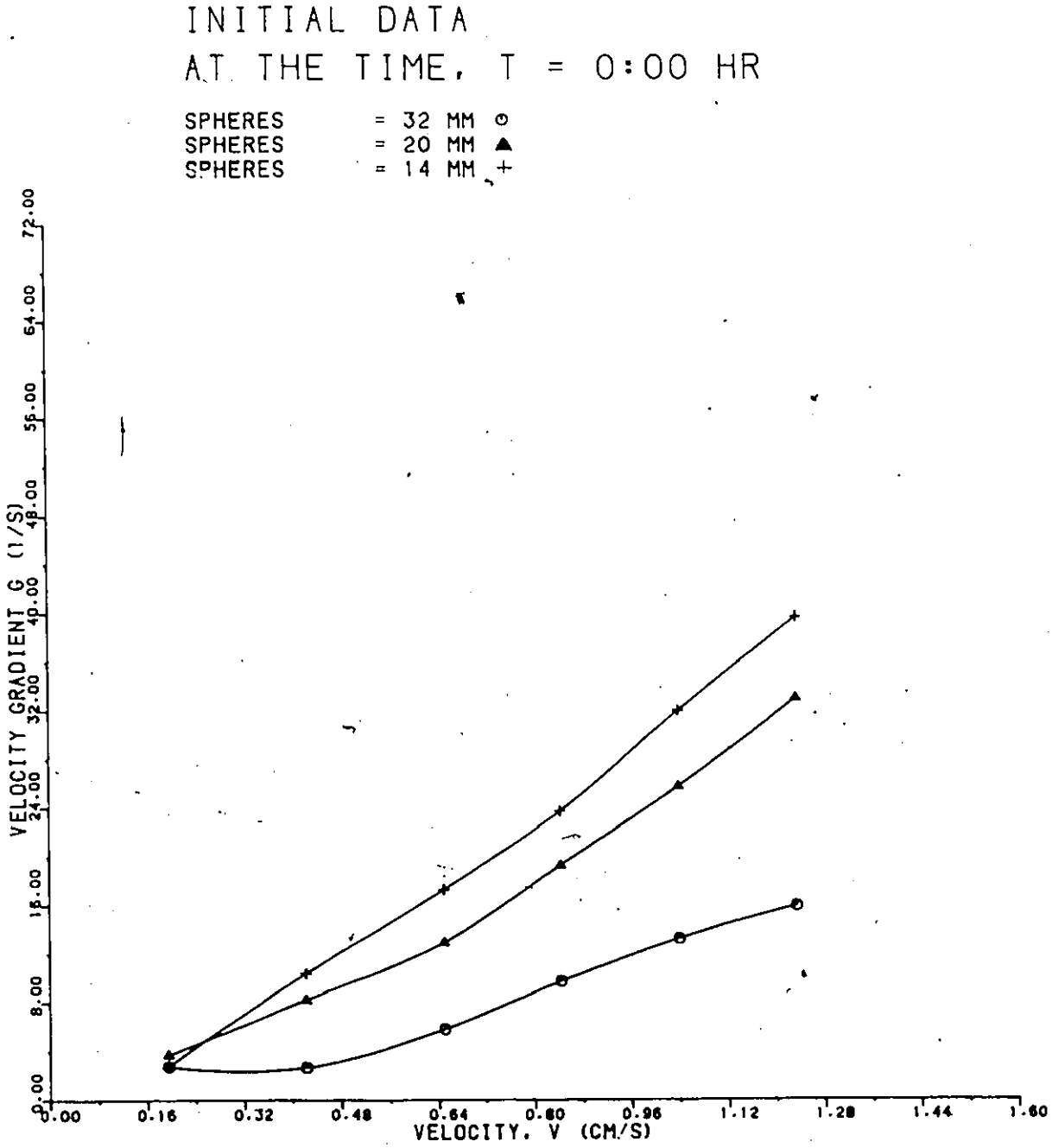

Figure 48: EFFECT OF MEDIA SIZE ON GRADIENT, INITIAL CONDITIONS

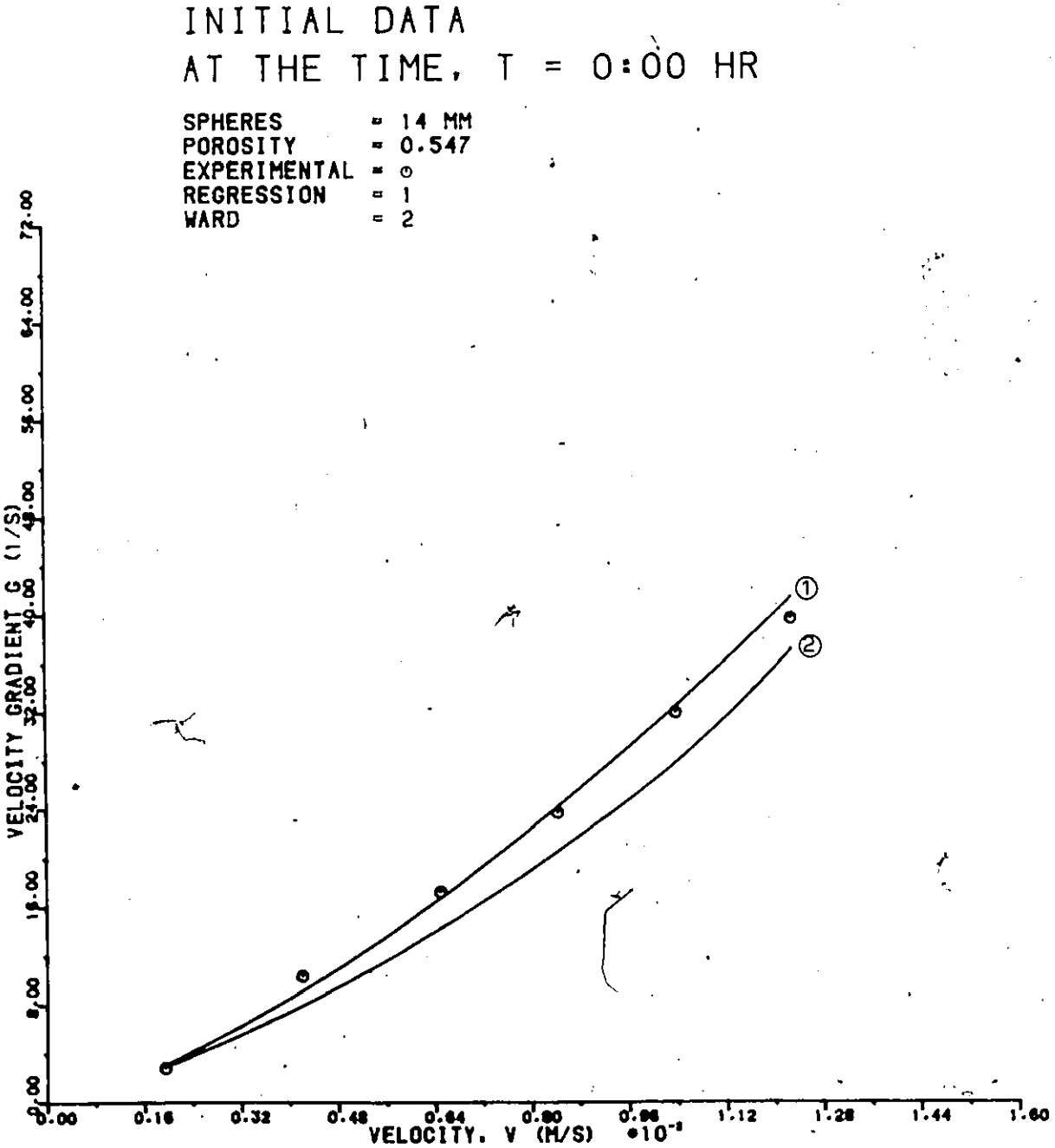

Figure 49: COMPARISON OF PREDICTED AND EXPERIMENTAL G, 14 MM SPHERES, INITIAL CONDITIONS

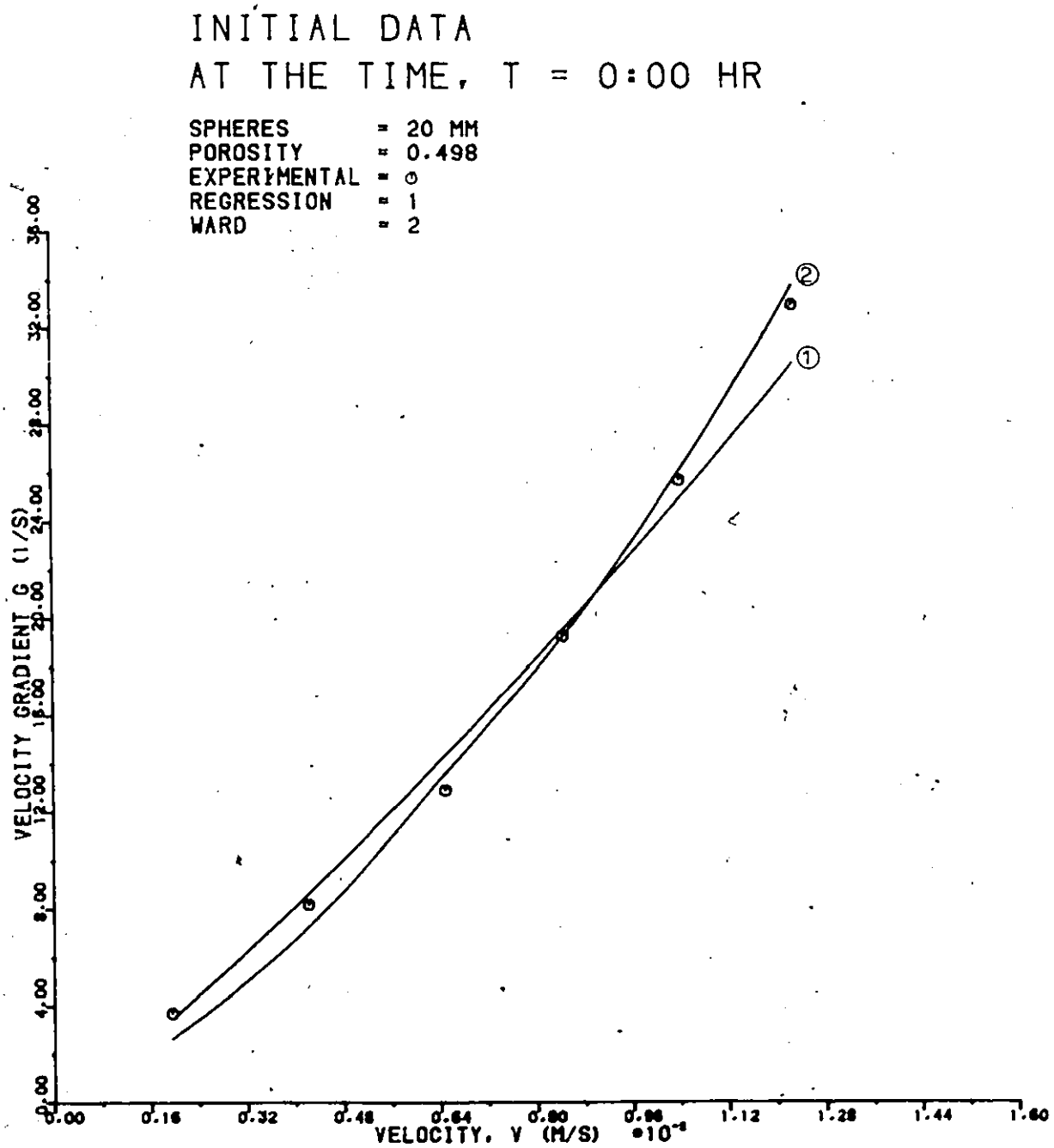

Figure 50: COMPARISON OF PREDICTED AND EXPERIMENTAL G, 20 MM SPHERES, INITIAL CONDITIONS

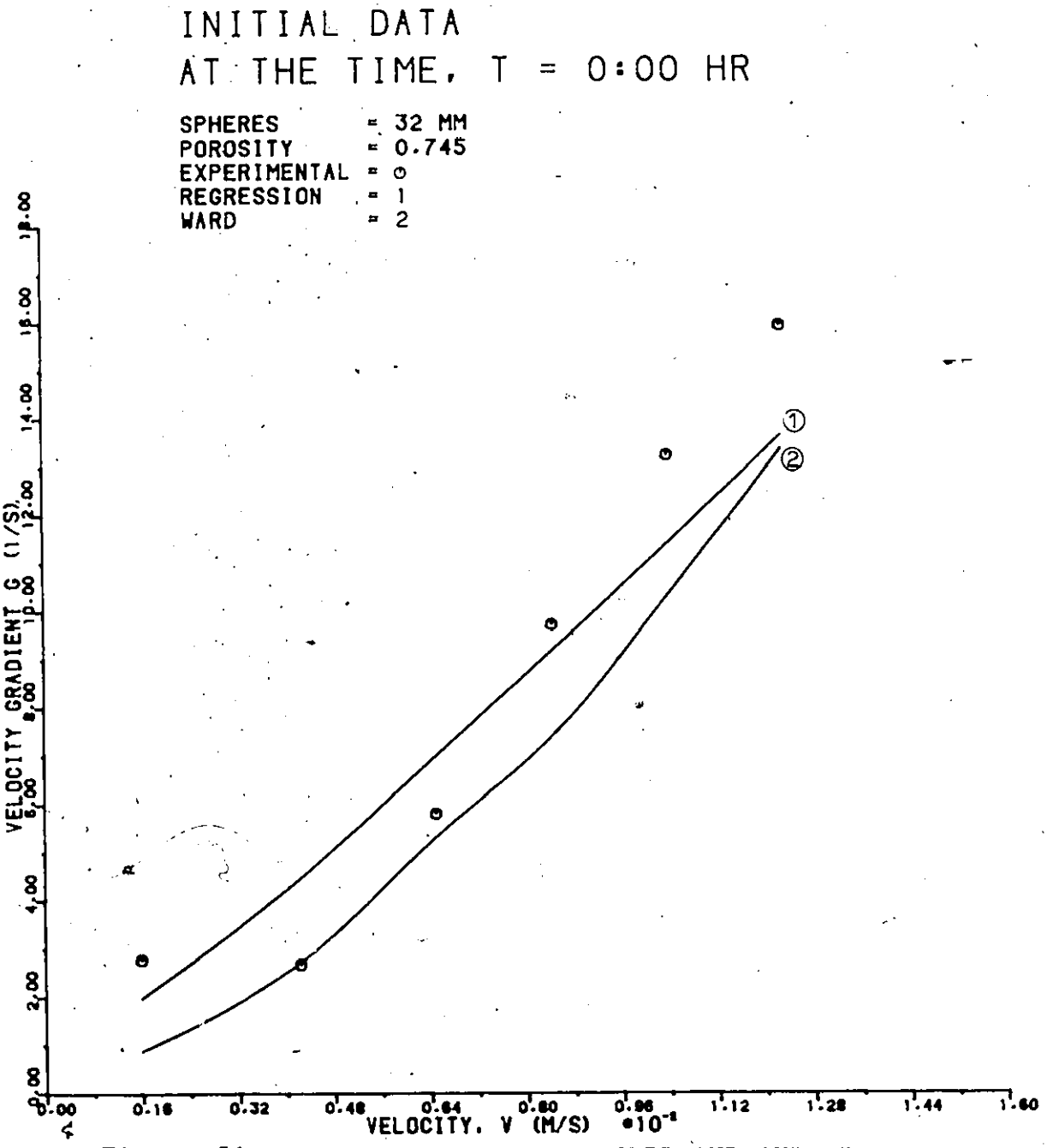

Figure 51: COMPARISON OF PREDICTED AND EXPERIMENTAL G, 32 MM SPHERES, INITIAL CONDITIONS

Table 14: Velocity Gradient and Velocity, Comparison of Calculated and Experimental Data

media size 32 mm, n = 0.745

Apparent Flow Velocity X 10 m/s	G,1/s								
	Time 00:00 HRS		Theoretical Formulas					Time 02:00 HRS	
	Experimental	Regression	Ergun	Schneebeli	Carman	Ward	Irmay	Experimental	Regression
0.195	2.79	1.99	0.59	2.64	0.59	0.90	0.44	1.35	1.33
0.422	2.68	4.46	1.72	6.90	1.65	2.73	1.17	4.07	3.87
0.650	5.81	6.99	3.31	12.52	3.08	5.32	2.14	5.95	7.01
0.845	9.72	9.18	4.60	17.15	4.24	7.41	2.95	9.82	10.06
1.040	13.23	11.40	6.38	23.27	5.79	10.33	4.01	15.71	13.37
1.230	15.92	13.63	8.22	29.59	7.39	13.34	5.12	16.27	16.95
media size 20 mm, n = 0.498									
0.195	3.71	3.47	2.32	3.82	2.48	2.67	2.08	3.24	3.17
0.422	8.19	8.63	6.18	9.51	6.38	7.26	4.98	8.24	8.53
0.650	12.90	14.34	11.48	16.80	11.48	13.59	8.52	15.53	14.75
0.845	19.27	19.55	16.15	23.32	15.97	19.26	11.67	18.68	20.60
1.040	25.73	24.97	21.83	31.01	21.29	26.13	15.30	27.40	26.79
1.230	32.98	30.58	28.14	39.48	27.12	33.77	19.27	34.67	33.35
media size 14 mm, n = 0.547									
0.195	2.84	3.07	2.50	5.27	2.68	2.96	2.29	2.67	2.87
0.422	10.37	9.13	6.49	12.74	6.77	7.96	5.40	9.58	9.32
0.650	17.28	16.75	11.48	21.52	11.71	14.29	8.94	19.12	17.90
0.845	23.72	24.24	16.40	29.95	16.48	20.60	12.28	26.70	26.65
1.040	31.99	32.48	22.06	39.44	21.87	27.89	15.99	35.92	36.46
1.230	39.67	41.38	29.17	51.00	28.43	37.11	20.42	45.35	47.32

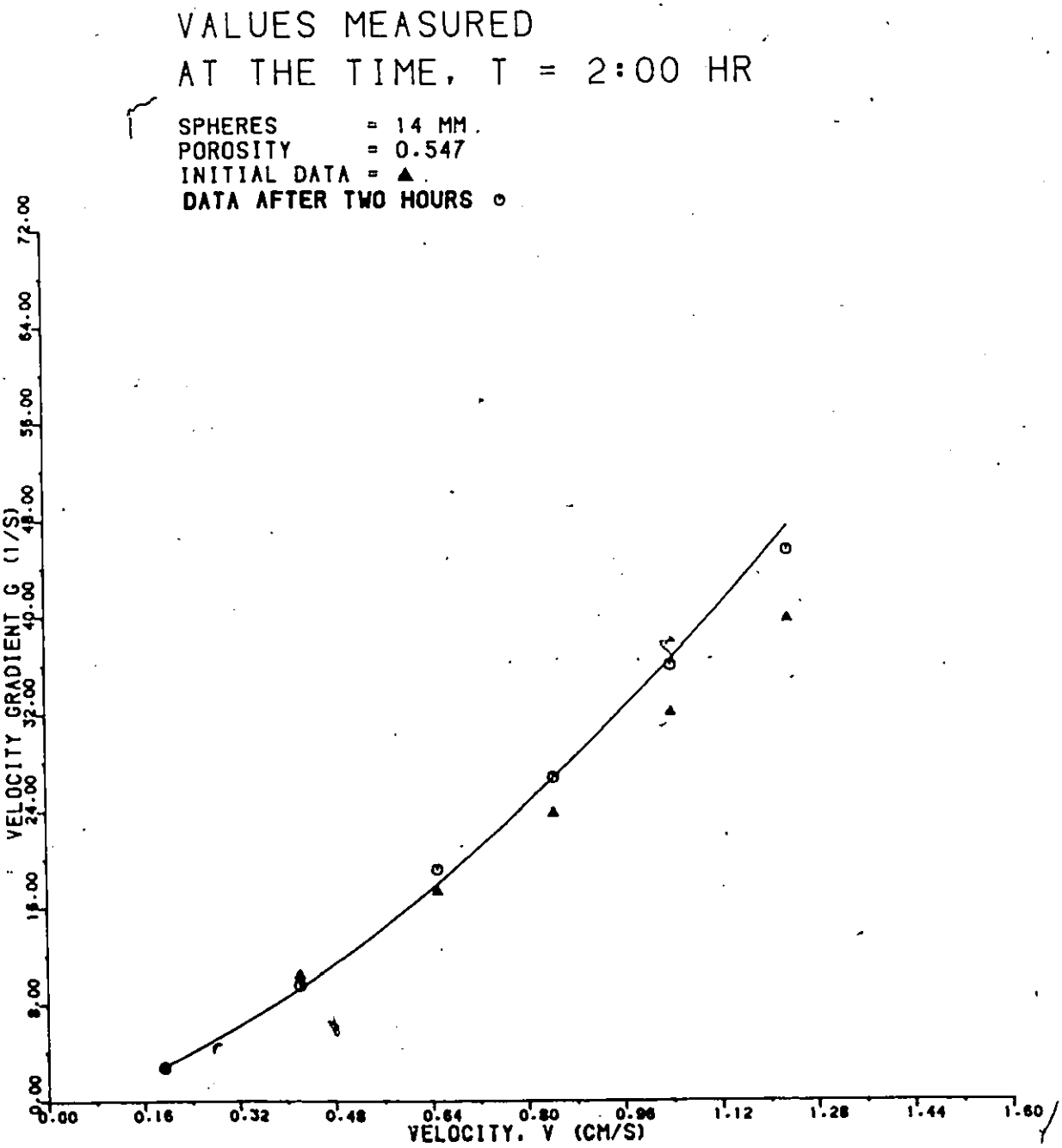

Figure 52: EFFECT OF LENGTH OF THE RUN ON G, 14 MM SPHERES, PARTIALLY CLOGGED MEDIA

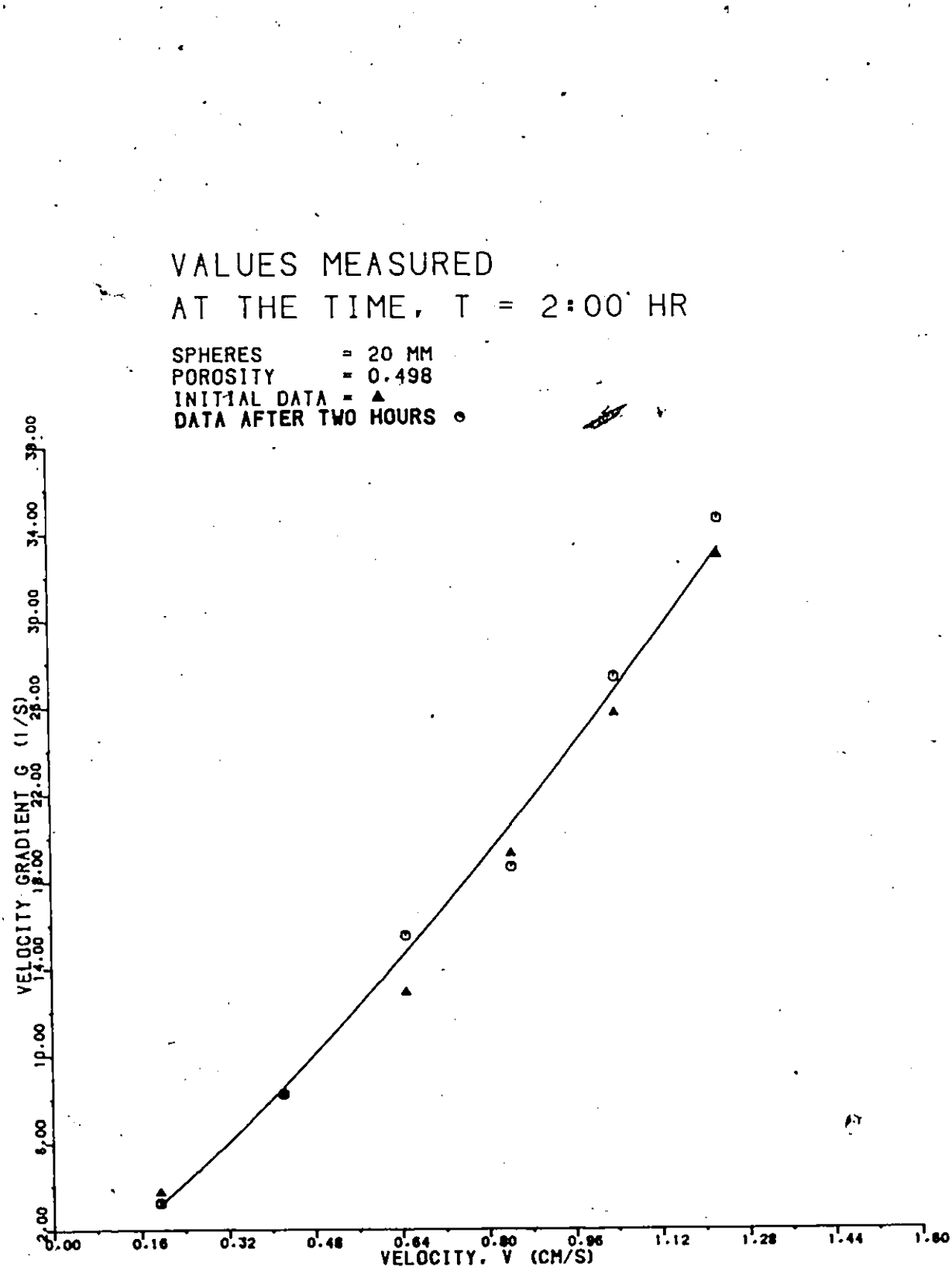

Figure 53: EFFECT OF LENGTH OF THE RUN ON G, 20 MM SPHERES, PARTIALLY CLOGGED MEDIA

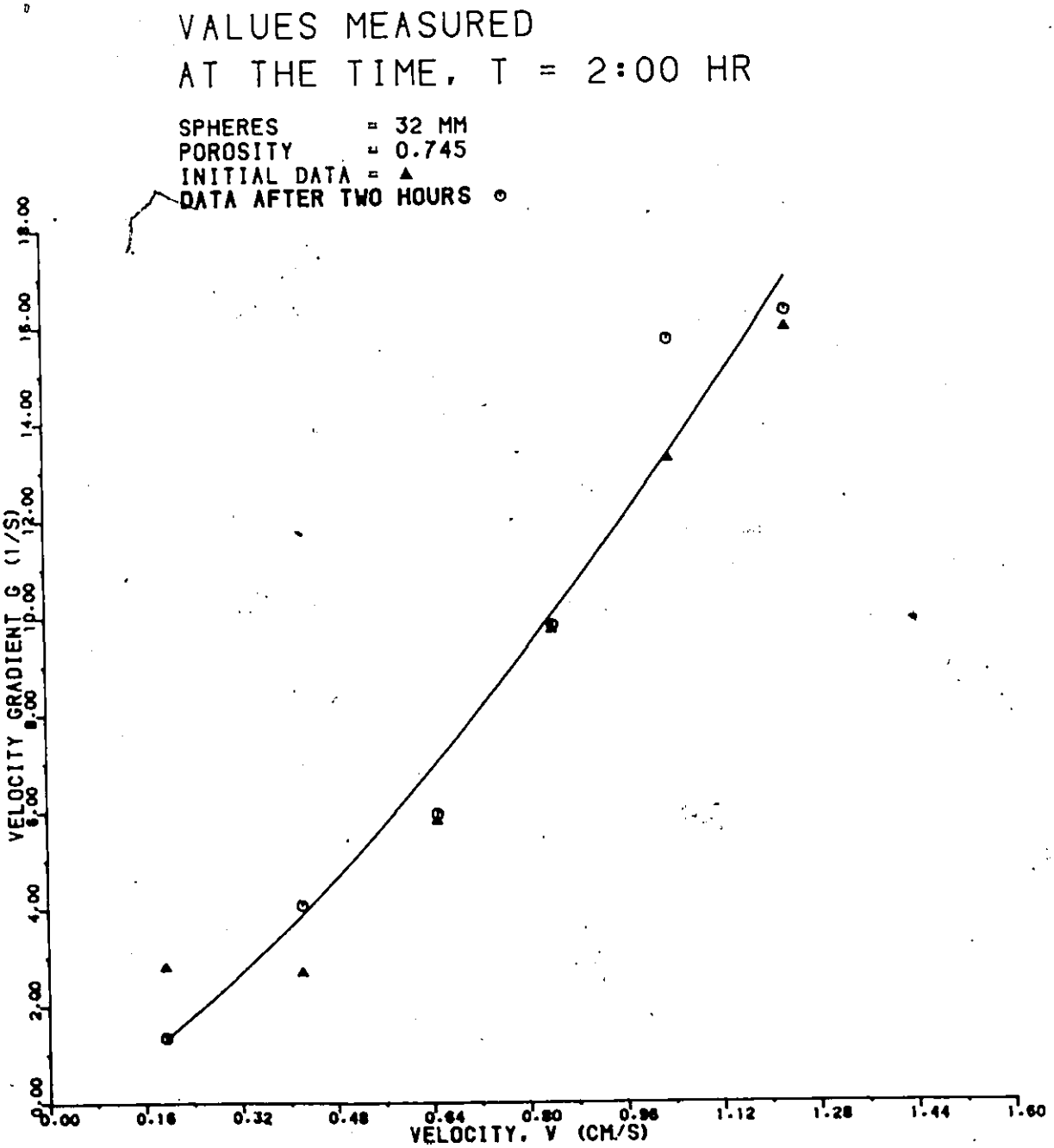

Figure 54: EFFECT OF LENGTH OF THE RUN ON G, 32 MM SPHERES, PARTIALLY CLOGGED MEDIA

CHAPTER V

CONCLUSIONS

The main objective of this study was to investigate the applicability of flow in granular media for purpose of flocculation.

It was assumed that media size and flow rate are fundamental parameters of successful flocculation. Furthermore, it was assumed that mixing properties of the media could be represented by a function of Reynold's number, R_K, defined in terms of permeability.

To achieve objective associated with this work, a series of tracer tests were carried out to estimate value of D with respect to R_K. Three different sizes of media were tested with six compatible flow velocities. In an analysis of the dispersion properties of the porous media, Scheidegger's (1960) development was used as a starting point.

To analyze the influence of flow rate and media size on flocculation, it was necessary to find a relation describing fluid motion in porous media. It was assumed that degree of clogging depends mainly on media size and initial flow velocity. During the flocculation studies, it was found that for "average" porosities, an equation developed by Ward (1964) accurately described flow properties in clean and partially clogged beds.

It was demonstrated that flocculation in granular media is a useful alternative to the commonly used paddle and baffle flocculators. The following major conclusions are drawn from the study:

1) The mixing properties of granular media described by dispersion coefficient can be successfully presented in the form of geometric function of Reynold's number. Similarly, the relation between dispersion coefficient and flow velocity closely follow theoretical findings; however, coefficient values are smaller.

2) In beds built of uniform spheres, particle size and media porosity are considered to be main parameters of successful flocculation. This study revealed weak response of the flocculator to the changing flow velocity.

3) It was found that above the R_K value of 7 exists a region where effectiveness of flocculation increases and adverse effects of clogging are minimized. The flow parameters in this region for clean and partially clogged media can be successfully described by means of the Ward flow equation.

4) Changes in flow rate and/or changes in coagulant feed result in increase of turbidity of settled sample. However, effluent has turbidity lower than raw water supplied into the flocculator.

5) The rate of decrease of primary particles can be better described by geometric function then by the exponential expression (Eq. 2.63) recommended by Richter (1977).

This behavior can be explained by the high R_k, where Harris' equation was developed for flocculation in purely laminar flow regimes.

6) Reynold's number based on permeability of the media, is considered to be a useful parameter for the monitoring and design of granular media flocculation.

CHAPTER VI

RECOMMENDATIONS FOR FUTURE WORK

The experience gained from this study allows the experimenter to formulate several suggestions which can help in further investigation of the topic.

1) Examination of a wide variety of media sizes of spherical and nonspherical shapes is suggested. Information obtained from such experiments would be helpful in understanding the influence of shape and porosity on the overall kinetic process.

2) Furthermore, an examination of R_K as a flocculation parameter, through tests in higher velocities and lower porosities is recommended. The study indicated great potential of R_K as a process monitoring and designing parameter.

3) Close monitoring of rate of deposition in the media, through measurement of total filterable solids is suggested. This would allow the influence of clogging on headloss, output rate and overall performance to be determined.

4) Examination and comparison between the constant flow and the declining flow rate regime is recommended. This would help in determining the influence of clog-

ging on development of critical velocity and kinetics of the process.

5) Finally, formulation and examination of the process kinetic equation which closely describes flocculation in nonlinear laminar flow regimes is recommended.

APPENDIX A

REGRESSION ANALYSIS

A regression analysis was performed on an Apple II C microcomputer using programs written in the BASIC programming language listed by Poole *et al.* (1979)

A.1 Fitting of J vs Flow Velocity Curves (Figs. 45-47)

Least squares approximation with polynomial of 2nd degree:

$$J = aV + bV^2 + c \qquad (A.1)$$

where: V = apparent flow velocity, m/s
J = hydraulic gradient

Table A.1 J vs Velocity Curves, Regression Parameters

Spheres mm	a	b	c	Coefficient CD	Coefficient CC	Standard Error
32	-9.296×10^{-4}	2.624×10^{-3}	4.621×10^{-4}	0.9641	0.9819	2.047×10^{-4}
20	-2.215×10^{-4}	8.359×10^{-4}	7.385×10^{-4}	0.9964	0.9982	2.715×10^{-4}
14	0.011	3.113×10^{-3}	-1.486×10^{-3}	0.9961	0.9981	4.043×10^{-4}

where: CD = coefficient of determination
CC = coefficient of correlation

A.2 Fitting of G vs Flow Velocity Curves (Figs. 48-51) For Initial Conditions and Partially Clogged Beds

Least square approximation with geometric expression:

$$G = aV^b \qquad (A.2)$$

where: G = velocity gradient, 1/s
V = flow velocity, m/s

Table A.2 G vs Velocity Curves, Regression Parameters, Initial Conditions

Spheres mm	a	b	CD	CC	Standard Error
32	76.881	1.041	0.8468	0.9202	0.3376
20	216.822	1.179	0.9922	0.9960	0.0796
14	429.366	1.408	0.9944	0.9972	0.0803

Table A.3 G vs Velocity Curves, Regression Analysis For Partially Clogged Bed

Spheres mm	a	b	CD	CC	Standard Error
32	15.344	1.377	0.9871	0.9935	0.1201
20	30.418	1.271	0.9958	0.9979	0.0630
14	42.410	1.515	0.9984	0.9992	0.0462

A.3 Fitting of N_o/N_m vs V Curves (Figs. 39-41)

Least squares approximation with polynomial of 2nd degree:

$$N_o/N_m = a + bV + cV^2 \qquad (A.3)$$

Table A.4 N_o/N_m vs V Curves, Regression Parameters

Spheres mm	a	b	c	CD	CC	Standard Error
32	1.129	1.159	-0.973	0.9638	0.9817	0.0249
20	1.966	-0.739	1.518	0.9933	0.9966	0.0516
14	2.756	-1.671	1.824	0.8111	0.9006	0.1619

A.4 Fitting of N_o/N_m vs R_K Curves (Figs. 41-44)

Least squares approximation with polynomial of 2nd degree:

$$N_o/N_m = a + bR_K + cR_K^2 \qquad (A.4)$$

Table A.5 N_o/N_m vs R_K Curves, Regression Parameters

Spheres mm	a	b	c	CD	CC	Standard Error
32	1.129	1.159	-0.973	0.9638	0.9817	0.0249
20	1.966	-0.739	1.518	0.9933	0.9966	0.0516
14	2.756	-1.671	1.824	0.8111	0.9006	0.1619

APPENDIX B

EXPERIMENTAL DATA

Table B.1 Flocculation Data, Media Size 32 mm

Time HRS	Flow rate x 10^{-3} m^3/s	Piezometer cm		Turbidity NTU		
		No.2	No.6	No.2	No.4	No.6
temperature 21 °C, C_o = 71 NTU						
0.0	0.1908	98.500	98.055	64	60	55
0.5		98.510	98.060	62	59	56
1.0	0.190	98.510	98.055	64	63	61
1.5		98.515	98.065	66	63	58
2.0	0.190	98.530	98.065	64	61	56
2.5	0.1901	98.550	98.080	66	63	58
temperature 21°C, C_o = 74 NTU						
0.0	0.1718	98.365	98.000	63	59	54
0.5		98.370	98.000	64	59	53
1.0	0.1709	98.375	97.990	64	58	53
1.5		98.290	97.890	61	58	54
2.0	0.1706	98.260	97.745	61	57	52
temperature 19°C, C_o = 71 NTU						
0.0	0.1385	98.060	97.805	66	64	64
0.5	0.1380	98.060	97.800	66	64	64
1.0	0.1376	98.060	97.805	63	63	62
1.5	0.1364	98.055	97.800	65	64	64
2.0	0.1345	98.060	97.800	64	62	62
temperature 24°C, C_o = 71 NTU						
0.0	0.098	100.715	100.610	56	51	44
0.5		100.715	100.610	58	54	48
1.0	0.097	100.715	100.605	58	55	50
1.5		100.710	100.600	54	50	44
2.0	0.096	100.710	100.600	54	52	48
2.5		100.700	100.590	56	52	50
3.0	0.095	100.680	100.580	62	59	54

Table B.1 Flocculation Data , continued

Time HRS	Flow rate x 10^{-3} m^3/s	Piezometer cm		Turbidity NTU		
		No.2	No.6	No.2	No.4	No.6
temperature 21°C, C_o = 66 NTU						
0.0	0.065	100.430	100.350	54	51	46
0.5	0.064	100.410	100.325	54	50	46
1.0	0.064	100.390	100.300	55	51	46
1.5	0.063	100.290	100.210	54	51	48
2.0	0.063	100.260	100.175	53	50	47
2.5	0.062	100.230	100.135	54	51	48
3.0	0.060	100.230	100.135	55	52	49
temperature 22°C, C_o = 69 NTU						
0.0	0.032	97.000	96.905	65	63	61
1.0	0.031	96.870	96.830	64	62	60
2.0	0.031	96.860	96.840	63	61	61
3.0	0.031	96.850	96.840	64	63	63
4.0	0.030	96.860	96.830	66	64	64
5.0	0.030	96.855	96.830	65	63	62

Table B.2 Flocculation Data, Media Size 20 mm

Time HRS	Flow rate x 10^{-3} m^3/s	Piezometer cm No.2	Piezometer cm No.6	Turbidity NTU No.2	Turbidity NTU No.4	Turbidity NTU No.6
temperature 21°C, C_o = 61 NTU						
0.0	0.197	83.825	81.915	34	29	23
1.0	0.196	83.970	81.965	38	33	24
2.0	0.194	84.065	81.955	34	32	24
3.0	0.193	84.230	81.970	33	29	23
4.0	0.193	84.300	81.975	37	33	24
5.0	0.193	84.355	81.965	36	30	24
6.0	0.190	84.405	81.965	44	37	28
temperature 20°C, C_o = 71 NTU						
0.0	0.165	83.130	81.750	39	42	27
1.0	0.163	83.265	81.745	42	44	30
2.0	0.162	83.350	81.750	47	40	30
3.0	0.161	83.395	81.750	44	35	28
4.0	0.158	83.430	81.740	37	34	26
5.0	0.158	83.460	81.750	50	35	26
6.0	0.158	83.500	81.740	50	38	28
7.0	0.157	83.535	81.740	53	42	30
temperature 19°C, C_o = 71 NTU						
0.0	0.137	82.575	81.575	55	50	33
1.0	0.122	82.410	81.505	53	41	31
2.0	0.120	82.440	81.500	57	46	34
3.0	0.119	82.435	81.475	53	43	30
4.0	0.118	82.430	81.465	55	43	33
5.0	0.117	82.450	81.470	39	36	26
temperature 21°C, C_o = 71 NTU						
0.0	0.104	81.850	81.295	33	29	23
1.0	0.103	82.000	81.330	40	38	26
2.0	0.102	82.125	81.320	43	37	23
3.0	0.102	82.190	81.315			
4.0	0.102	82.225	81.315	40	33	27
5.0	0.102	82.335	81.315	37	33	26
6.0	0.101	82.340	81.290	37	33	24
7.0	0.103	82.385	81.315	50	36	32
temperature 17°C, C_o = 72 NTU						
0.0	0.066	81.345	80.965	54	51	44
1.0	0.061	81.325	80.965	49	47	43
2.0	0.060	81.340	80.955	49	46	37
3.0	0.059	81.375	80.960	49	46	40
4.0	0.058	81.395	80.950	56	51	40
5.0	0.058	81.405	80.950	52	51	37
6.0	0.058	81.400	80.930	52	40	33

Table B.2 Flocculation Data, continued

Time HRS	Flow rate x 10^{-3} m^3/s	Piezometer cm		Turbidity NTU		
		No.2	No.6	No.2	No.4	No.6
temperature 18°C, C_o = 71 NTU						
0.0	0.030	80.755	80.590	45	42	38
1.0	0.028	80.695	80.570	58	62	36
2.0	0.027	80.700	80.575	55	47	36
3.0	0.027	80.695	80.575	48	44	35
4.0	0.026	80.590	80.570	50	44	38
5.0	0.026	80.690	80.575	53	48	39
6.0	0.025	80.695	80.575	53	45	39
7.0	0.025	80.665	80.570	54	47	39
8.0	0.025	80.665	80.565	51	39	36

Table B.3 Flocculation Data, Media Size 14mm

Time HRS	Flow rate x 10^{-3} m^3/s	Piezometer cm		Turbidity NTU		
		No.2	No.6	No.2	No.4	No.6
temperature 24°C, C_o = 71 NTU						
0.0	0.193	84.875	82.345	34	32	28
1.0	0.186	85.245	82.350	32	26	19
2.0	0.184	85.425	82.060	31	26	20
3.0	0.190	86.240	82.135	42	38	30
4.0	0.192	86.270	82.075	28	26	26
5.0	0.193	86.245	82.070	28	25	20
temperature 20°C, C_o = 70 NTU						
0.0	0.165	84.065	81.885	32	30	30
1.0	0.161	84.460	81.930	36	32	26
2.0	0.160	84.680	81.930	38	32	25
3.0	0.158	84.930	81.945	31	27	20
4.0	0.158	84.720	81.935	32	27	21
5.0	0.156	85.240	81.915	31	27	21
temperature 19°C, C_o = 71 NTU						
0.0	0.135	83.255	81.740	49	43	38
1.0	0.134	83.465	81.745	52	44	35
2.0	0.132	83.675	81.755	47	39	31
3.0	0.126	83.735	81.735	42	35	28
4.0	0.121	83.740	81.690	39	31	25
5.0	0.112	83.570	81.545	49	35	26
temperature 19°C, C_o = 69 NTU						
0.0	0.103	82.395	81.350	51	43	34
1.0	0.101	82.550	81.385	48	39	30
2.0	0.099	82.670	81.390	40	34	25
3.0	0.098	82.835	81.395	44	37	31
4.0	0.098	82.955	81.380	40	31	26
5.0	0.097	83.065	81.380	53	31	27

Table B.3 Flocculation Data, continued

Time HRS	Flow rate x 10^{-3} m^3/s	Piezometer cm		Turbidity NTU		
		No.2	No.6	No.2	No.4	No.6
temperature 21°C, C_o = 71 NTU						
0.0	0.067	81.585	81.005	38	34	29
1.0	0.054	81.430	80.945	35	30	28
2.0	0.051	81.425	80.930	47	41	28
3.0	0.050	81.395	80.905			
4.0	0.049	81.410	80.895	40	34	29
5.0	0.046	81.395	80.860	36	33	30
6.0	0.045	81.380	80.835	52	43	29
7.0	0.044	81.375	80.835	48	42	30
8.0	0.044	81.365	80.790	49	38	32
9.0	0.043	81.390	80.795	stop-and-start		
9.0	0.046	81.520	80.795	37	33	26
10.0	0.043	81.505	80.825	43	40	28
11.0	0.041	81.490	80.820	43	38	22
12.0	0.040	81.475	80.805	51	44	29
13.0	0.039	81.445	80.795	48	43	28
14.0	0.038	81.430	80.780	44	41	27
15.0	0.038	81.430	80.780	39	37	28
16.0	0.036	81.415	80.765	44	39	31
17.0	0.035	81.395	80.750	34	30	24
18.0	0.033	81.390	80.745	39	34	29
19.0	0.033	81.365	80.730	50	42	30
20.0	0.032	81.310	80.695	44	38	28
21.0	0.031	81.290	80.685	54	48	30
22.0	0.030	81.285	80.670	57	44	33
23.0	0.030	81.270	80.660	50	40	32
24.0	0.030	81.265	80.650	50	39	32
temperature 21°C, C_o = 71 NTU						
0.0	0.029	80.675	80.585	46	38	31
1.0	0.028	80.610	80.545	45	37	28
2.0	0.026	80.620	80.535	55	46	36
3.0	0.025	80.635	80.510	45	36	26
4.0	0.024	80.660	80.495	35	29	24
5.0	0.021	80.675	80.340	37	27	22

Table B.4 Calculation of Permeability, k, using Ward's method, (units CGS)

$$k = \{ [c\rho V^2 + (c^2\rho^2V^4 + 4\mu VJ)^{1/2}]/2J \}^2$$

$c = 0.55$

Apparent Velocity V $\times 10^{-2}$ m/s	Piezometer $\times 10^{-2}$ m No.2	No.6	J = $\delta H/1.88$ $\times 10^{-3}$	Temp. °C	k cm^2
media size 32 mm					
0.188	97.000	96.905	0.095	22 R	0.0651
0.435	100.430	100.350	0.425	21 R	0.0554
0.669	100.715	100.610	0.558	24	0.1660
0.877	98.060	97.805	1.356	19	0.1110
1.070	98.365	98.000	1.941	21	0.1300
1.250	98.500	98.055	2.367	21	0.1330
			average k =		0.1350
media size 20 mm					
0.195	80.755	80.590	0.878	18 R	0.0595×10^{-2}
0.429	81.345	80.965	2.021	17	0.2610×10^{-2}
0.676	81.850	81.295	2.021	21	0.7530×10^{-2}
0.890	82.575	81.575	5.319	19	0.6980×10^{-2}
1.070	83.130	81.750	7.340	20	0.7710×10^{-2}
1.280	83.825	81.915	10.159	21	0.8180×10^{-2}
			average k =		0.6600×10^{-2}
media size 14 mm					
0.188	80.675	80.585	0.479	21	0.1730×10^{-2}
0.435	81.675	81.005	3.085	21	0.1190×10^{-2}
0.669	82.395	81.350	5.558	19	0.2040×10^{-2}
0.877	83.255	81.885	8.058	19	0.2870×10^{-2}
1.070	84.065	81.885	11.595	20	0.3090×10^{-2}
1.250	84.875	82.345	13.457	24	0.4290×10^{-2}
			average k =		0.2530×10^{-2}

R - rejected

Table B.5 Preliminary Data, Turbidity Variation with Time

Sample without alum.

Raw Water	Settled sample	
NTU	1 HR	20 HR
71	66	64
72	68	65

Unsettled sample with alum

Medium Size	Flow Rate	Raw Water		Sampling point	
mm	Lps		settled	No. 2	No.6
14	0.131	71	66	65	64
20	0.029	71	65	64	64

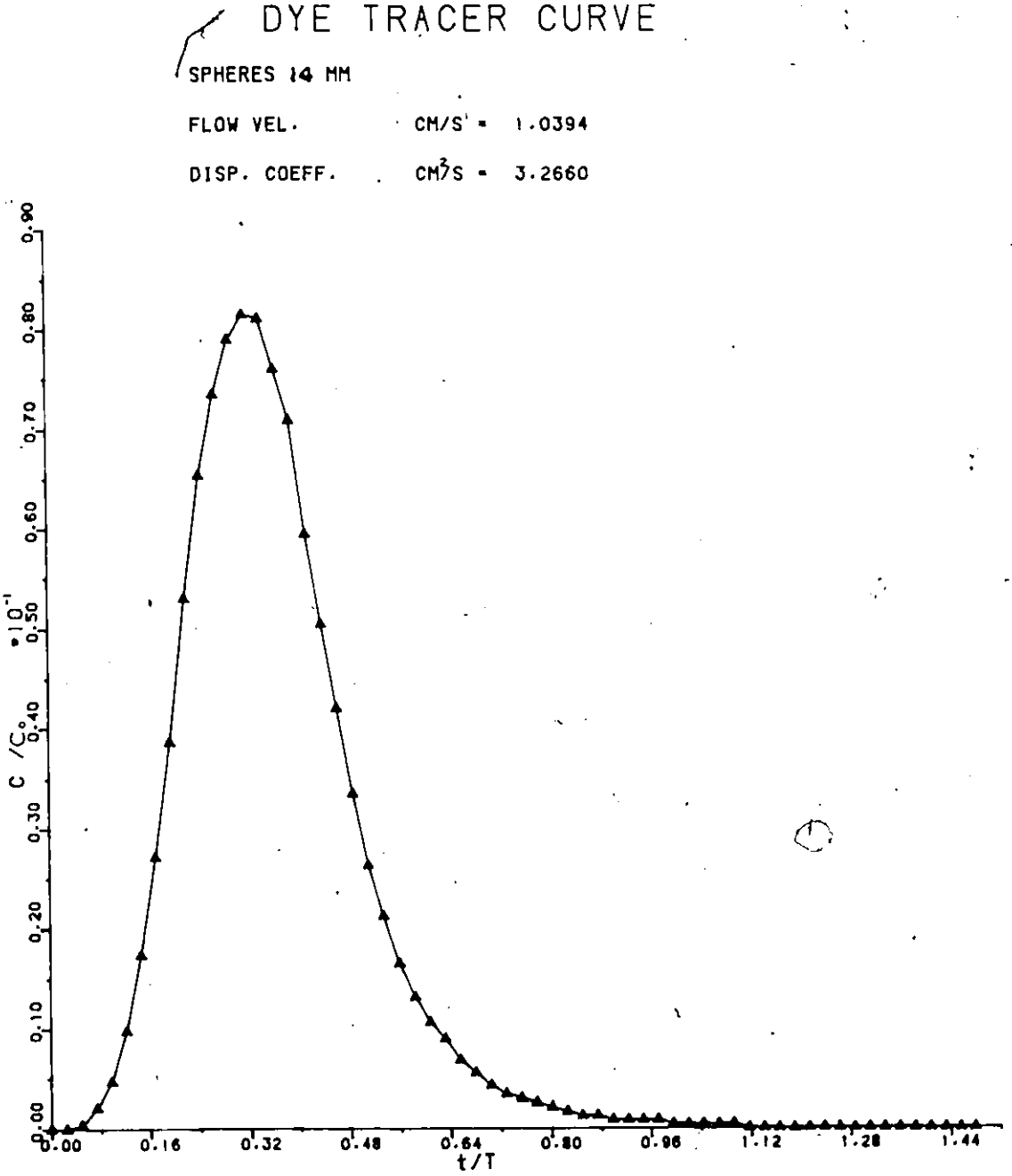

Figure B.1: TRACER TEST

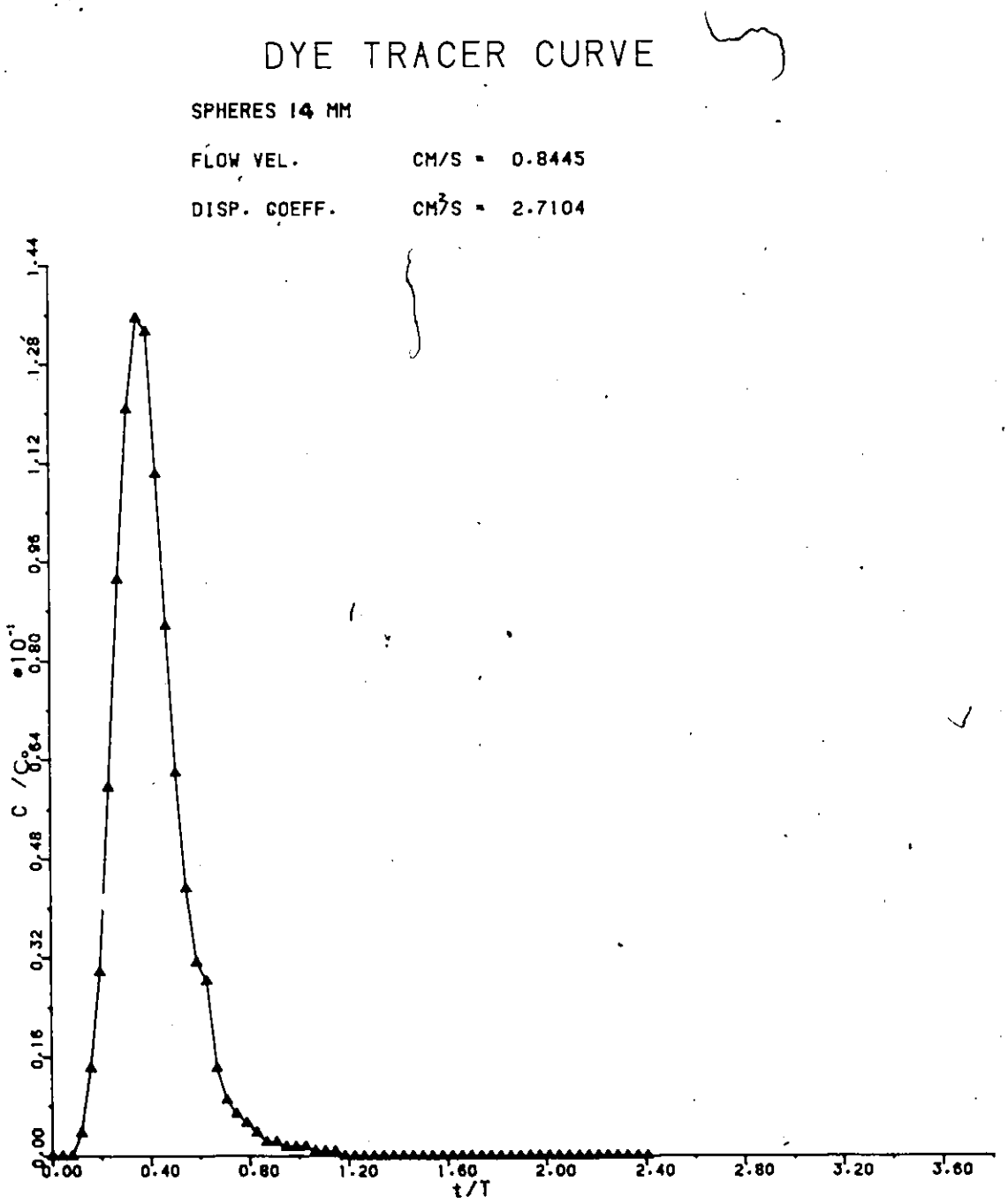

Figure B.2: TRACER TEST

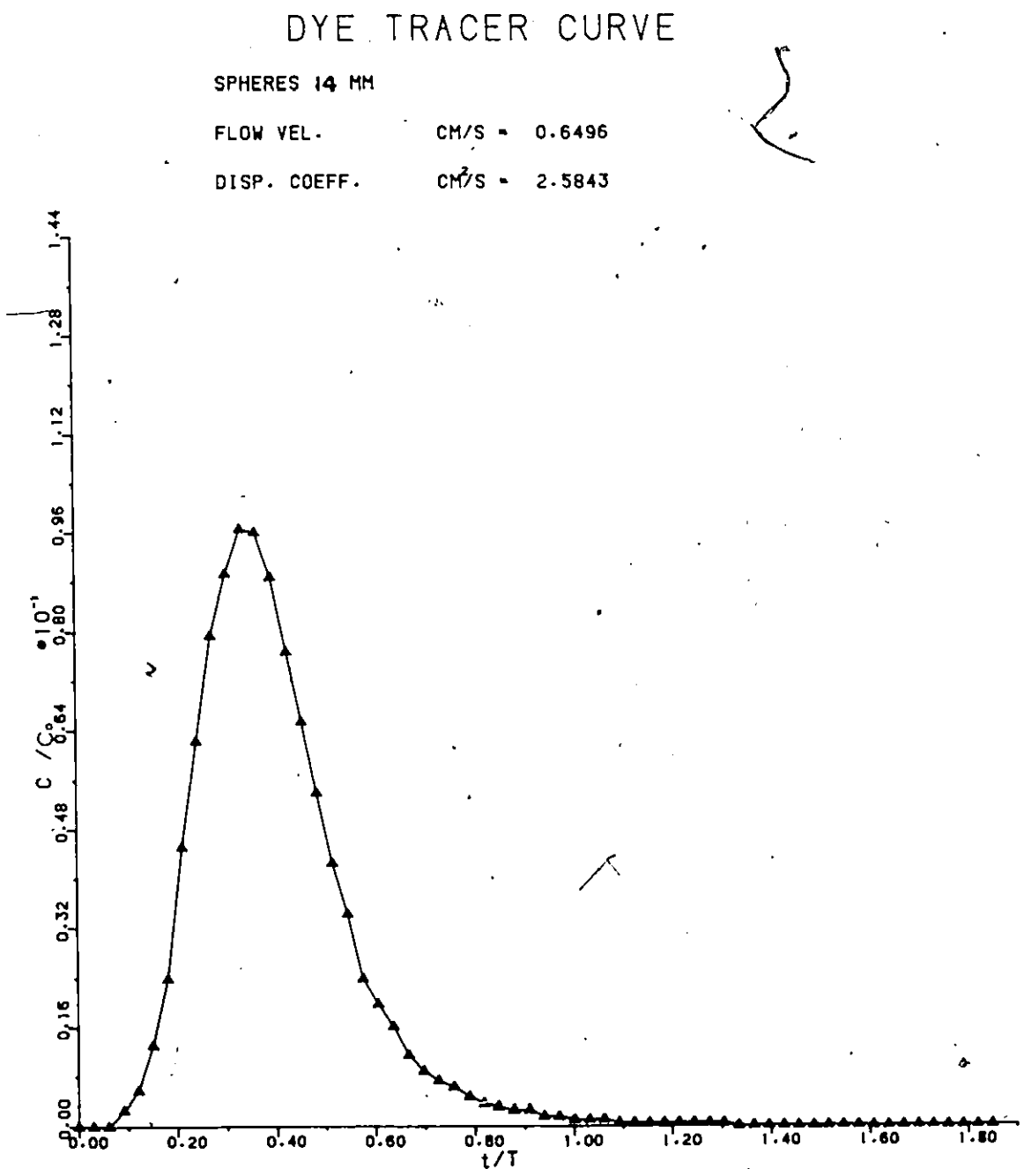

Figure B.3: TRACER TEST

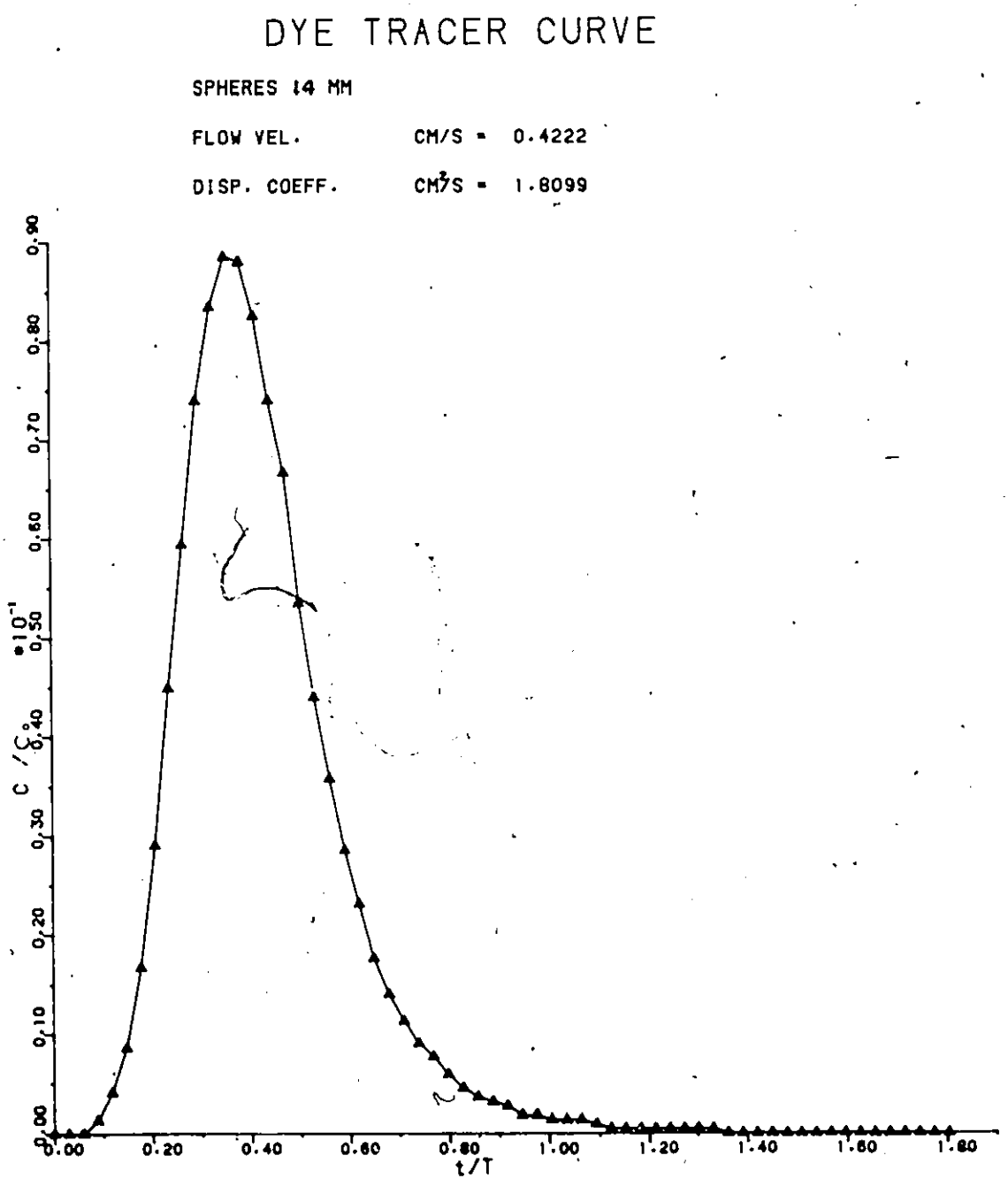

Figure B.4: TRACER TEST

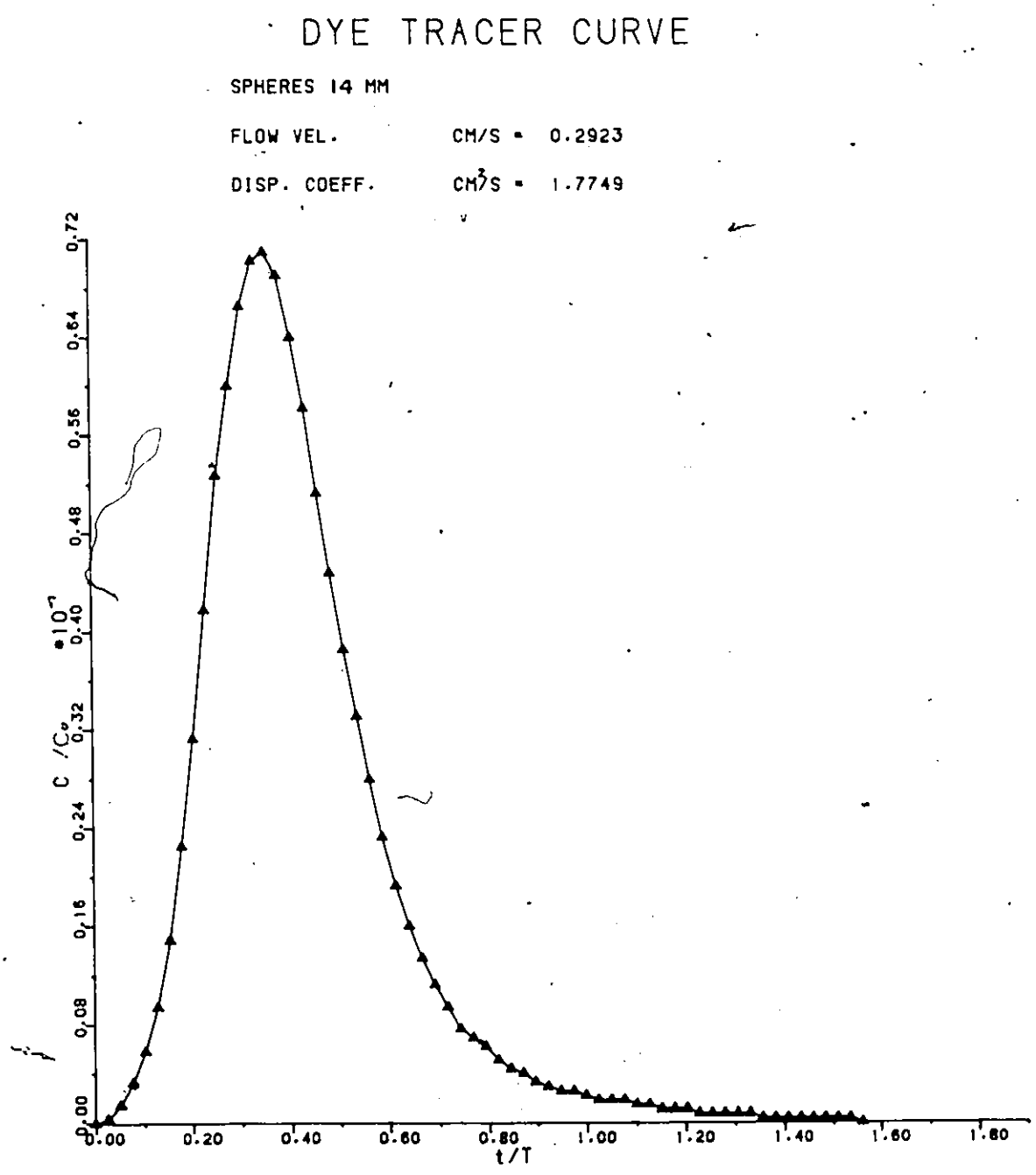

Figure B.5: TRACER TEST

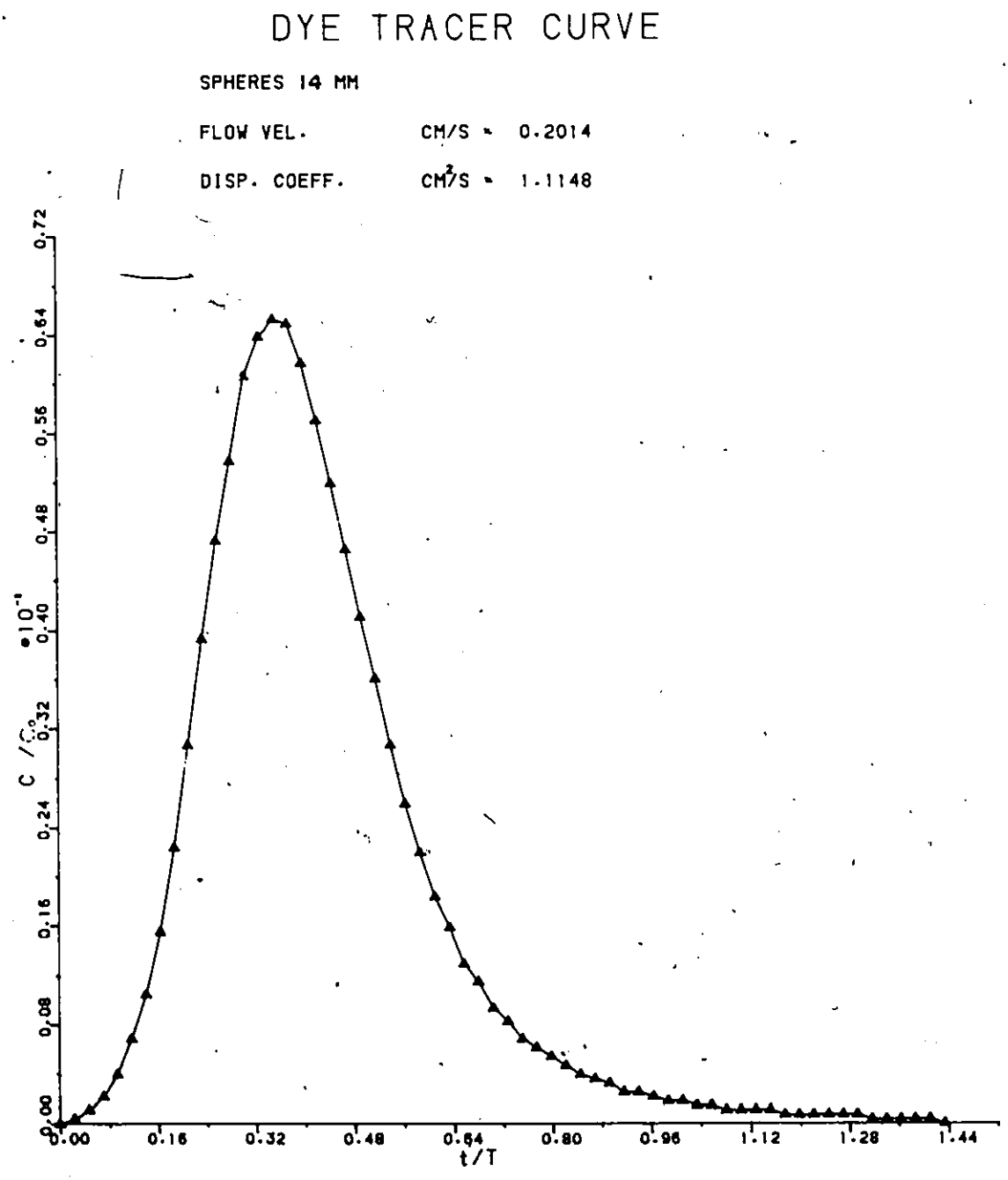

Figure B.6: TRACER TEST

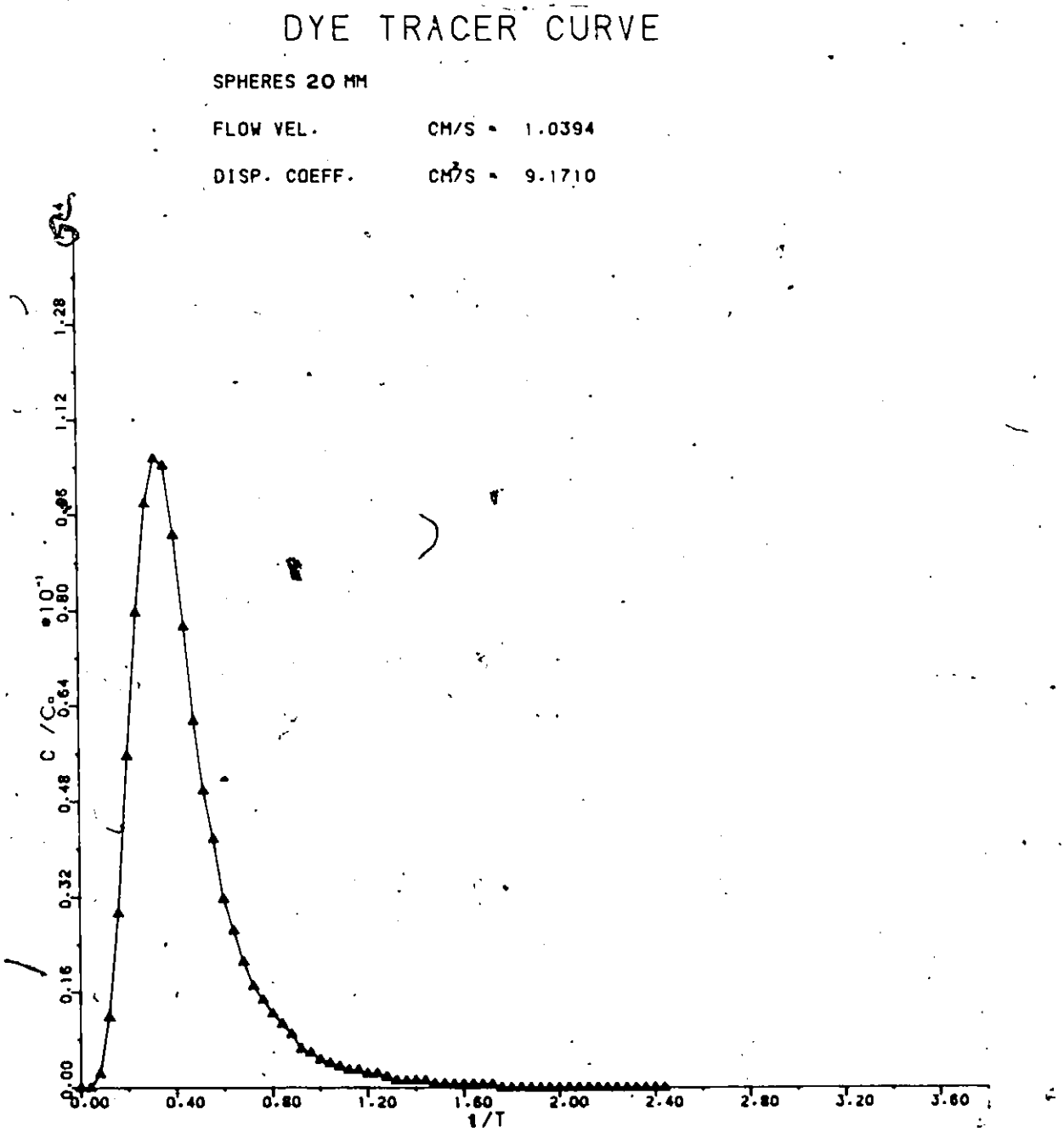

Figure B.7: TRACER TEST

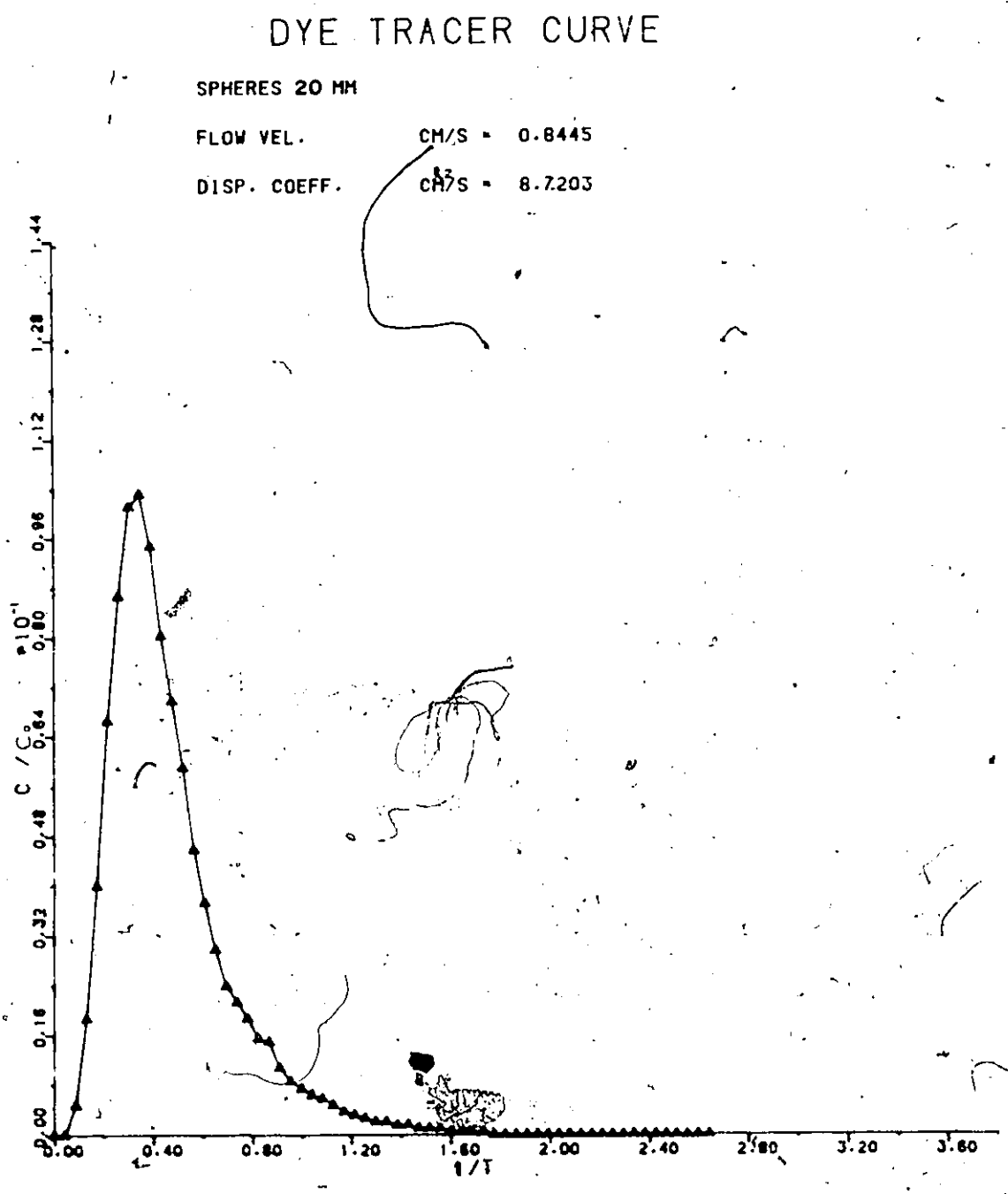

Figure B.8: TRACER TEST

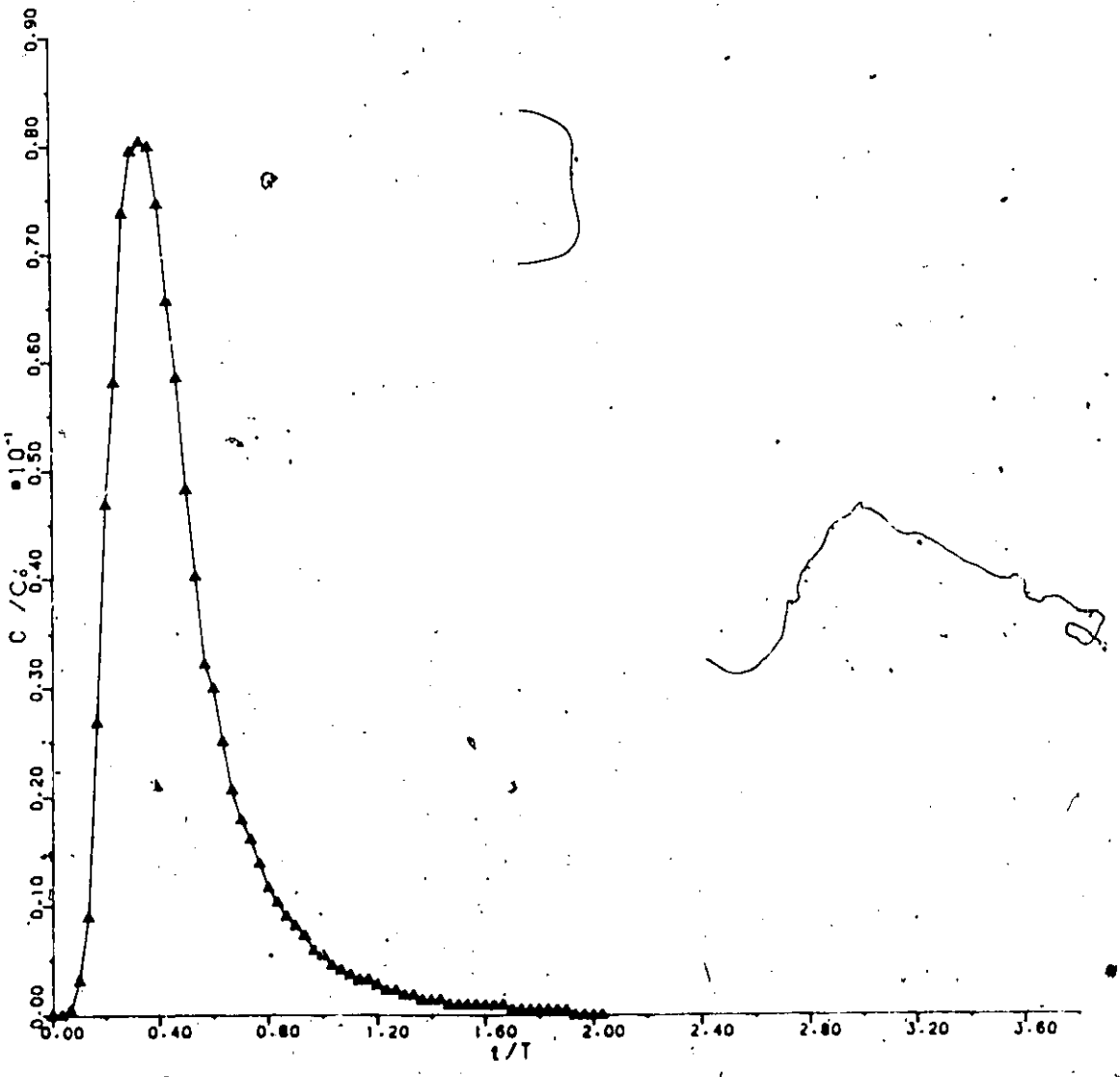

Figure B.9: TRACER TEST

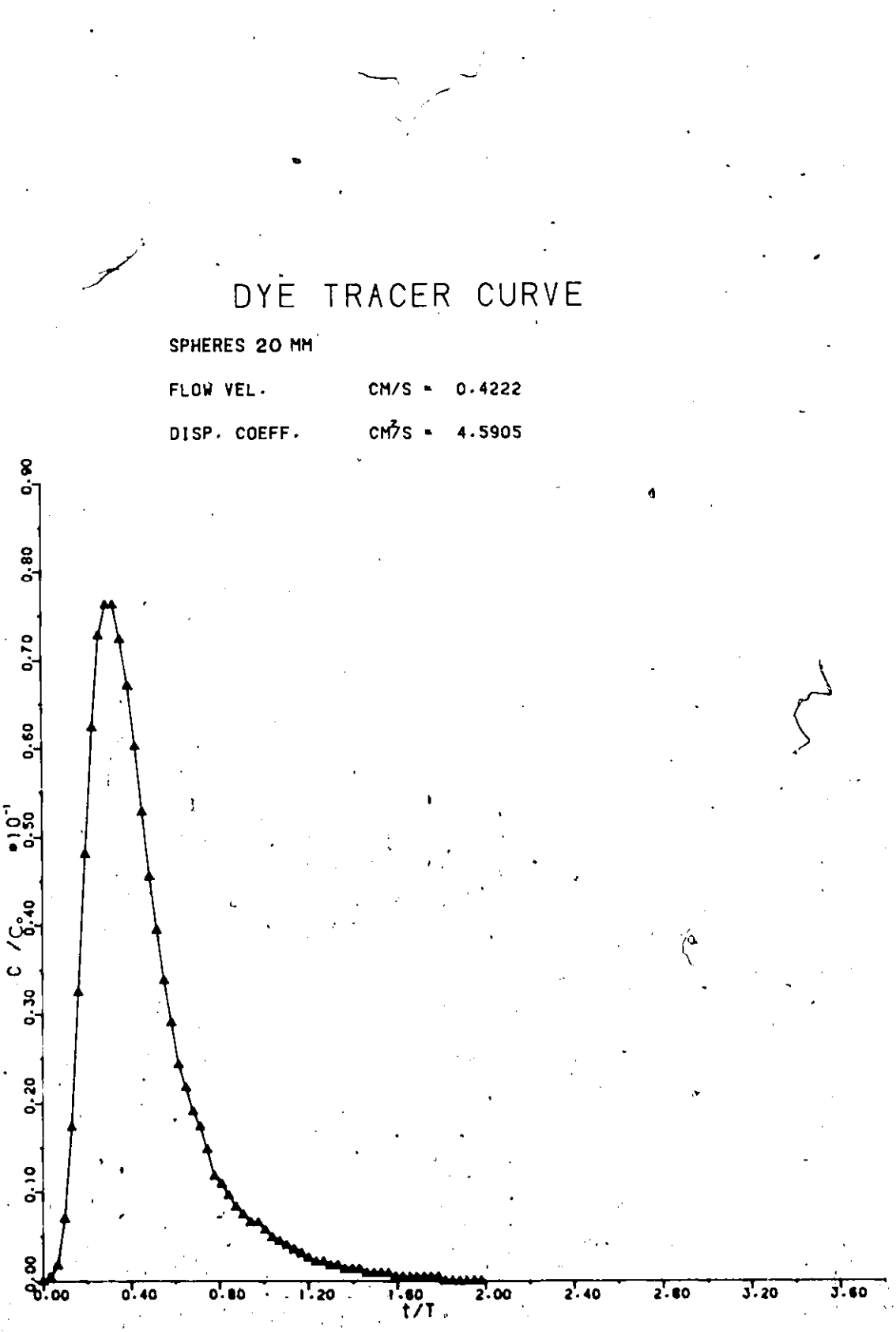

Figure B.10: TRACER TEST

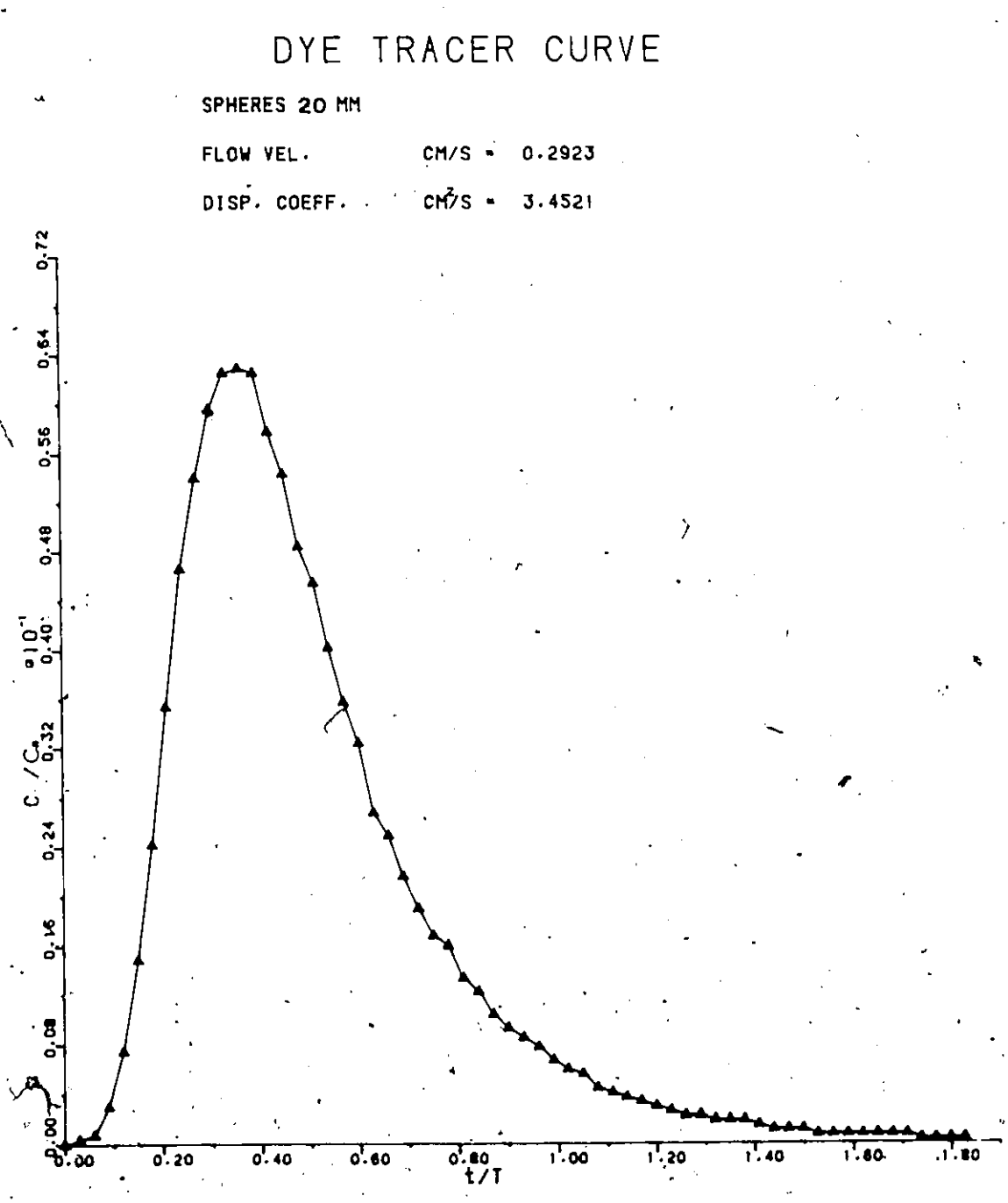

Figure B.11: TRACER TEST

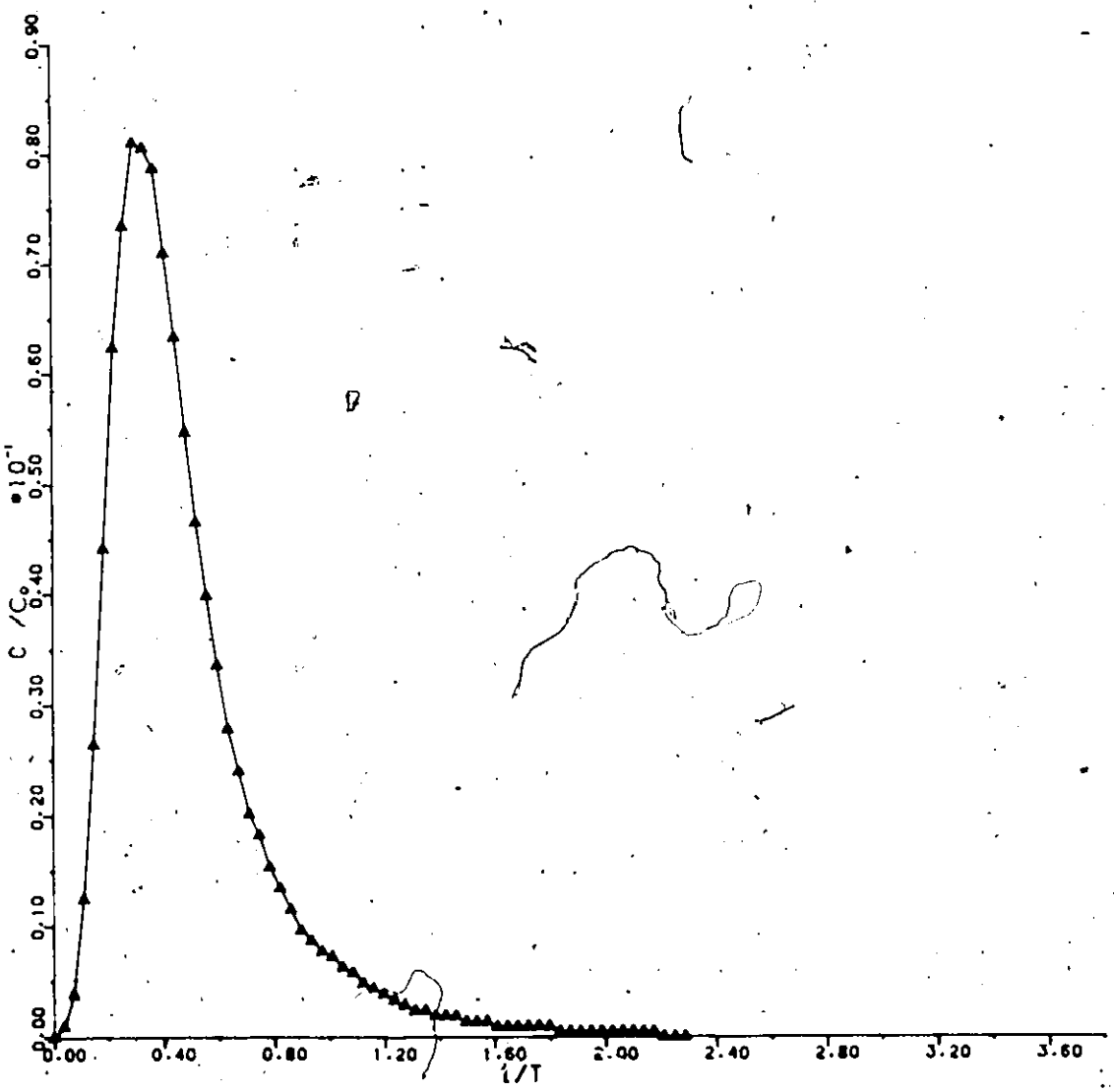

Figure B.12: TRACER TEST

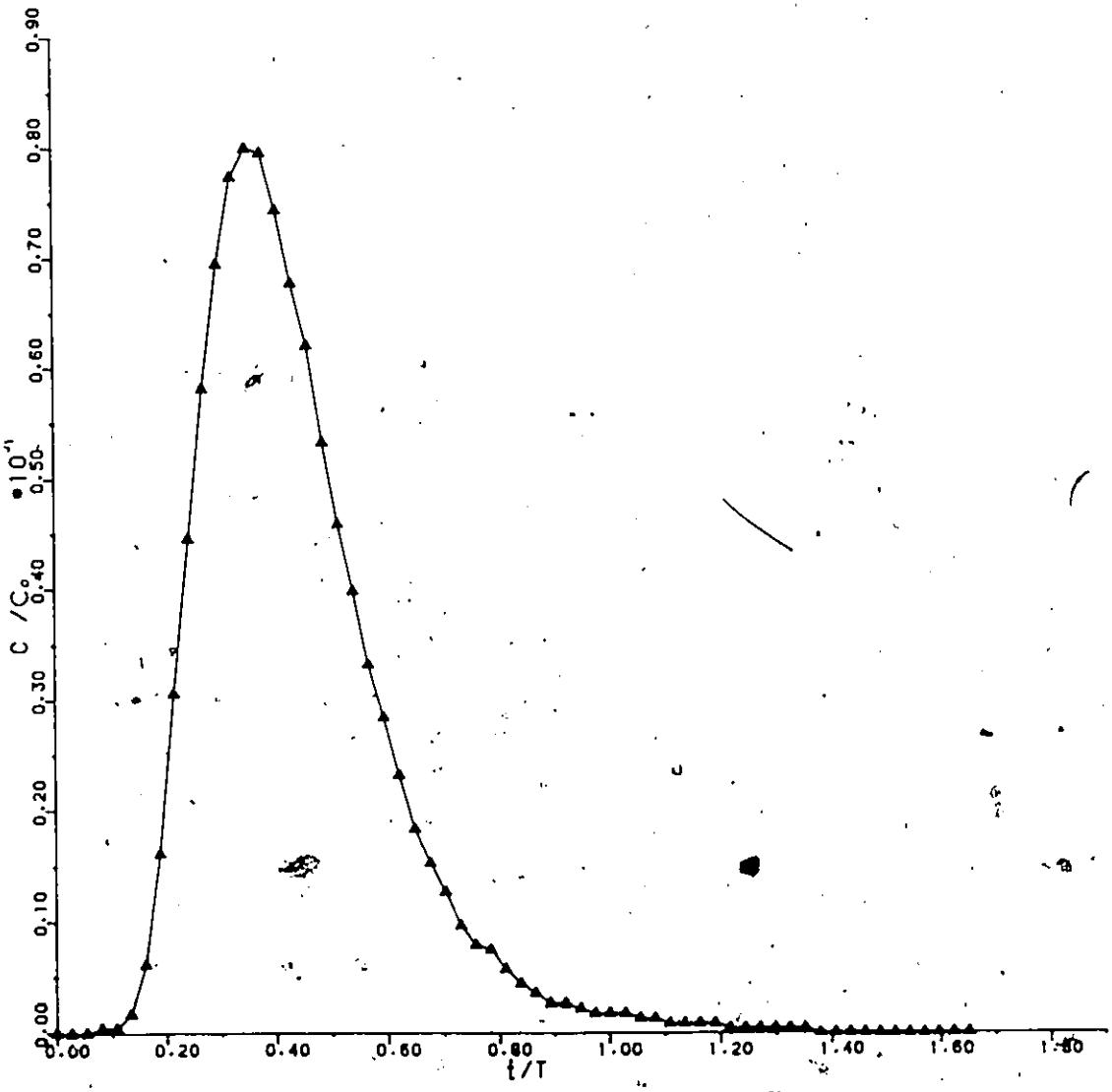

Figure B.13: TRACER TEST

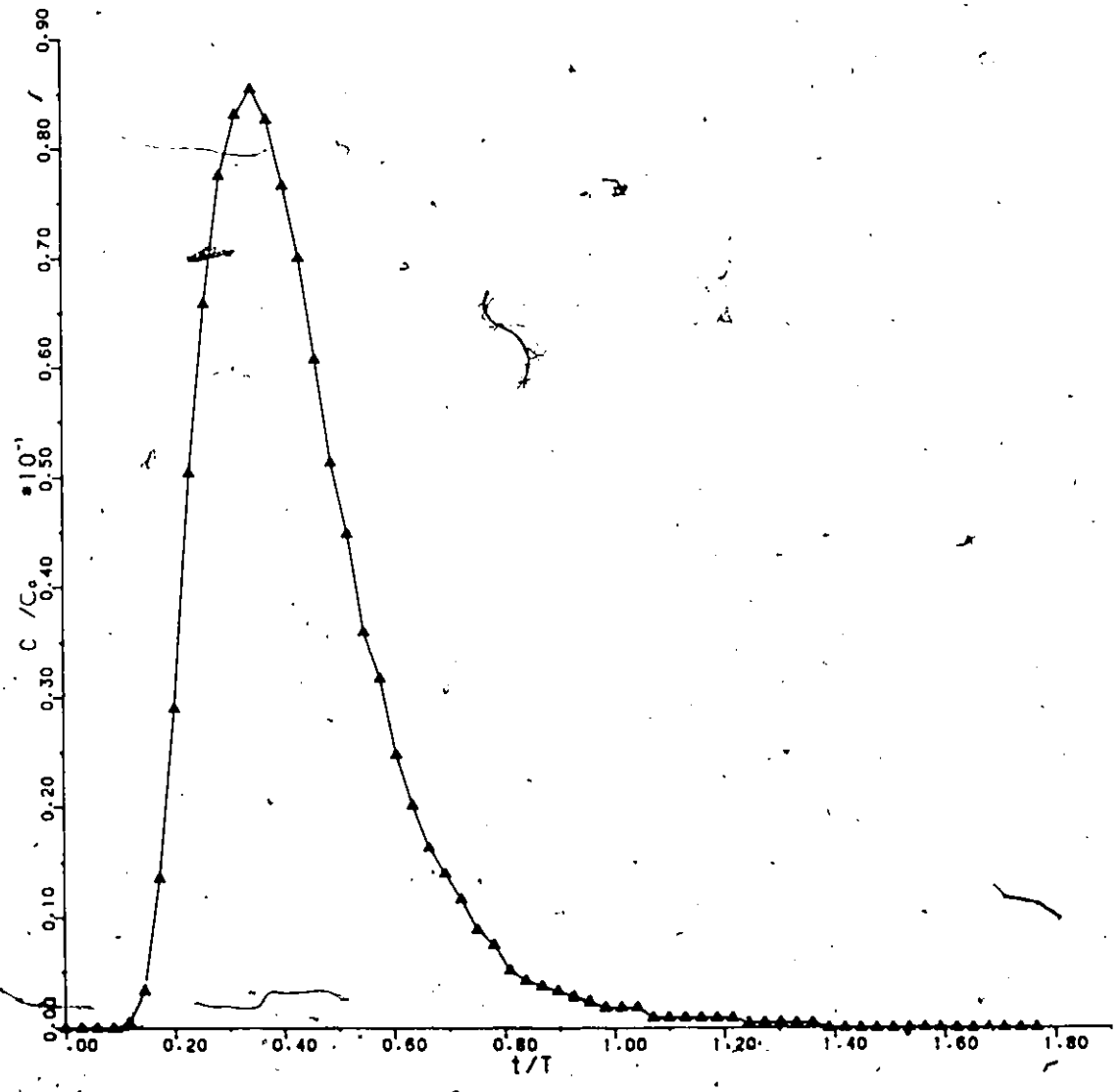

Figure B.14: TRACER TEST

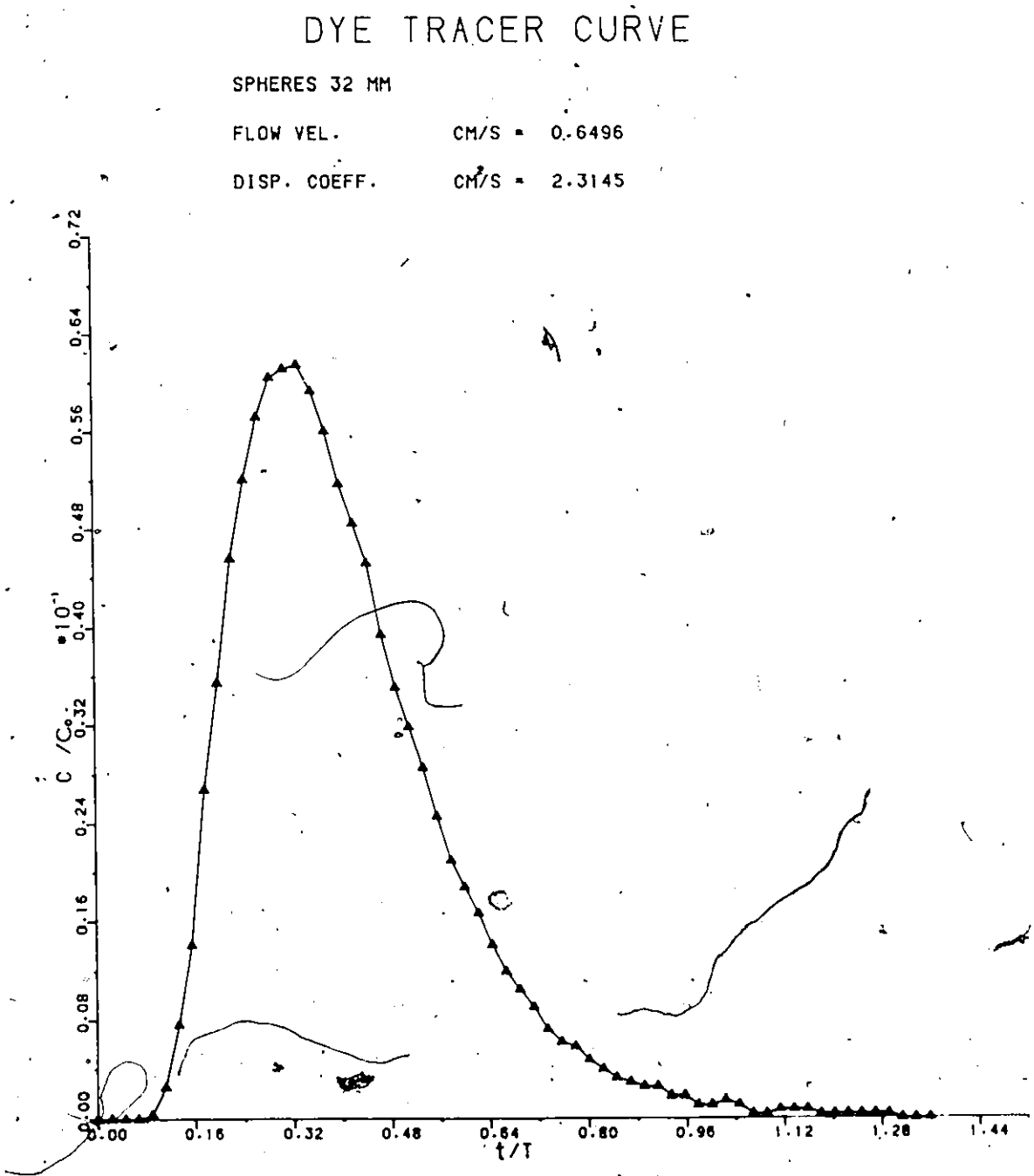

Figure B.15: TRACER TEST

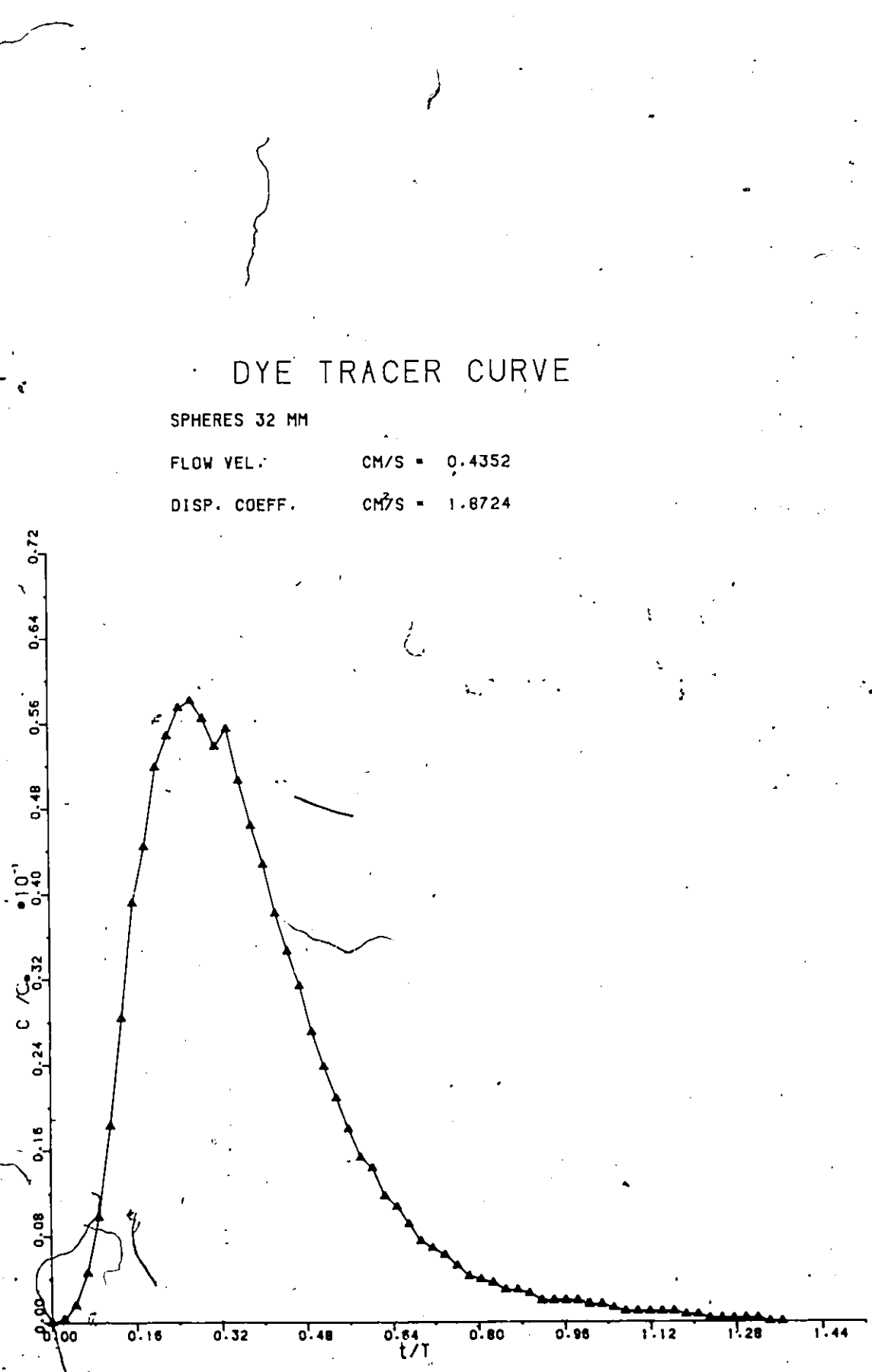

Figure B.16: TRACER TEST

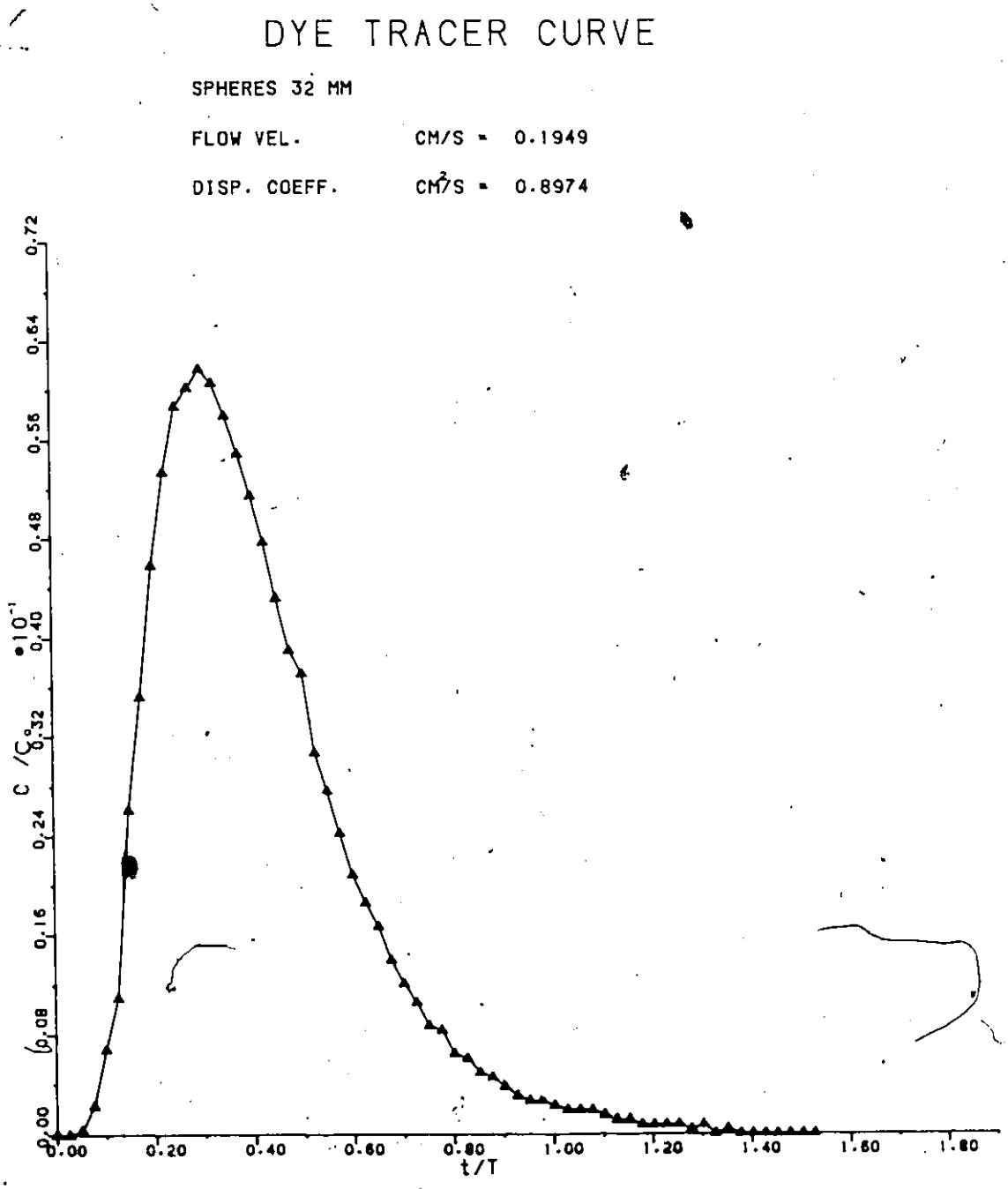

Figure B.17: TRACER TEST

REFERENCES

Adin, A. and Rebhun, M. 1974. High-Rate Contact Flocculation-Filtration with Cationic Polyelectrolytes. *Journal American Water Works Association*, 66, 2, pp.109-117 (Feb. 1974)

Adin, A. and Rebhun M. 1977. A Model to Predict Concentration and Headloss Profiles in Filtration. *Journal American Water Works Association*, 69, 8, pp. 444-453 (Aug. 1977)

Andreu-Villegas, R., Letterman, R.D. 1976. Optimizing Flocculator Power Input. *Journal of the Environmental Engineering Division, ASCE,* 102, EE2, April, pp. 251-263.

Arboleda, J. 1974. Hydraulic Control Systems of Constant and Declining Flow Rate in Filtration. *Journal American Water Works Association*, 66, 2, pp.67-84 (Feb. 1974)

Argaman, Y. and Kaufman, W.J. 1970. Turbulence and Flocculation. *Journal Sanitary Engineering Division, ASCE* 96, SA2, April, pp. 223-241.

Argaman, Y. 1971. Pilot-Plant Studies of Flocculation. *Journal American Water Works Association*, 63, 12, pp.775-777 (Dec. 1971)

Bear, J. 1972. *Dynamics of Fluids in Porous Media.* American Elsevier Scientific Publishing Company, New York.

Bhole, A.G. and Mhaisalkar, V.A. 1977. Study of a Low Cost Sand-Bed-Flocculator for Rural Areas. *Indian Journal Environmental HLTH.*, 19, 1, pp. 33-53.

Bird, R.B., Stewart W.E. and Lightfoot, E.N. 1960, *Transport Phenomena.* John Wiley & Sons Inc. N.Y.

Bischoff, K.B., Levenspiel, O. 1962. Fluid Dispersion-Generalization and Comparison of Mathematical Models. *Chemical Engineering Science*, 17, Feb., pp 245-264.

Bratby, J.R. 1977. Design of Flocculation Systems from Batch Test Data. *Water S.A.*, 3. 4. pp.173-180.

Bratby, J.R. 1980. *Coagulation and Flocculation.* Uplands Press Ltd, England.

Camp, T.R., Stein, P.C. 1943. Velocity Gradients and Internal Work in Fluid Motion. *Journal Boston Society Civil Engineers*, 30, 4, pp.219-237.

Camp, T.R. 1946. Sedimentation and the Design of Settling Tanks. *Transactions ASCE*, III, 909.

Camp, T.R. 1955. Flocculation and Flocculation Basins. *Transactions ASCE*, 120, 1, pp.4-16.

Camp, T.R. 1968. Floc volume concentration. *Journal American Water Works Association*, 60, 6, pp.656-673 (Jun. 1968).

Camp, T.R. 1969. discussion to Agglomerate Size Changes in Coagulation. *Journal of Sanitary Engineering Division, ASCE*, 481, SA6, Dec., pp. 1210-1214.

Carman, P.C. 1937. Fluid Flow Through a Granular Bed. *Transactions of the Institution of Chemical Engineers*, London, pp. 150-156.

Danckwerts, P.V. 1953. Continuous Flow Systems Distribution of Residence Times. *Chemical Engineering Science*, 2, 1, Feb., pp. 1-13.

Dullien, F.A.L. 1979. *Porous Media, Fluid Transport and Pore Structure*. Academic Press, NY.

Ebach, E.A., White, R.R. 1958. Mixing of Fluids Flowing Through Beds of Packed Solids. *Advances In Chemical Engineering, Journal*, 4, 2, Jun., pp. 161-169.

Ergun, S. 1952. Fluid Flow Through Packed Columns. *Chemical Engineering Progres*, 48, pp. 89-94.

Fair, G.M. and Gemmell, R.S. 1964. A Mathematical Model of Coagulation. *Journal of Colloid Science*, 19, pp. 360-372.

Forchheimer. 1901. Wasserbewegung durch Boden. *Zeischrift des Verrines deutscher ingenieure*, Dec., pp. 1736-1788.

Freeze, R.A. and Cherry, J.A. 1979. *Groundwater*. Prentice-Hall, NY.

Greenkorn, R.A. 1964. Flow Models and Scaling Laws For Flow Through Porous Media. *Industrial and Engineering Chemistry*, 56, 6, pp. 32-37.

Greenkorn, R.A. 1970. *Dispersion in Heterogenous Nonuniform Anisotropic Media*. EPA No. 16060 DLL

Gupta, S.P. 1972. Dispersion and Adsorption in Porous Media. Ph.D Thesis, Purdue University, Dec.

Harris, H.S., Kaufman, W.J. and Krone, R.B. 1966. Orthokinetic Flocculation in Water Purification. *Journal Sanitary Engineering Division, ASCE*, 95, SA6, Dec., pp.95-111.

Herzig, J.P., Leclerc, D.M. and Le Goff, P. 1970. Flow of Suspensions Through Porous Media, Application to Deep Filtration, *Industrial and Engineering Chemistry*, 62, 5, pp.8-35.

Holland, F.A. 1973. *Fluid Flow for Chemical Engineers*. Edward Arnold Ltd., London.

Hudson, H.E. 1965. Physical Aspects of Flocculation. *Journal American Water Works Association*, 57, 7, pp.885-892 (July 1965).

Hudson, H.E. 1981. *Water Clarification Processes Practical Design and Evaluation*. Van Nostrand Reinhold Company, N.Y.

Huck, P.M. and Murphy, K.L. 1978. Kinetic Model for Flocculation with Polymers. *Journal of the Environmental Engineering Division, ASCE*, 104, EE4, August, pp.767-784.

Hutchinson, W., Foley, P.D. 1974. Operational and Experimental Results of Direct Filtration. *Journal American Water Works Association*, 66, 2, pp.79-87 (Feb. 1974).

Irmay, S. 1954. On the Hydraulic Conductivity of Unsaturated Soils. *Transaction of the American Geophysics Union*, 35, pp. 463-468.

Ives, K.J., Sholji, I. 1965. Research on Variables Affecting Filtration. *Journal Sanitary Engineering Division, ASCE*, 91, SA4, August, pp. 1-18.

Ives, K.J. 1978. *The Scientific Basis of Flocculation*. Sijthoff and Noordhoff, The Netherlands.

Kao, S.V., Mason, S.G. 1975. Dispersion of Particles by Shear. *Nature*, 253, pp. 619-621.

Kawamura, S. 1973. Coagulation Consideration. *Journal American Water Works Association*, 65, 6, pp.417-423 (June 1973).

Kawamura, S. 1976. Consideration on Improving Flocculation. *Journal American Water Works Association*, 68, 6, pp.328-336 (June 1976).

Kradile, J.N. 1983. Development of Simple and Economic Filtration Methods For Rural Water Supplies. *Water Supply*, 1, Berlin, pp. 113-126.

LaMer, V.K., Healy, T.W. 1963. Absorption-Flocculation Reactions of Macromolecules at the Solid-Liquid Interface. *Review of Pure and Applied Chemistry*, Australia, 13, 3, Sept., pp. 112-133.

Levenspiel, O., Smith, W.K. 1957. Notes on the Diffusion-type Model for the Longitudinal Mixing of fluids in flow. *Chemical Engineering Science*, 6, Feb., pp. 227-233.

Levich, V.G. 1962. *Physicochemical Hydrodynamics*. Prentice-Hall, Inc, New York.

Maroudas, A. and Eisenklam, P. 1965. Clarification of Suspensions: A study of Particle Deposition in Granular Media. I, II, *Chemical Engineering Science*, 20, March, pp. 867-873.

Matsuo, T., Unno, H. 1981. Forces Acting on Floc and Strength of Floc. *Journal of the Environmental Engineering Division, ASCE*, 107, SA1, June, pp. 257-263.

Marcom, A.R. 1946. Fluid Flow Through Granular Materials. *Transaction of the Institution of Chemical Engineers*, 24, pp. 30-43.

Morris, J.K., Knoche, W.R. 1984. Temperature Effects on the Use of Metal-Ion Coagulants for Water Treatment. *Journal American Water Works Association*, 76, 3, pp.74-79 (Mar. 1984).

Neung-Won Han, Jayendra Bhakta and Carbonell, R.G. 1985. Longitudinal and Lateral Dispersion in Packed Beds: Effect of Column Length and Particle Size Distribution. *Advances In Chemical Engineering, Journal*, 31, 2, pp. 277-288.

Ogata, A., Banks, R.B. 1961. A Solution to the Differential Equation of Longitudinal Dispersion in Porous Media. Geological Survey Professional Paper 411-A, Washington 1961.

Parker, D.S. 1970. Characteristics of Biological Flocs in Turbulent Regime. University of California, Berkeley, Ph.D.

Parker, D.S., Kaufman, W.J., Jenkins, D. 1972. Floc Breakup in Turbulent Flocculation Processes. *Journal Sanitary Engineering Division, ASCE*, 98, SA1, Feb., pp. 79-99.

Poole, L. and Borchers, M. 1979 *Some Common Basic Programs*. Osborne/McGraw-Hill, Berkeley, C.A.

Purchas, D.B. 1978. *Solid/Liquid Separation Equipment Scale-Up*. Upiands Press Ltd., England.

Rebhun, M. Fuhrer, Z. and Adin, A. 1984. Contact Flocculation - Filtration of Humic Substances. *Water Resources*. 18, 8, pp. 963-970.

Richter, C.A. 1977. Water Treatment Plant for Small Communities. SANEPAR, Brazil.

Sanks, R.L. 1978. *Water Treatment Plant Design*. Ann Arbor Science, Mich.

Schneebeli, G. 1955. Experiences sur la limite de validite de la loi de Darcy et l'apparition de la turbulence dans une ecoulement de filtration. *La Huile Blanche*, 2, 10, pp. 141-149.

Scheidegger, A.E. 1960. *The Physics of Flow Through Porous Media*. University of Toronto Press.

Schulz, Ch.R., and Okun, D.A. 1984. *Surface Water Treatment for Communities in Developing Countries*. John Wiley & Sons, N.Y.

Shamir, U.Y., Harleman, D.R.F. 1967. Numerical Solutions for Dispersion in Porous Mediums. *Water Resources Research*. 3, 2, pp. 557-581.

Shea, T.G., Gates, W.E., Argaman, Y.A. 1971. Experimental Evaluation of Operating Variables in Contact Flocculation. *Journal American Water Works Association*, 63, 1, pp.41-48, (Jan. 1971).

Standard Methods for the Examination of Water and Wastewater, 15th Ed. *APHA, AWWA, WPCF*.

Stark, K.P. 1972 A numerical study of the nonlinear laminar regime of flow in an idealized porous medium. Fundamentals of Transport Phenomena in Porous Media. *IAHR*, Elsevier Publishing Company.

Stumm, W., Morgan, J.J. 1962 Chemical Aspects of Coagulation. *Journal American Water Works Association*, 54, 8, pp.971-992 (Aug. 1962).

Stumm, W., O'Melia, Ch.R. 1968. Stoichiometry of Coagulation. *Journal American Water Works Association*, 60, 5, pp.514-539 (May 1968).

Sutherland, D.N. 1967. A Theoretical Model of Floc Structure. *Journal of Colloid and Interface Science*, 25, pp. 373-380.

Tambo, N. and Watanabe, Y. 1979a. Physical Characteristics of Flocs. *Water Research*, 13, pp.409-421.

Tambo, N. and Watanabe, Y. 1979b. Physical Aspects of Flocculation Process. *Water Research*, 13, pp. 429-441.

Tchobanoglous, G. and Eliassen, R. 1970. Filtration of Treated Sewage Effluent. *Journal Sanitary Engineering Division, ASCE*, 96, SA2, April, pp. 243-265.

TeKippe, R.J., Ham, R.K. 1970. Coagulation Testing: A Comparison of Techniques, I and II. *Journal American Water Works Association*, 62, 9, pp.594-602 (Sep. 1970), 62, 10, pp.620-628 (Oct. 1974).

Thomas, D.G.1964. Turbulent Disruption of Flocs in Small Particle Suspensions. *Advances In Chemical Engineering Journal*, 10, 3, pp. 517-523.

Vigneswaran, S. and Ben Aim R. 1985. The Influence of Suspended Particle Size Distribution in Deep-Bed Filtration. *Advances In Chemical Engineering Journal*, 31, 2, pp. 321-324.

Vold, M.J. 1963. Computer Simulation of Floc Formation in a Colloidal Suspension. *Journal of Colloid Science*, 18, pp. 684-695.

Von Smoluchowski, M. 1916. *Drei Vortrage uber Diffusion, Brownshe Molekular Beweging und Koagulation von Kolloidteilchen*. Physik. Z., 17, 557.

Von Smoluchowski, M. 1917. *Versuch einer Mathematischen Theorie der Koagulatinskinetik Kolloid Losungen*. Z. Physik. Chem., 92, 155.

Wagner, G.E. 1983. The Latin American Approach to Improving Water Supplies. *Journal American Water Works Association*, 75, 4, pp.168-173 (Apr. 1983).

Ward, J.C. 1964. Turbulent Flow in Porous Media. *Proceedings of ASCE*, 90, HY5, Sep., pp. 1-12.

Weber, W.J. 1972. *Physicochemical Processes for Water Quality Control*. Wiley-Interscience. N.Y.

Yalin, S.M. 1971. *Theory of Hydraulic Models*. Macmillan.

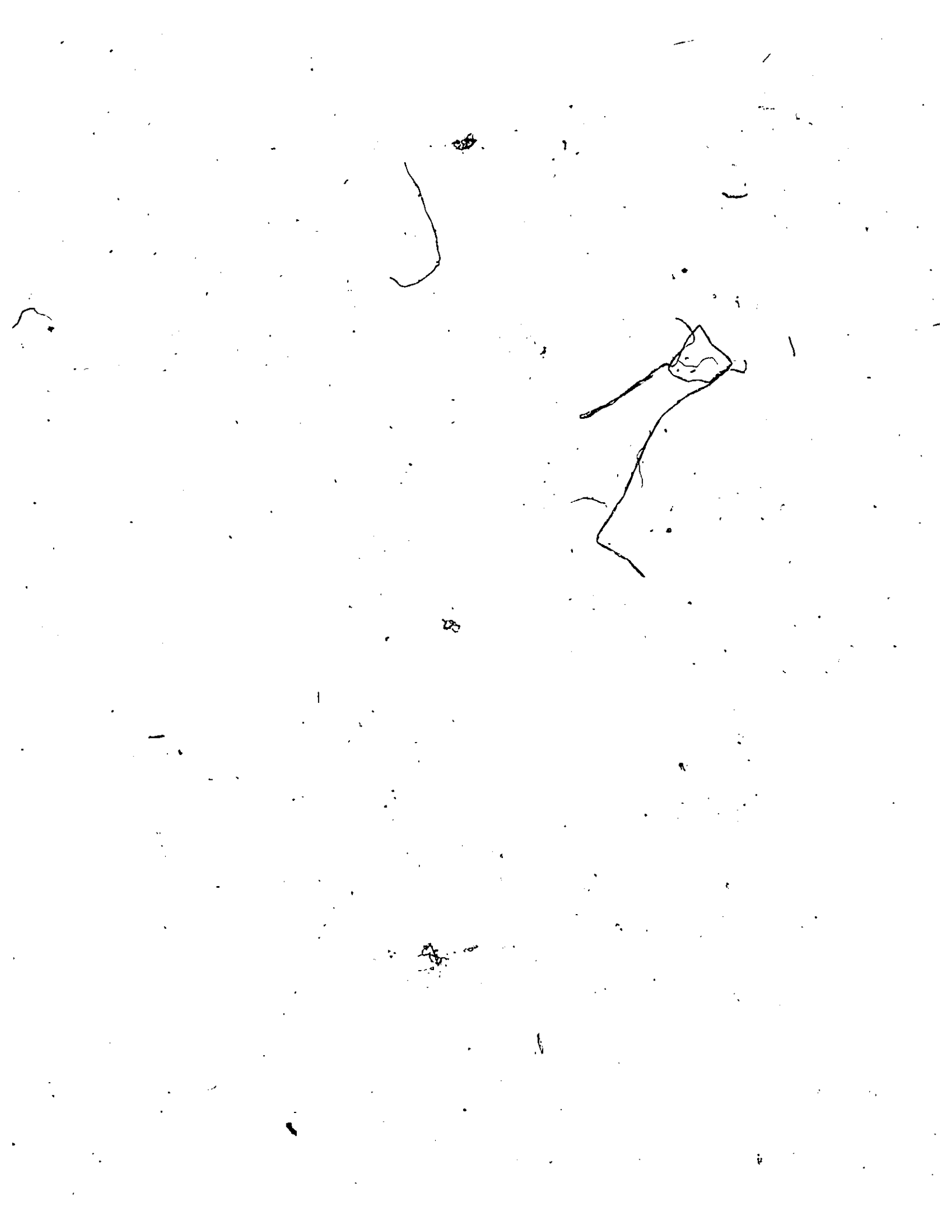

UNIVERSITÉ D'OTTAWA
UNIVERSITY OF OTTAWA